ASTM Committee Meeting
E08.07.03 Surface Cracks

E740 and E2899

May 3, 2016

Doug Wells & Phillip Allen
NASA MSFC
Damage Tolerance Assessment Branch

Agenda

A. Approval of the minutes from November 2015 meeting in Tampa, FL

B. Old Business

- E2899 status
- Analytical round robin phase II, report writing update
- E740 future plans - Work Item 50037
- Review of critical angle evaluation

C. New Business

- None, unless offered by task group

E2899-15 Release

- Three previous ballot items were incorporated in the -15 revision along with some editorial comments and corrections.

- No pending revisions

- Next planned ballot revision actions:
  - Incorporation of second round robin report reference
  - Potential revision for improved substantiation of precision and bias statements based on round robin results

Analytical Round Robin Phase II

- Preliminary results from the round robin were presented in November 2014.
- Full analysis and reporting of the result set is in process.
- Planned publication of the RR results as a NASA Technical Memorandum (public release) currently in draft state
- Decided separate publication of critical angle determination by analysis is needed
  - Technical content reviewed herein
- Round robin result overview included in back-up

E740 Items

ASTM E740-10 Status

- E740 is a surface crack residual strength test method. No crack front parameters are evaluated as a part of this method, with exception of the stress intensity during precracking.

- Standard renewed in 2010, and has been submitted for ballot for renewal without changes. Ballot out on next opportunity.

Forward plan:

- Keep E740 active
- Established work item for E2899 to accommodate residual strength evaluations as an Annex.
    - Annex to be used directly or in support of field collapse test evaluation
- Once approved into E2899, Ballot E740 for withdrawal

E740 Items

Work Item 50037 has been established:

Summary:
ASTM E2899 provides an updated framework for the evaluation of initiation fracture toughness in surface cracks. The long-standing surface crack standard, ASTM E740, is in need of update. In contrast to the initiation toughness measure provided by E2899, E740 provides only a measure of the residual strength in the presence of a surface crack. The residual strength assessment in E740 is currently very limited. There is a desire to develop a more robust residual strength evaluation for the surface crack geometry in the E2899 standard, particularly to handle tests which fall into E2899s field collapse regime, meaning the deformation state in the specimen has exceeded the currently specified limits of validity for determination of the J-Integral fracture toughness parameter. The intent is to develop an annex for E2899 to handle the residual strength surface crack test. Once developed and integrated into E2899, the proposed plan is to ballot E740 for withdrawal. In the meantime, E740 will remain active.

MT Aerospace (Germany), a frequent user of E740, and has expressed potential interest in collaborating on the E740 revision.

Dust up on initiation angle, ϕ_i

Noted in the development of surface crack round robin phase II report that independent documentation of the process for determining initiation angle is needed

Little record of task group seeing details on the process for many years, so providing a brief overview here

The Surface Crack Set-up

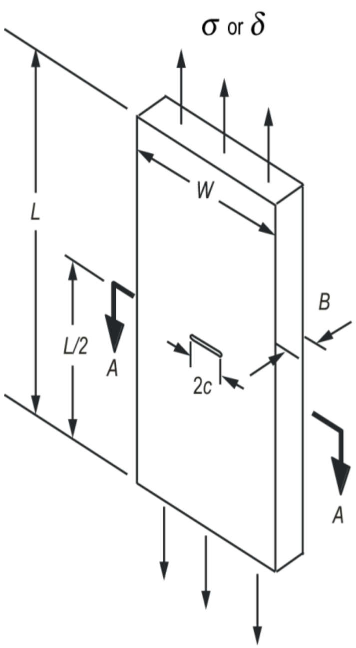

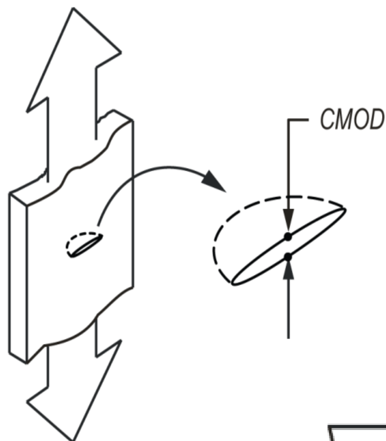

Parametric angle, ϕ

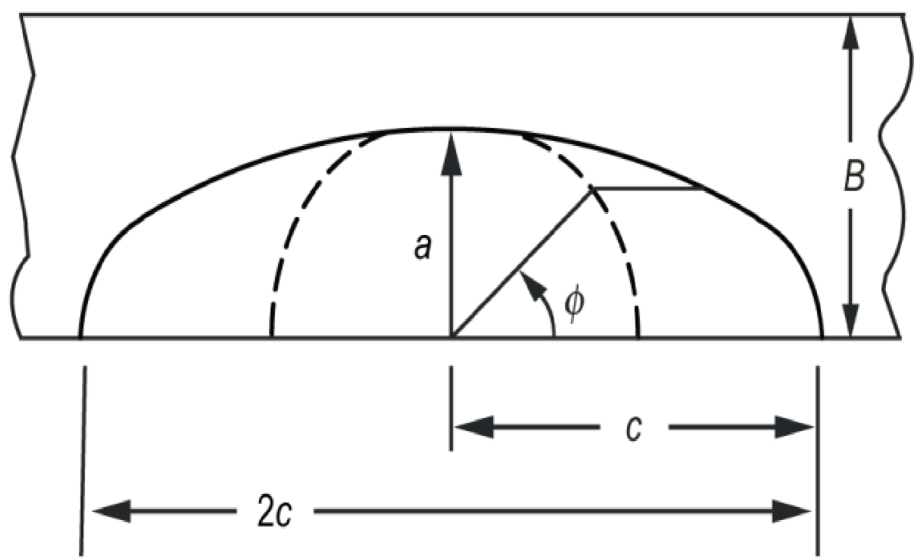

Section A-A

Critical Angle Determination

Damage Tolerance Assessment Branch
MSFC Engineering Directorate

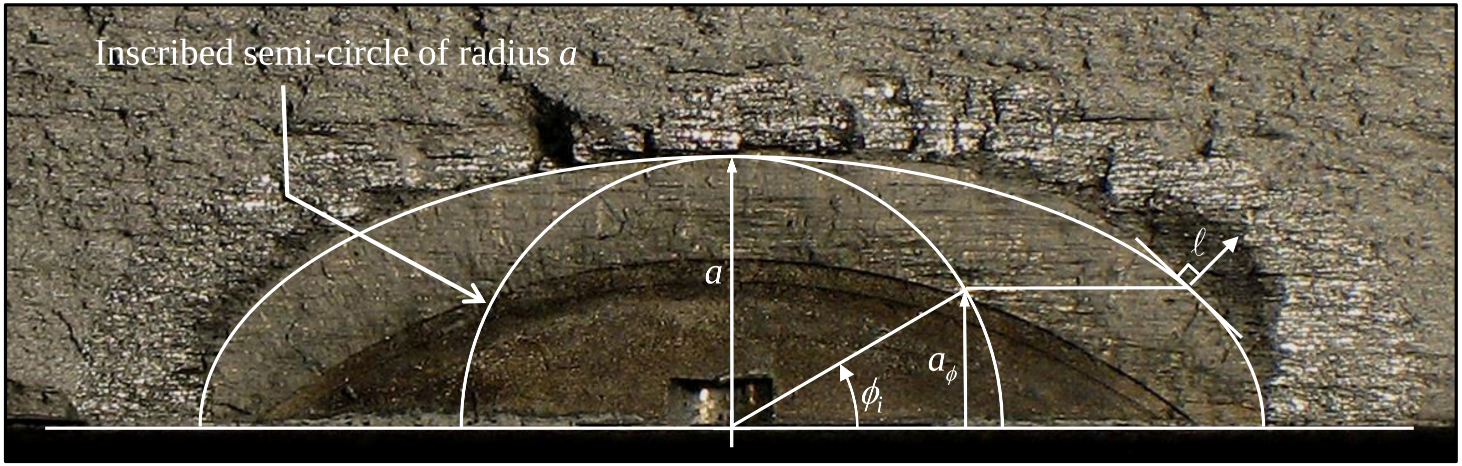

Tearing location clear

RR Phase II: Tearing location in ductile tearing region not clear

(cleavage initiation site is visible, but not part of standard at this time)

Critical Angle Determination

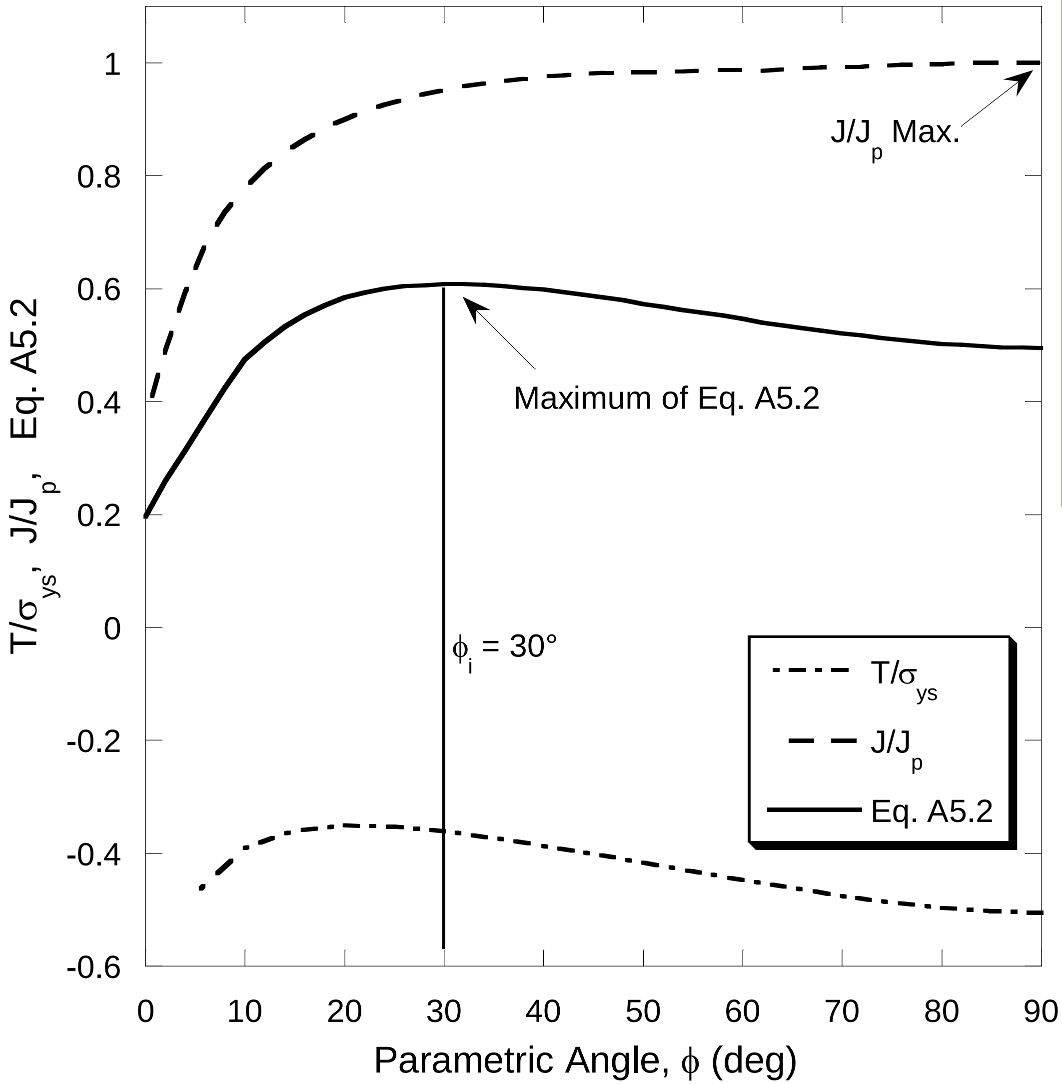

ϕ_i defined at maximum of

$$f(\phi) = \frac{J_\phi}{J_p}\left(\frac{T}{\sigma_{ys}} + 1\right) \quad \text{for } \frac{T}{\sigma_{ys}} \le 0$$

$$f(\phi) = \frac{J_\phi}{J_p}\left(\frac{T}{4\sigma_{ys}} + 1\right) \quad \text{for } \frac{T}{\sigma_{ys}} > 0$$

- Product of driving force and constraint
- Follows work of Newman et al. on J-α_h
- Elastic-plastic solution needed for reliable predictions

Critical Angle Determination

WHY?

ϕ_i defined at maximum of

$$f(\phi) = \frac{J_\phi}{J_p}\left(\frac{T}{\sigma_{ys}} + 1\right) \quad \text{for } \frac{T}{\sigma_{ys}} \le 0$$

$$f(\phi) = \frac{J_\phi}{J_p}\left(\frac{T}{4\sigma_{ys}} + 1\right) \quad \text{for } \frac{T}{\sigma_{ys}} > 0$$

- Why T/σ_{ys} ?
- Use of $(T/\sigma_{ys} + 1)$ form
- Deformation limit methodology

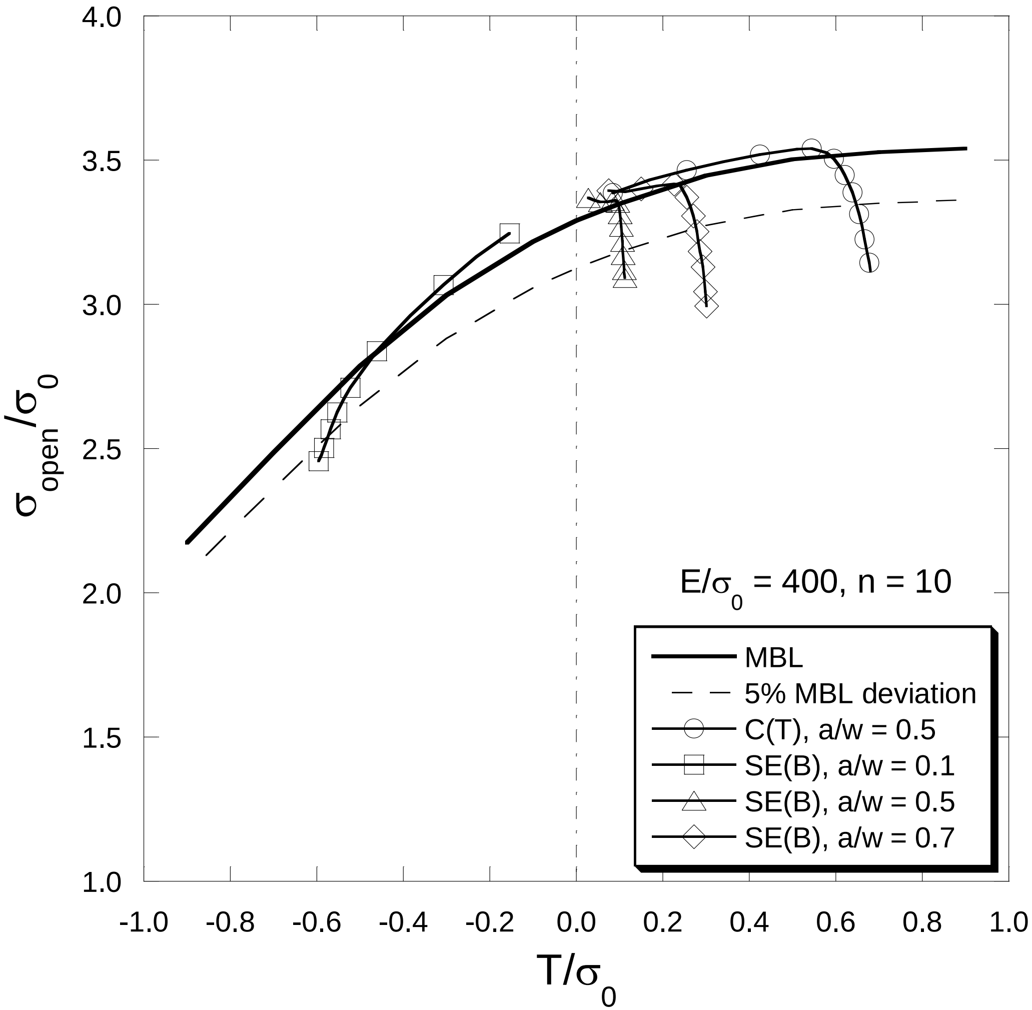

Critical Angle Determination

$$Q \equiv \frac{\sigma_{yy} - \left(\sigma_{yy}\right)_{T=0}}{\sigma_0} \text{ at } \theta = 0 \text{ and } \frac{r\sigma_0}{J} = 2,$$

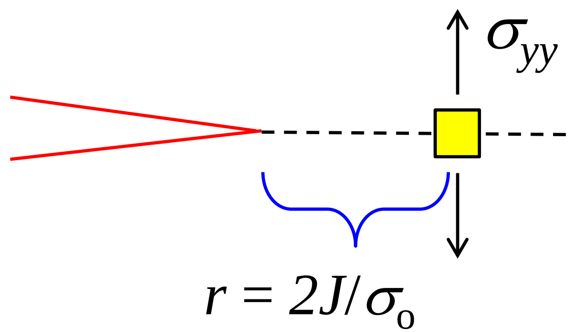

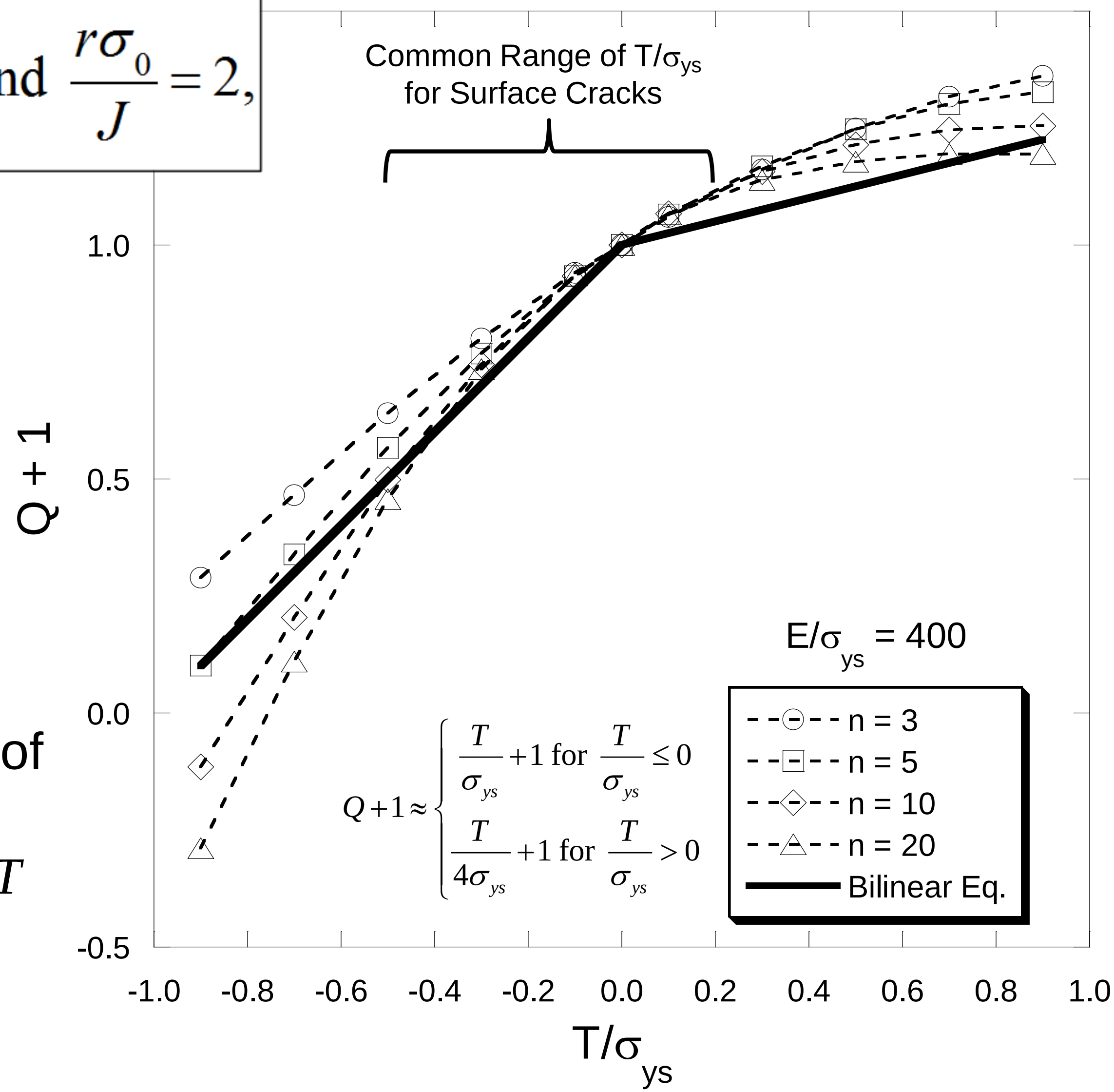

- Simple bilinear form in T follows the Q constraint parameter for prediction of crack tip conditions
- Deformation limits keep T a suitable parameter for relative influence in determination of ϕ_i

Critical Angle Determination

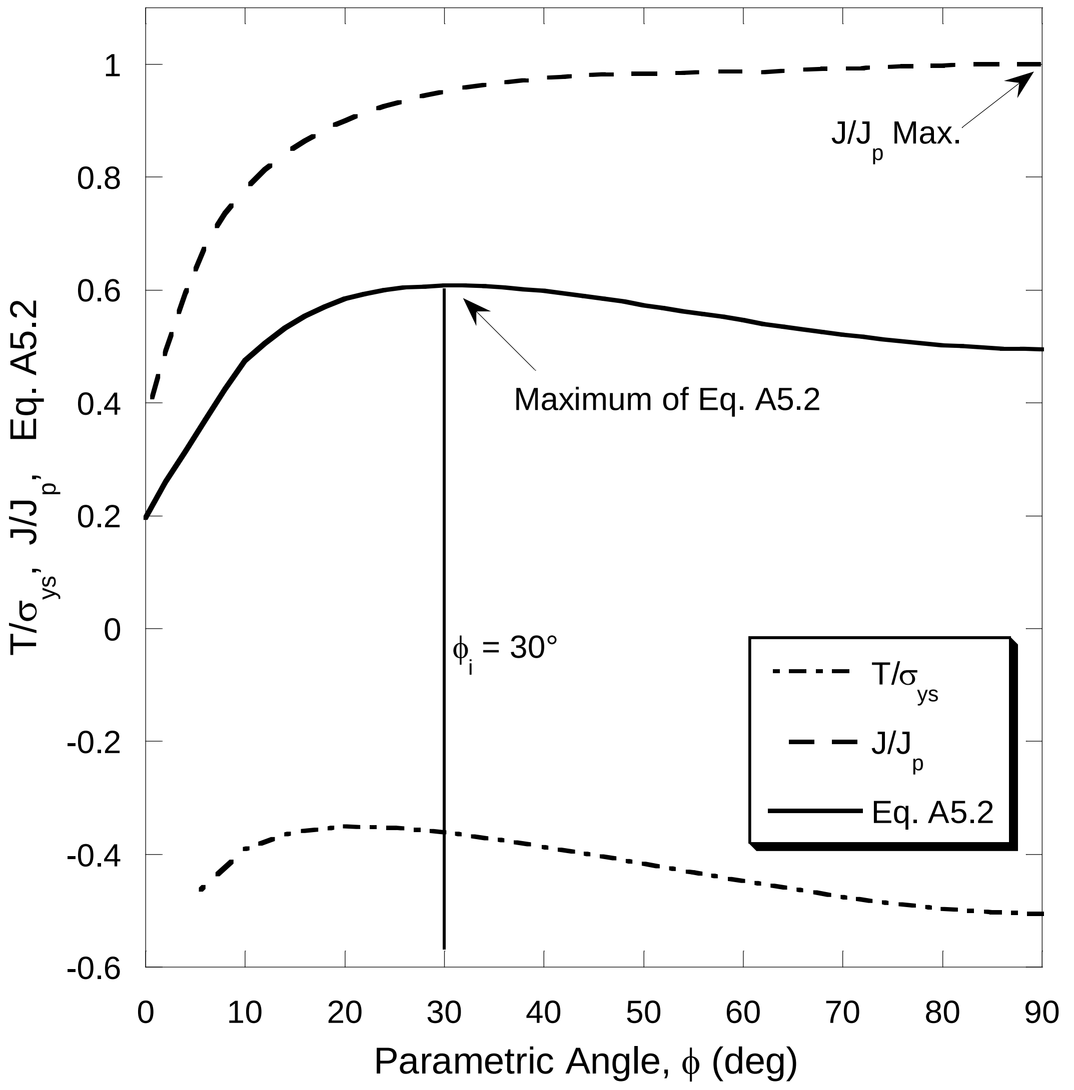

Critical Angle Determination

2219-T8 SC Tension and Bending Data

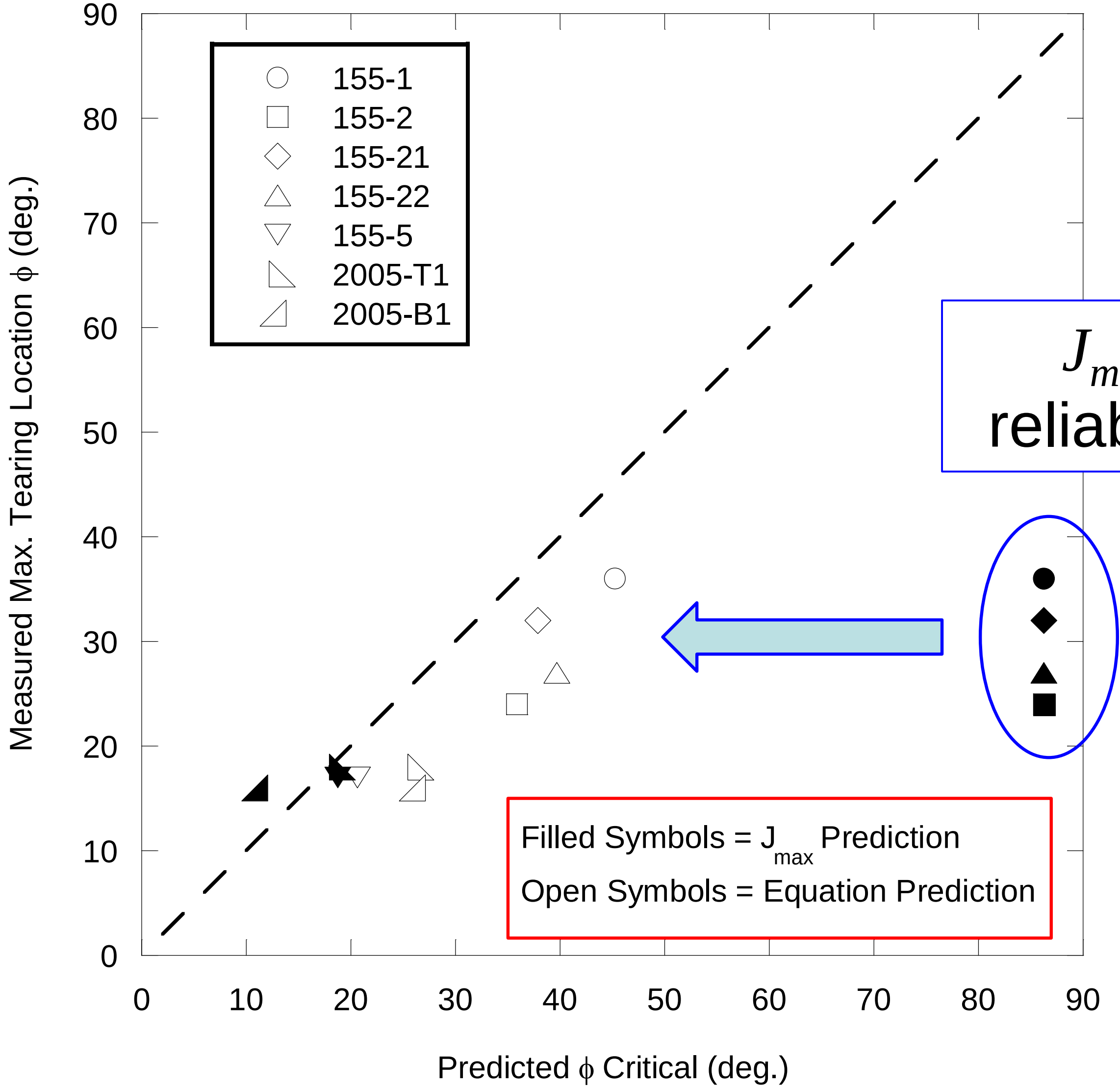

J_{max} is not a reliable predictor

D6AC Steel Surface Crack Tests

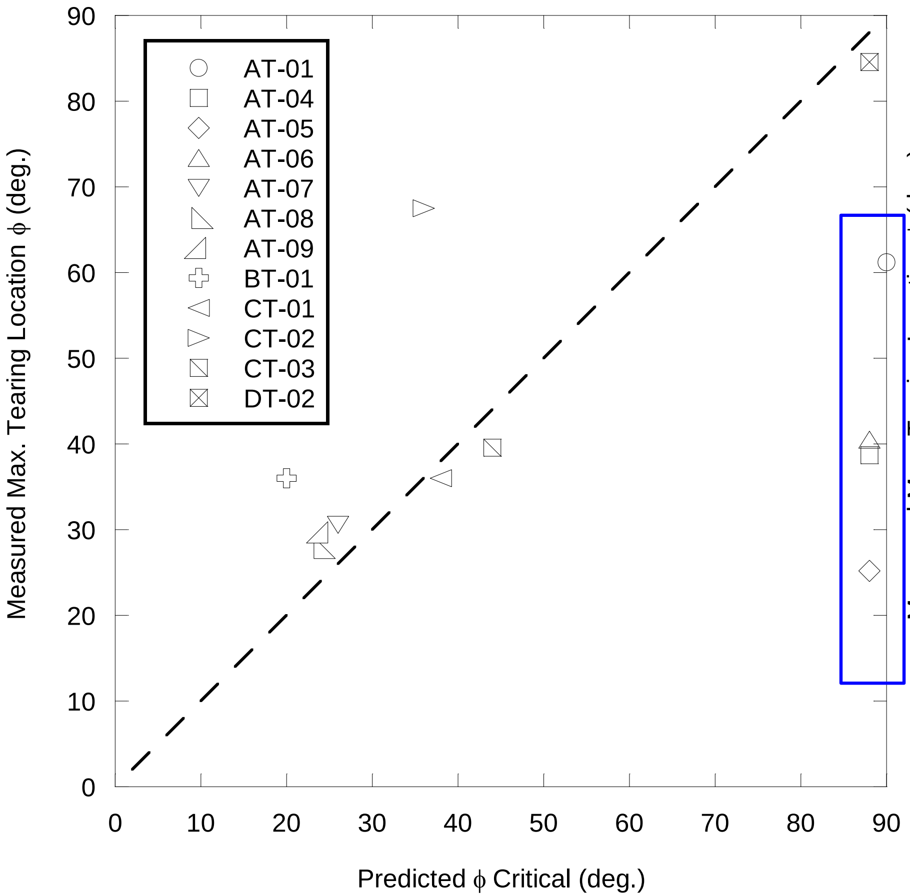

J_{max} prediction

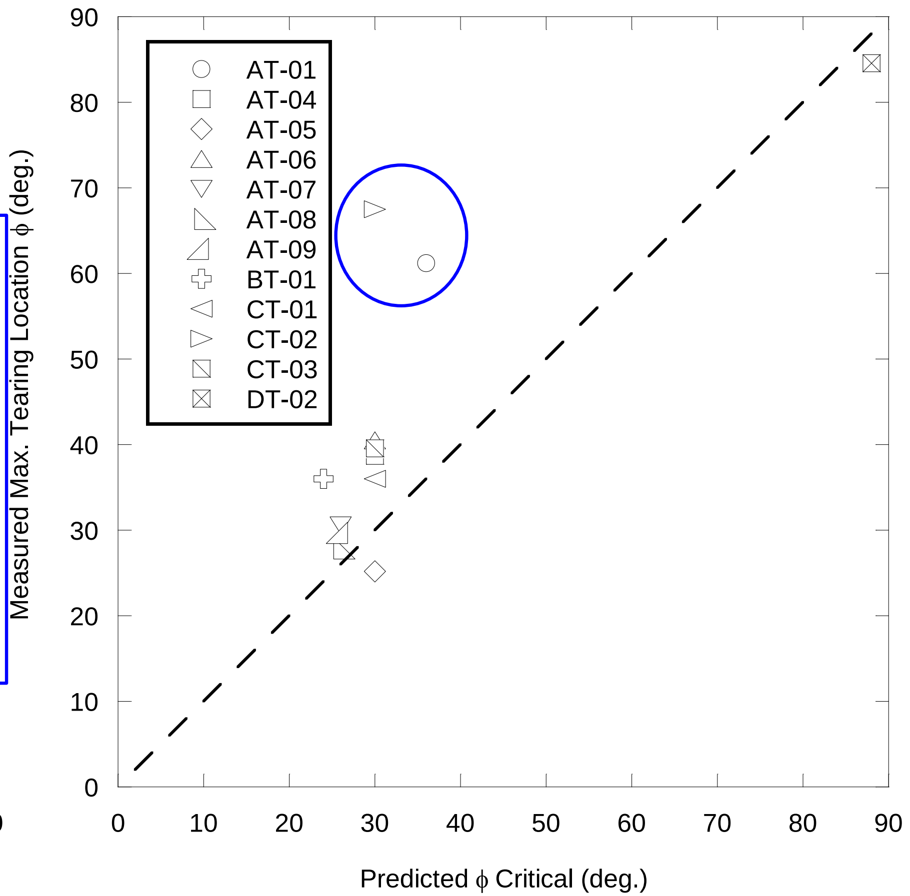

Eqn. A5.2 prediction

Critical Angle Determination

Round Robin II: Prediction of Initiation Angle, ϕ_i

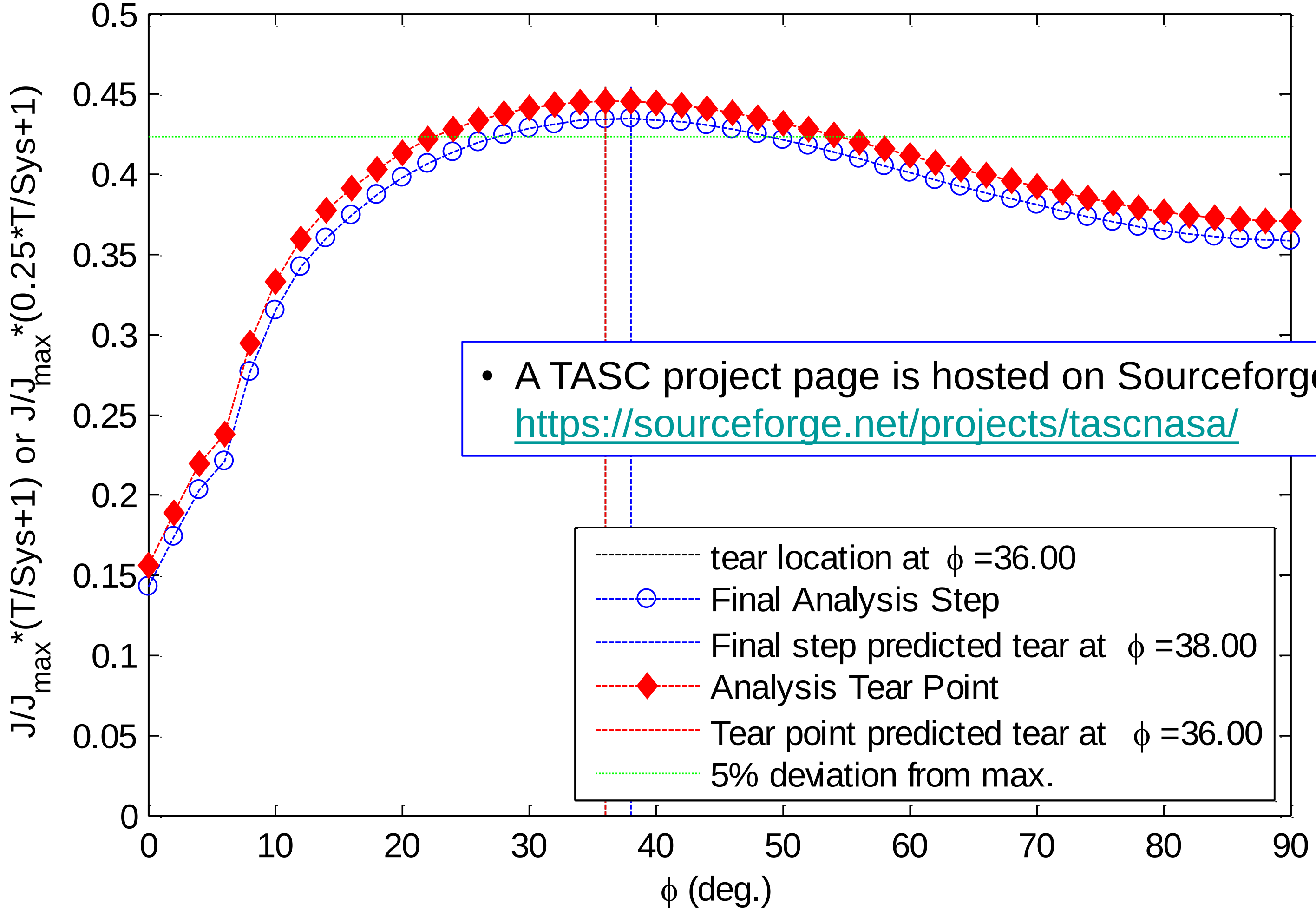

- A TASC project page is hosted on Sourceforge.net at: https://sourceforge.net/projects/tascnasa/

Round Robin II: Prediction of Initiation Angle, ϕ_i

Lab	ϕ_i		
Lab-1	37.5		
Lab-1-T	36.0		
Lab-2	35.0	Max.	42.80
Lab-2-T	36.0	Avg.	35.43
Lab-3	40.4	Min.	25.00
Lab-4	37.1	Std. Dev.	4.68
Lab-5	32.5		
Lab-6-T	38.0		
Lab-7	34.9		
Lab-8	42.8		
Lab-9-T	30.0		
Lab-10	25.0		

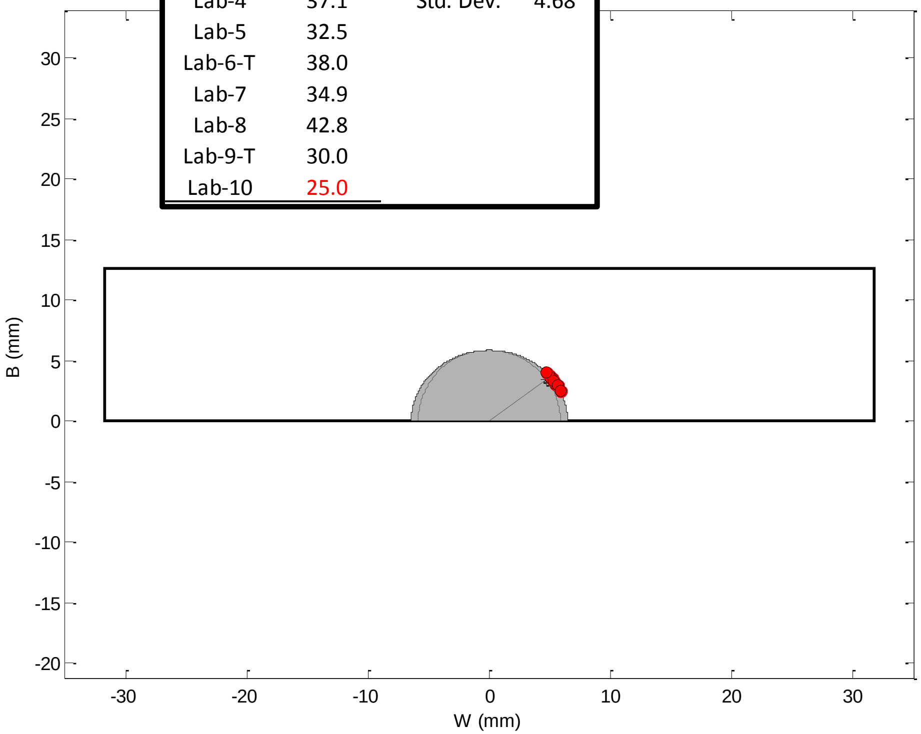

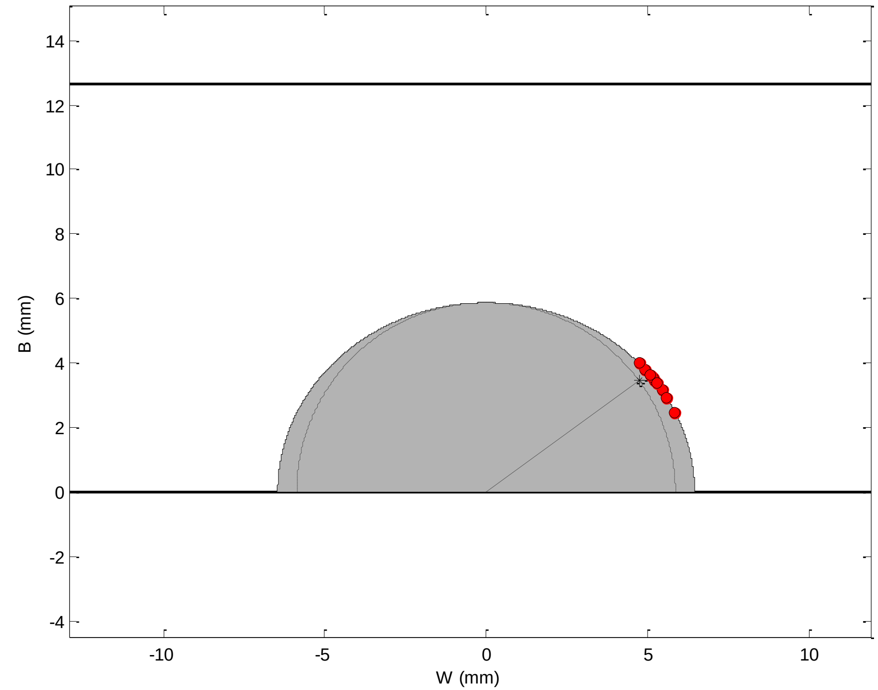

Note: Lab-10 had a error in their T-stress calculation which resulted in a incorrect calculation of ϕ_i. The Lab-10 corrected value is ϕ_i = 35°.

Critical Angle Determination

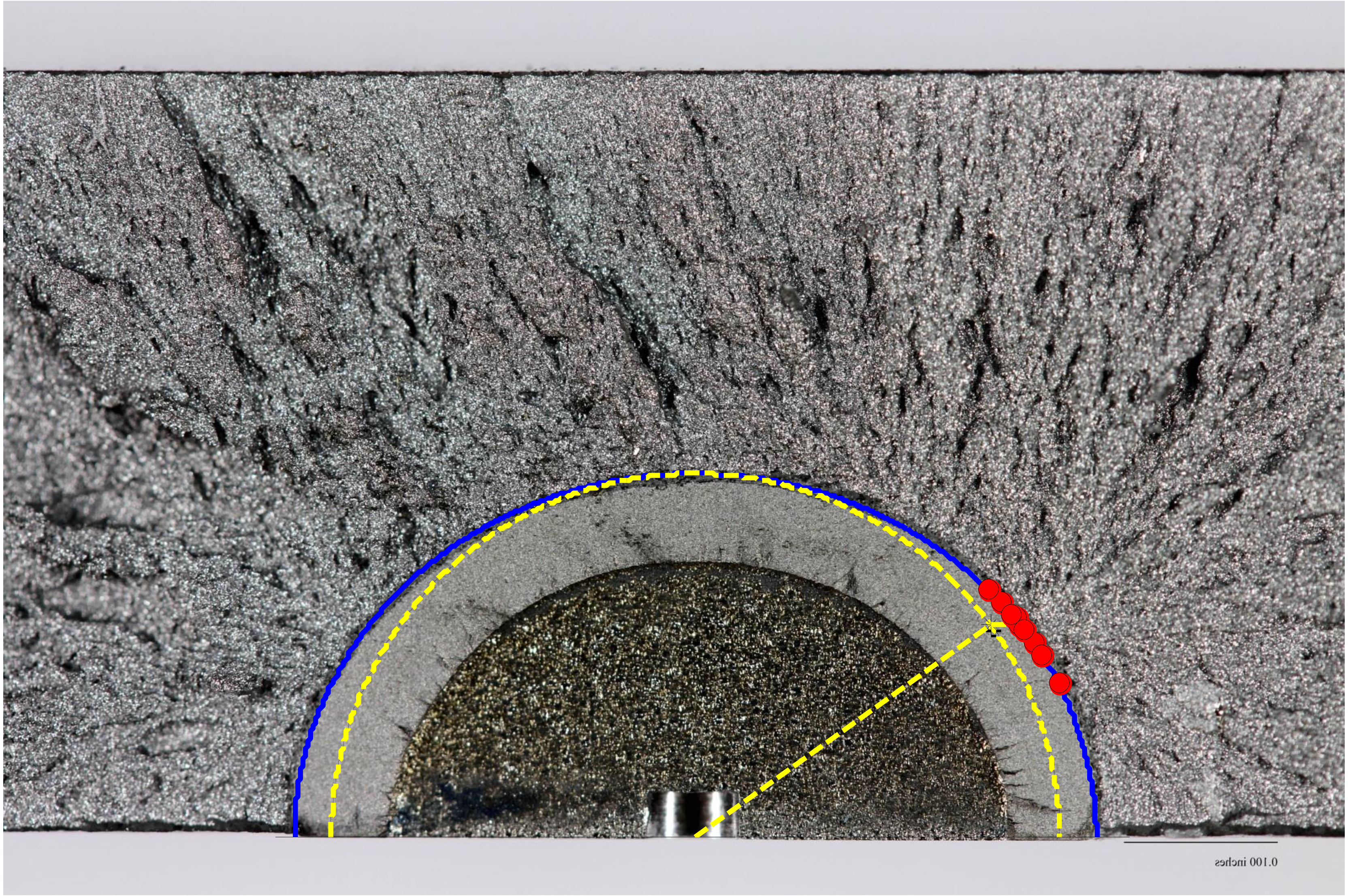

Backup

Round Robin Objectives:

1) Determine the consistency in the interpretation of the test evaluation requirements in E2899.
2) Provide guidance/feedback for E2899 A6 - *METHODOLOGY FOR PERFORMING ELASTIC-PLASTIC FINITE ELEMENT ANALYSIS AND COMPARISON TO TEST RECORD*
3) Provide additional information on the analytical consistency of finite element (FE) methods as prescribed in the standard for future revision of the precision and bias statements.
4) Evaluate use of interpolated nonlinear FE solutions as an alternative to traditional FE analysis through use of TASC*.

* Tool for Analysis of Surface Cracks (TASC), https://sourceforge.net/projects/tascnasa/

RR Phase II based on 4142 steel SC(T) test

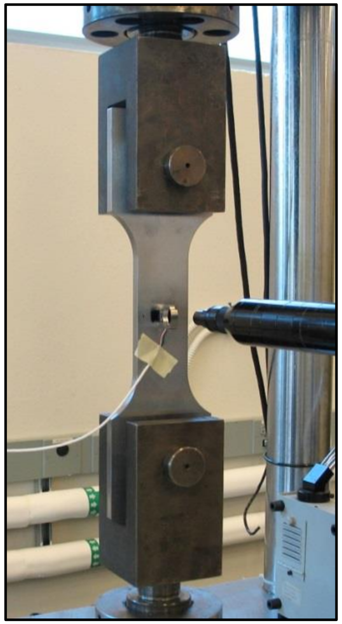

- Participants given specimen dimensions, fracture surface photo, material tensile test data, and SC(T) force-CMOD data.
- Asked to follow E 2899 and evaluate the test

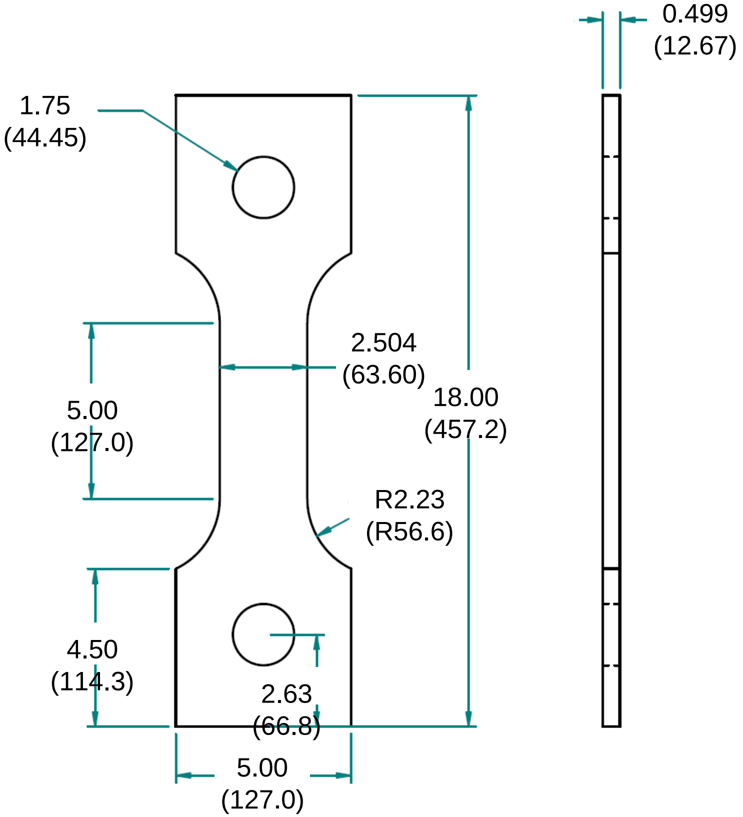

RR Phase II participants in random order

- Enrico Lucon – NIST
- Greg Thorwald – Quest Integrity Group
- Igor Varfolomeev - IWM
- Jason Bely – Alcoa
- Steven Altstadt – Stress Engineering Services
- Michael Windisch – MT Aerospace
- Ryan Sherman – Purdue University
- Francisco Martin – Purdue University
- Dawn Phillips – NASA MSFC
- Phillip Allen (Lab 1) – NASA MSFC

- Participants evaluated the test results using elastic-plastic finite element analysis per E 2899 A6 and/or using TASC

Force-CMOD Comparison, E 2899 A6.3 and A6.4

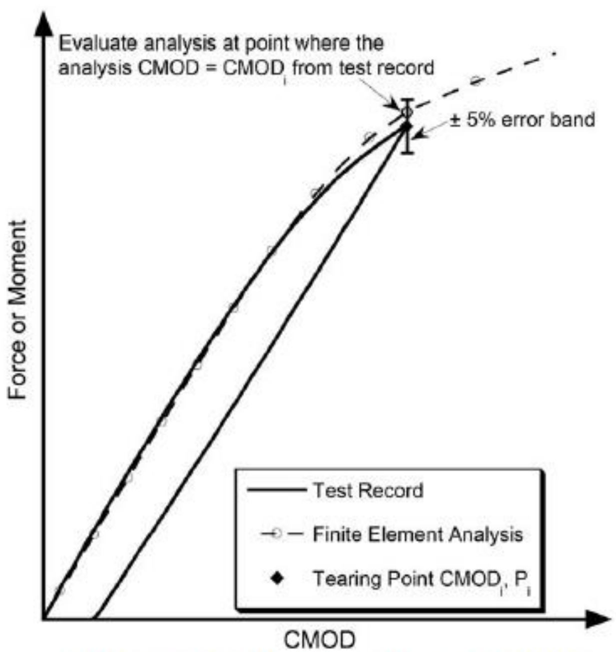

FIG. A6.1 Evaluate the test analysis by matching CMOD values

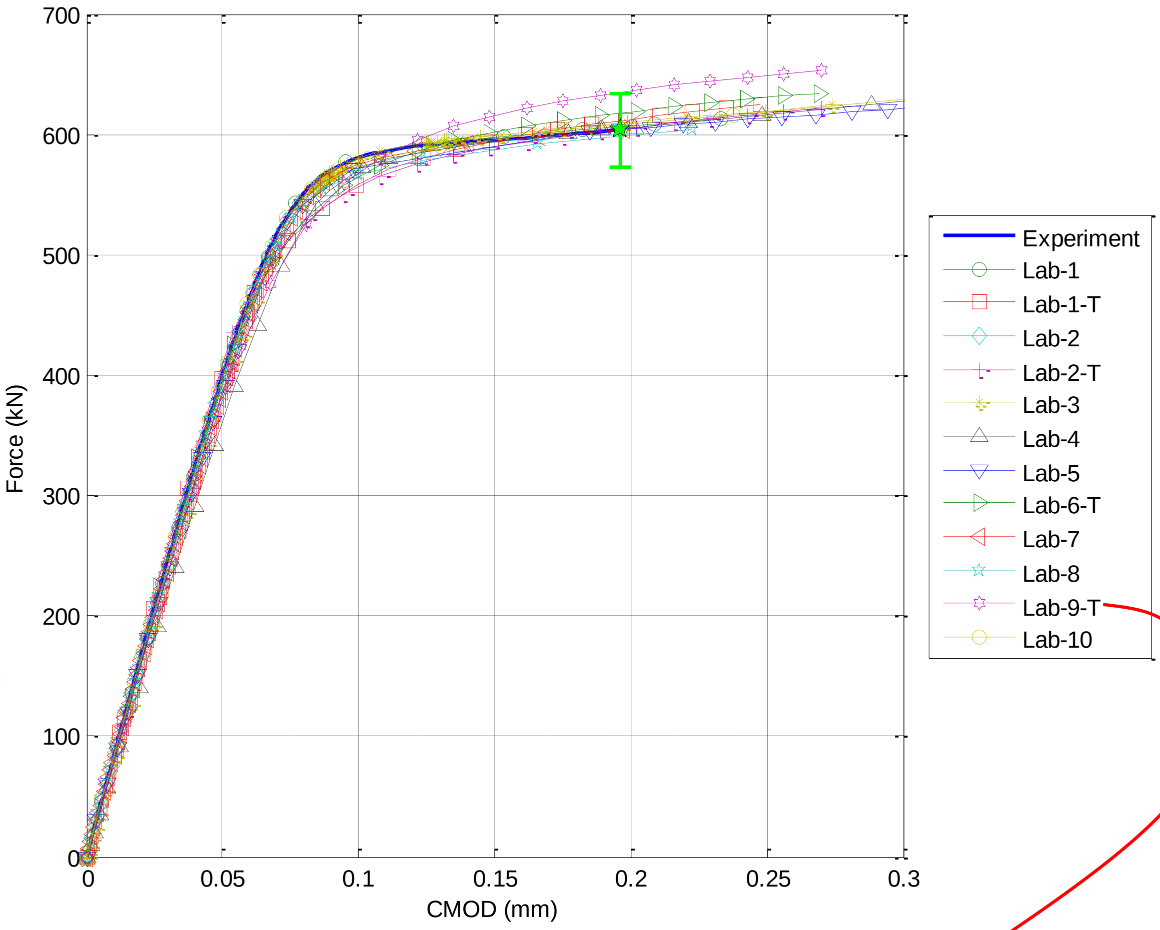

Note: Lab-9-T force at *CMOD*$_i$ exceeds the test *P*$_i$ by 5.25%, but the analysis results are still included in the following evaluations.

Elastic Compliance Evaluation, E 2899 A6.3

Comparison for Lab-1

Experiment Elastic Slope Determined Using Linear Fit to 20-50% of Max Data Range

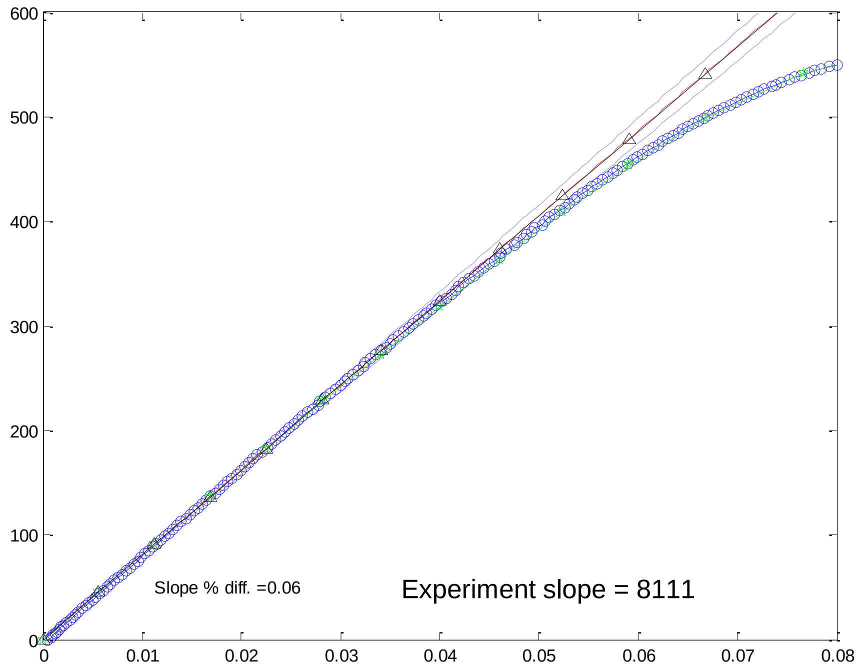

Experiment Elastic Slope Determined Using SDAR Graham-Adler Fitting Algorithm

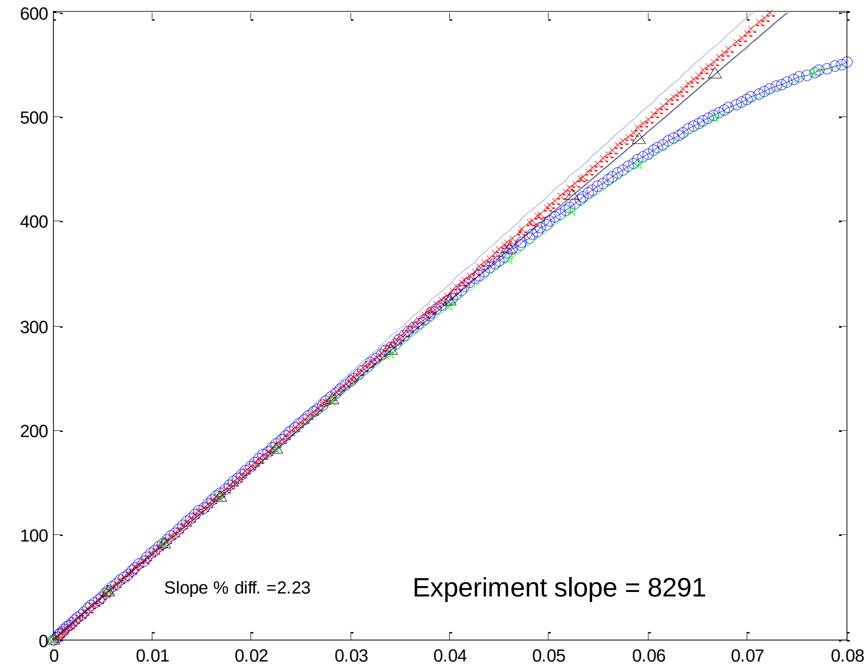

Elastic Compliance Evaluation, E 2899 A6.3

Experiment Elastic Slope Determined Using Linear Fit to 20-50% of Max Data Range

Lab	Elastic Slope % Diff.
Lab-1	0.06
Lab-1-T	-2.88
Lab-2	-0.69
Lab-2-T	-5.55
Lab-3	2.16
Lab-4	9.27
Lab-5	2.33
Lab-6-T	-2.47
Lab-7	1.49
Lab-8	-0.63
Lab-9-T	3.30
Lab-10	-1.07

Experiment Elastic Slope Determined Using SDAR Graham-Adler Fitting Algorithm

Lab	Elastic Slope % Diff.
Lab-1	2.23
Lab-1-T	-0.66
Lab-2	1.49
Lab-2-T	-3.27
Lab-3	4.28
Lab-4	11.23
Lab-5	4.44
Lab-6-T	-0.25
Lab-7	3.62
Lab-8	1.55
Lab-9-T	5.39
Lab-10	1.11

Analytical Round Robin Phase II

Damage Tolerance Assessment Branch
MSFC Engineering Directorate

Critical Angle, ϕ_i, Evaluation, E 2899 A5.2

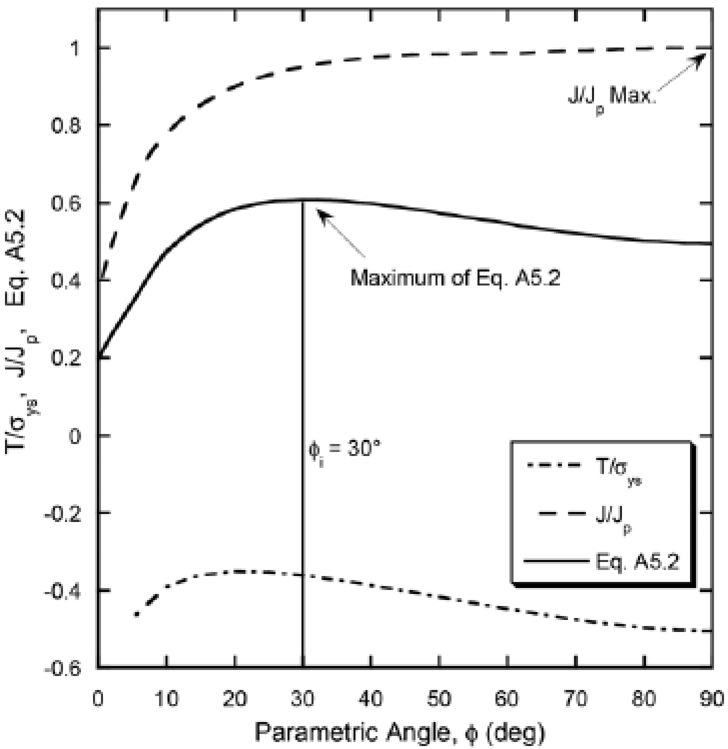

FIG. A5.2 Example of determination of ϕ_i by finding the maximum of Eq A5.2.

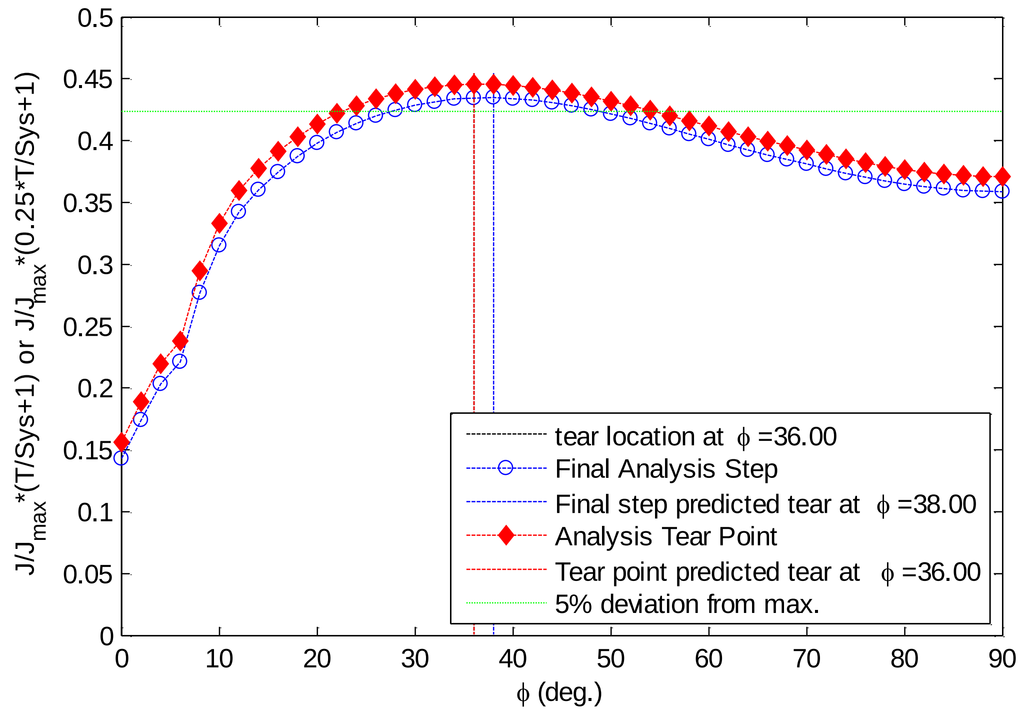

$$f(\phi)=\frac{J(\phi)}{J_p}\left(\frac{T(\phi)}{\sigma_{YS}}+1\right)\quad \text{for } \frac{T(\phi)}{\sigma_{YS}}\leq 0$$
$$f(\phi)=\frac{J(\phi)}{J_p}\left(\frac{T(\phi)}{4\sigma_{YS}}+1\right)\quad \text{for } \frac{T(\phi)}{\sigma_{YS}}>0 \qquad \text{(A5.2)}$$

Critical Angle, ϕ_i, Evaluation, E 2899 A5.2

Lab	ϕ_i		
Lab-1	37.5		
Lab-1-T	36.0		
Lab-2	35.0	Max.	42.80
Lab-2-T	36.0	Avg.	35.43
Lab-3	40.4	Min.	25.00
Lab-4	37.1	Std. Dev.	4.68
Lab-5	32.5		
Lab-6-T	38.0		
Lab-7	34.9		
Lab-8	42.8		
Lab-9-T	30.0		
Lab-10	25.0		

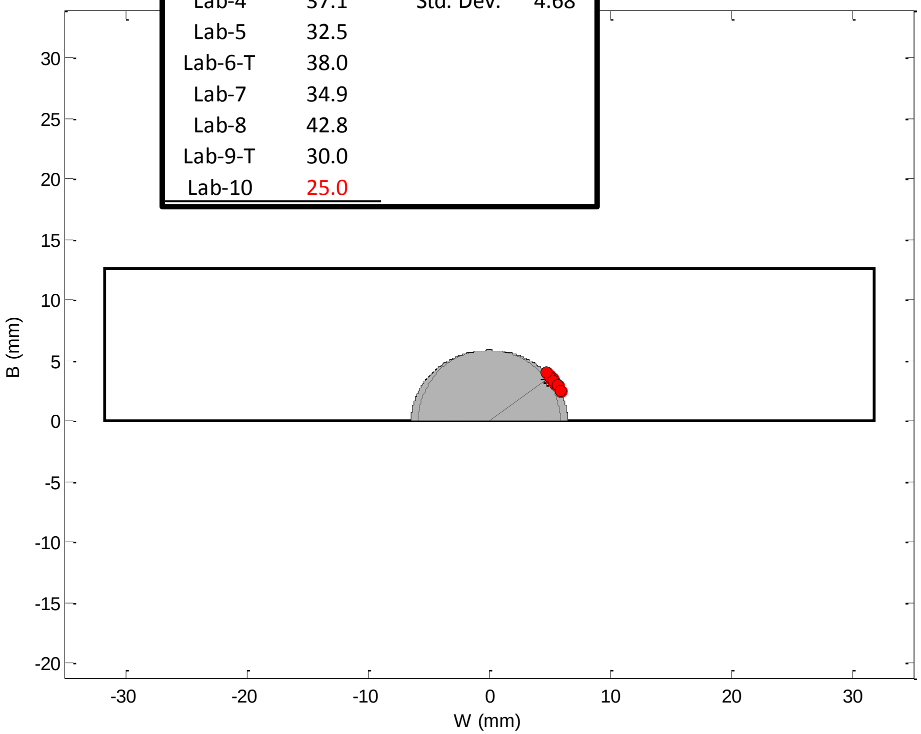

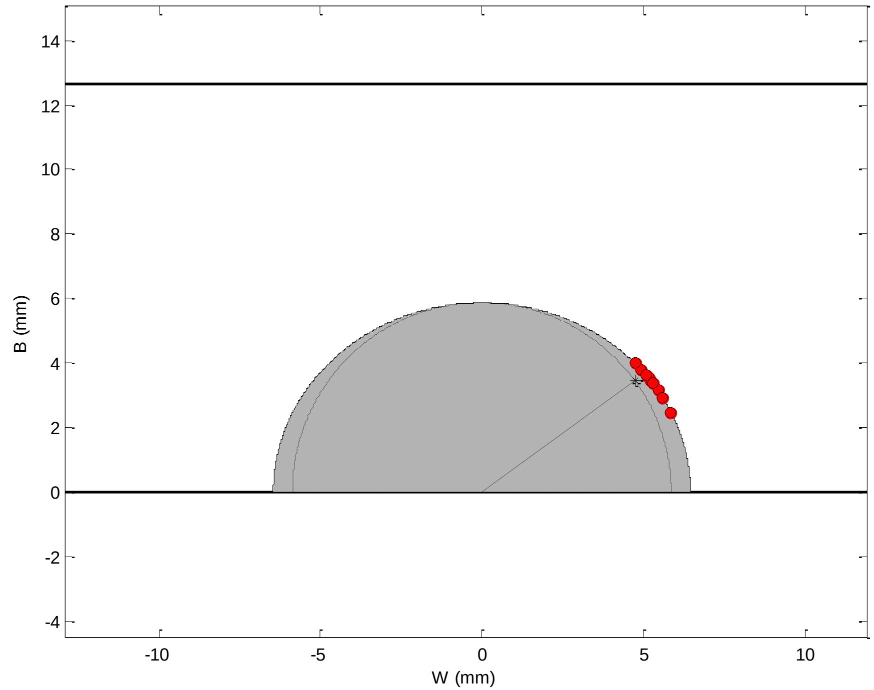

Note: Lab-10 had a error in their T-stress calculation which resulted in a incorrect calculation of ϕ_i. The Lab-10 corrected value is ϕ_i = 35°.

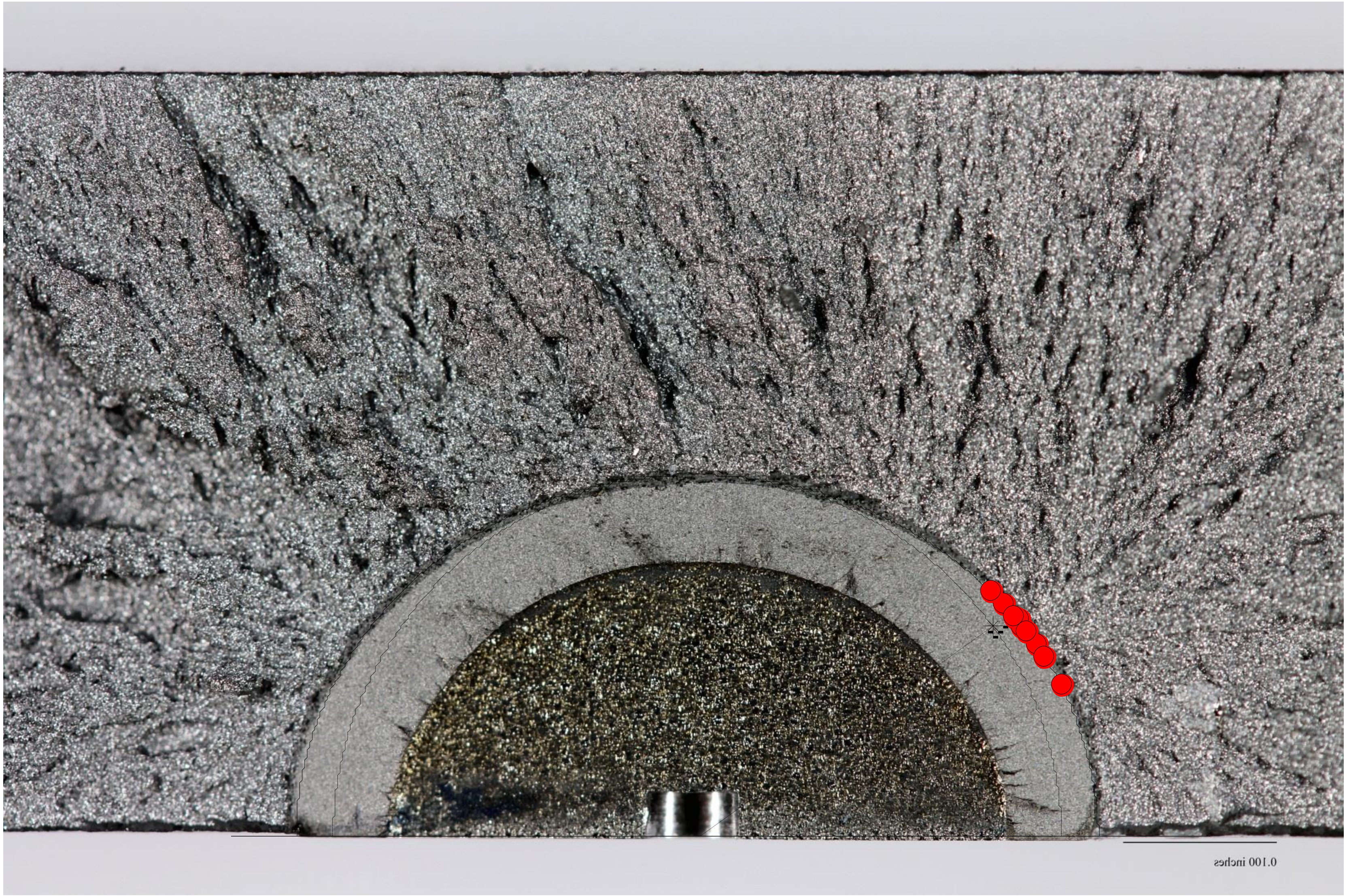
0.100 inches

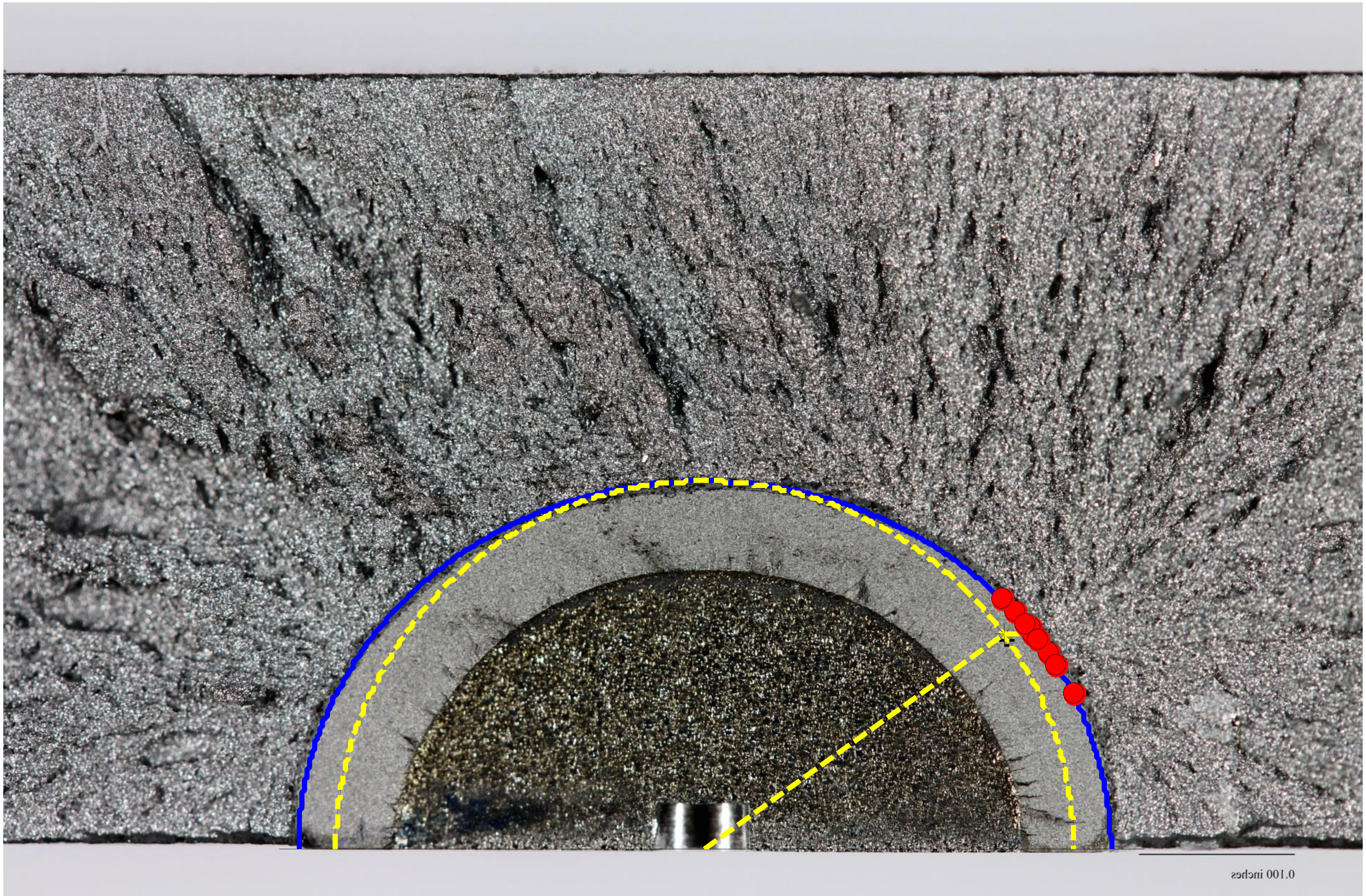
0.100 inches

Analytical Round Robin Phase II

Damage Tolerance Assessment Branch
MSFC Engineering Directorate

Elastic-Plastic Regime Assessment, E 2899 9.22

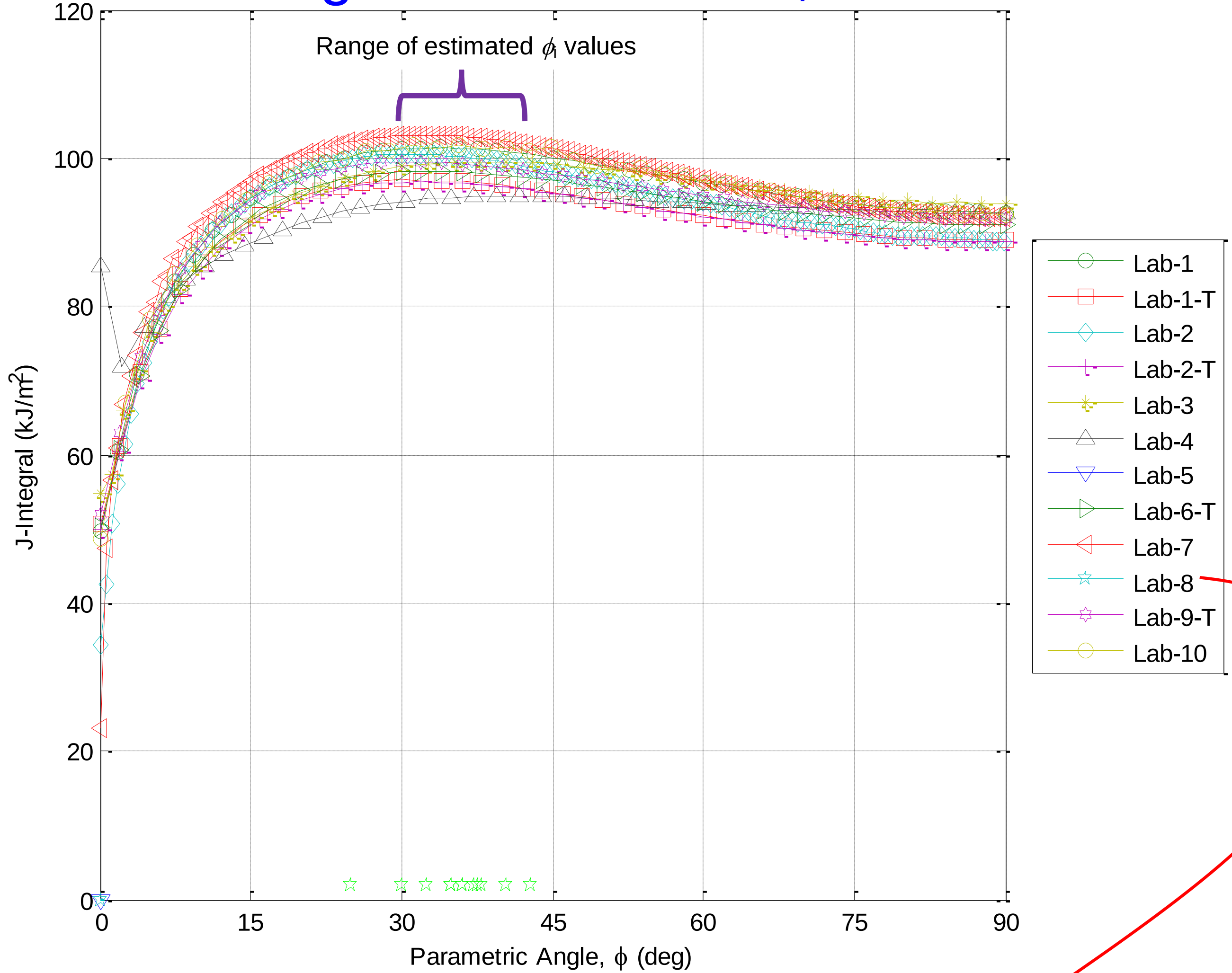

Note: Lab-8 reported J values were approx. ½ of the actual values likely due to a symmetry plane accounting error in the domain integral calculation. Therefore all Lab-8 values were multiplied by 2 for inclusion in the study.

Elastic-Plastic Regime Assessment, E 2899 9.22

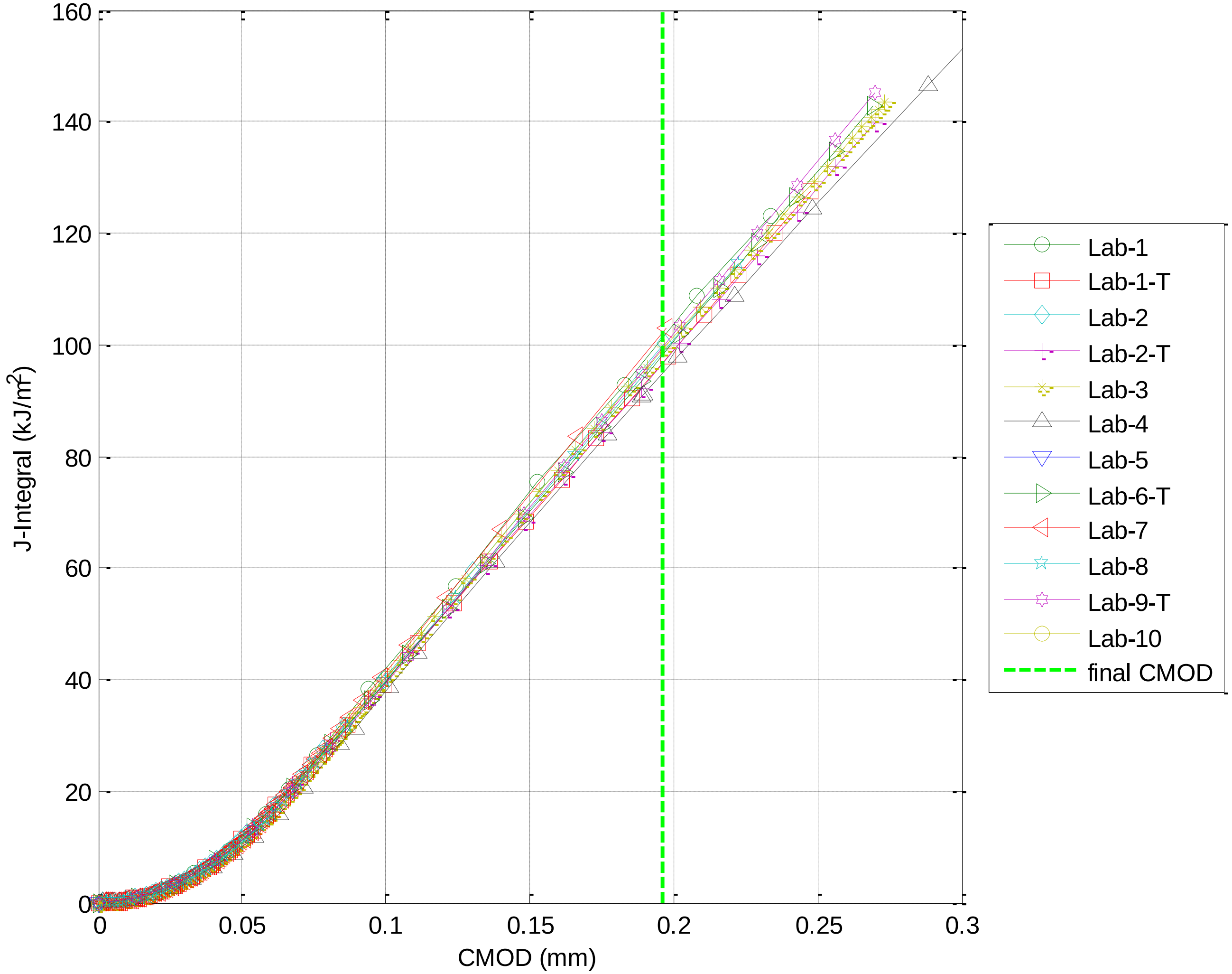

Elastic-Plastic Regime Assessment, E 2899 9.22

Range of J values at *CMOD*$_i$

Lab	J at ϕ_i
Lab-1	101.19
Lab-1-T	96.80
Lab-2	100.17
Lab-2-T	96.67
Lab-3	99.50
Lab-4	94.31
Lab-5	91.24
Lab-6-T	98.04
Lab-7	102.97
Lab-8	98.52
Lab-9-T	99.49
Lab-10	100.17

Max.	102.97
Avg.	98.26
Min.	91.24
Std. Dev.	3.17

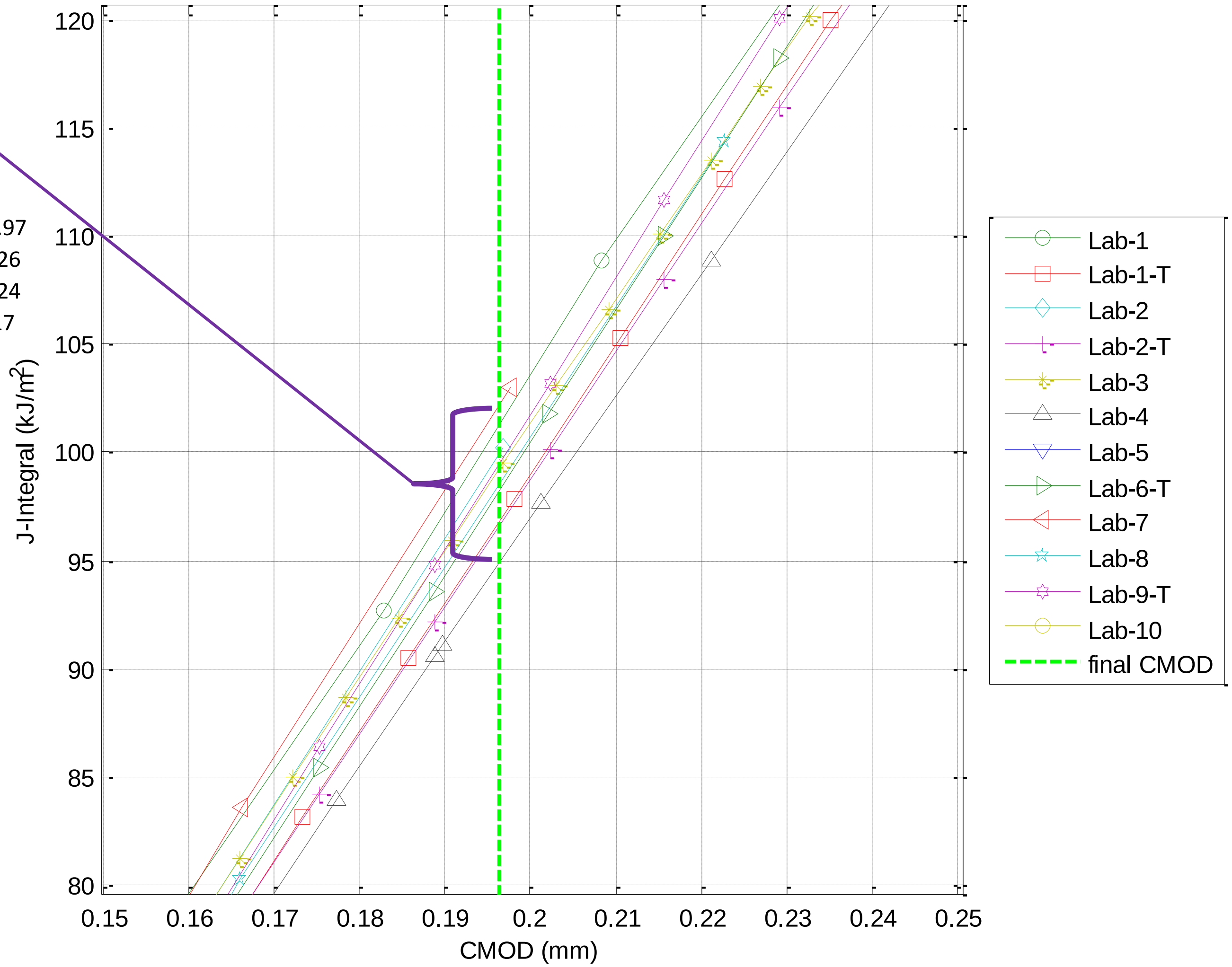

Elastic-Plastic Regime Assessment, E 2899 9.22

As reported values

Lab	J at ϕ_i
Lab-1	101.19
Lab-1-T	96.80
Lab-2	100.17
Lab-2-T	96.67
Lab-3	99.50
Lab-4	94.31
Lab-5	91.24
Lab-6-T	98.04
Lab-7	102.97
Lab-8	114.36
Lab-9-T	99.49
Lab-10	100.17

Max.	114.36
Avg.	99.58
Min.	91.24
Std. Dev.	5.63

Corrected Lab 8 value to $CMOD_i$

Lab	J at ϕ_i
Lab-1	101.19
Lab-1-T	96.80
Lab-2	100.17
Lab-2-T	96.67
Lab-3	99.50
Lab-4	94.31
Lab-5	91.24
Lab-6-T	98.04
Lab-7	102.97
Lab-8	98.52
Lab-9-T	99.49
Lab-10	100.17

Max.	102.97
Avg.	98.26
Min.	91.24
Std. Dev.	3.17

Elastic-Plastic Regime Assessment, E 2899 9.22

Crack front conditions and deformation regime assessment

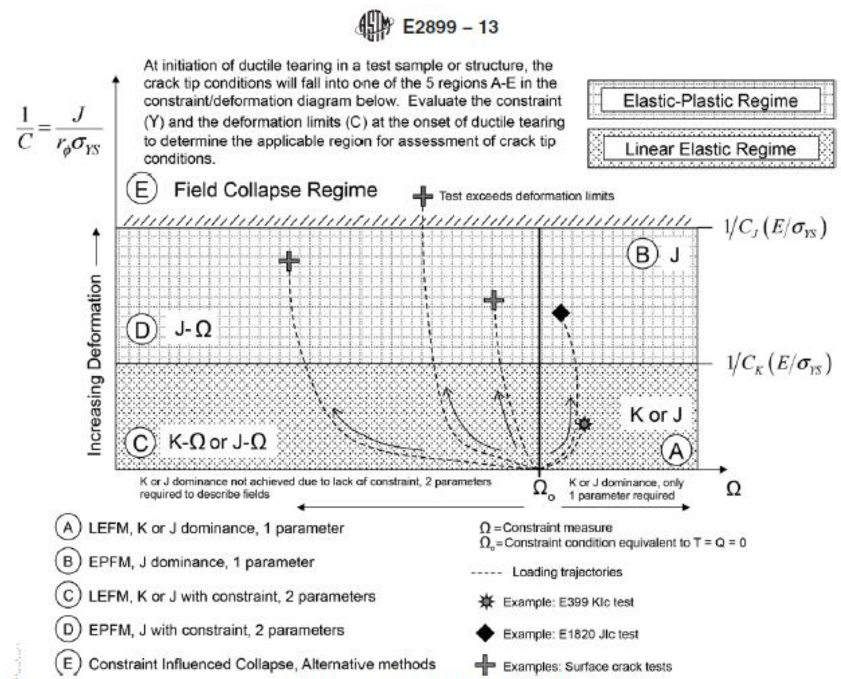

FIG. 8 Assessment of Crack Front Conditions

Two parameter, elastic-plastic regime

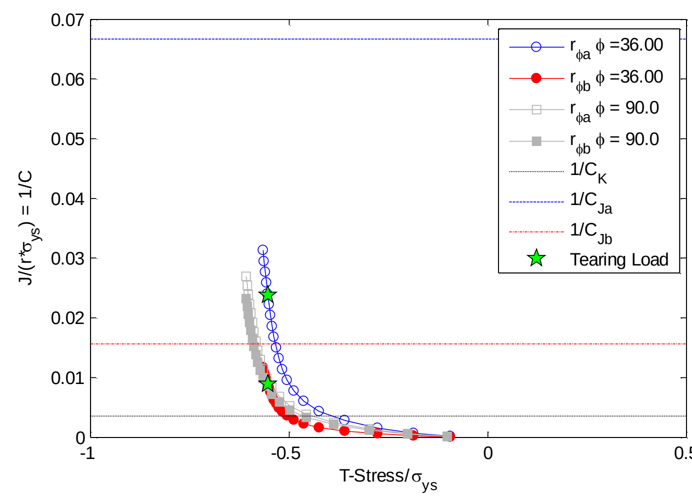

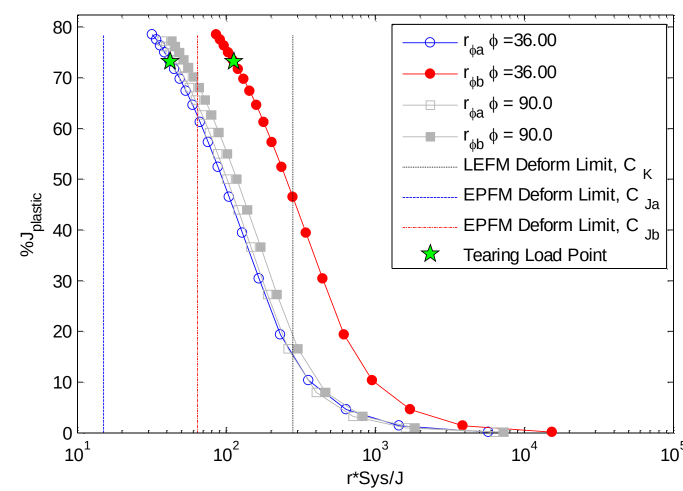

TASC Update

Damage Tolerance Assessment Branch
MSFC Engineering Directorate

What is TASC?

- TASC (Tool for Analysis of Surface Cracks) is a computer program created by NASA MSFC that enables easy computation of three-dimensional, nonlinear *J*-integral (fracture energy) solutions for surface cracked plates in tension.

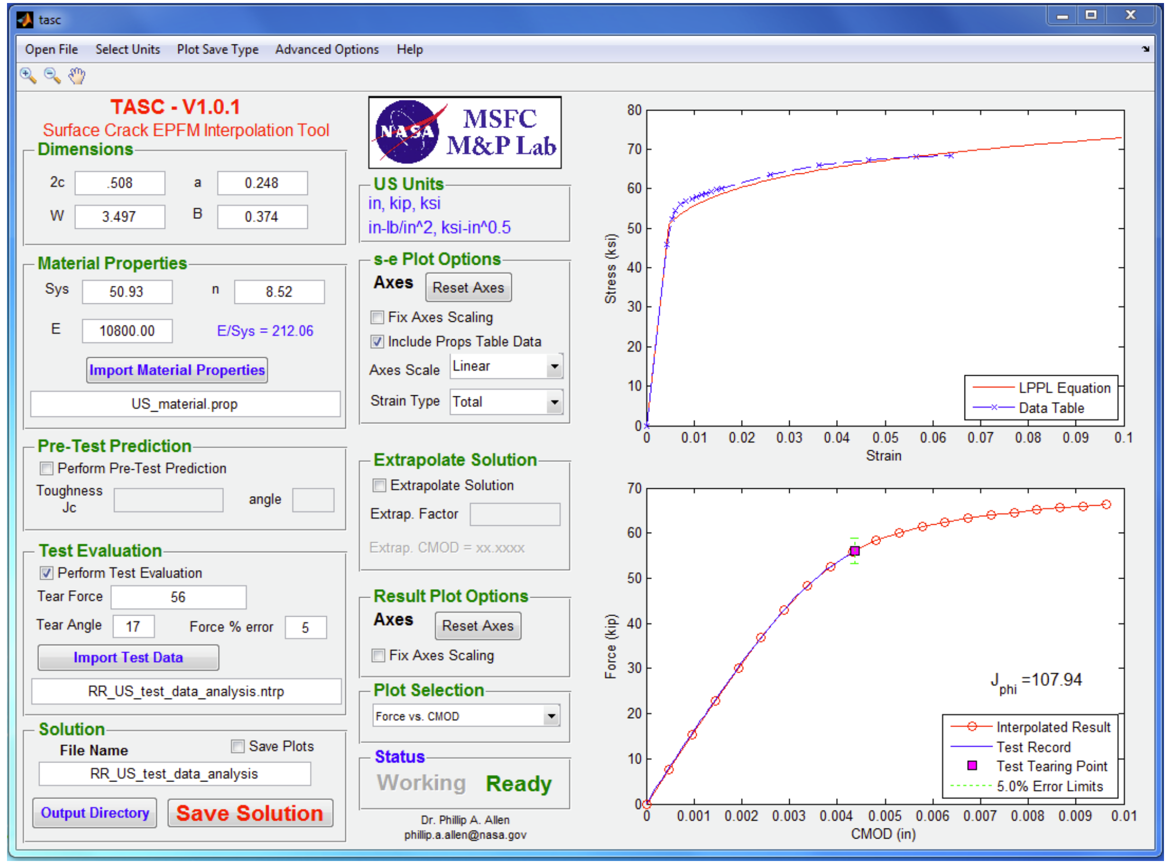

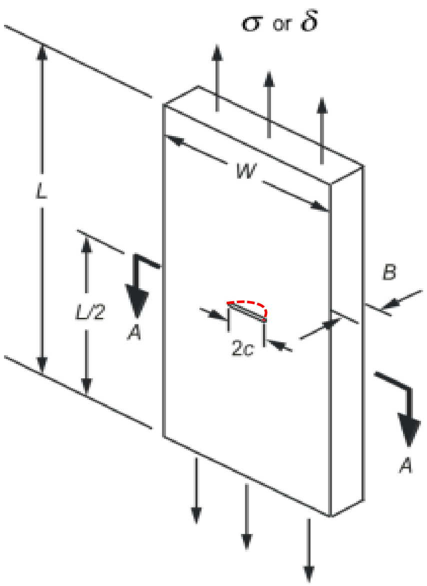

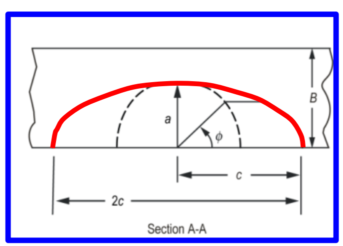

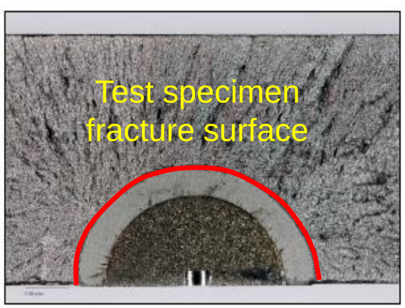

TASC Accessibility

- A TASC project page is hosted on Sourceforge.net at: https://sourceforge.net/projects/tascnasa/

- TASC can be freely downloaded in Windows® 64-bit standalone executable, Mac OS X® 64-bit standalone application, and MATLAB source file formats.

- No MATLAB license is required for the standalone executable versions license due to the royalty-free MATLAB Complier Runtime distribution provided with the program installation package, and no MATLAB experience is needed due to the simple GUI.

- TASC is released under the NASA Open Source Agreement Version 1.3.

- TASC was posted on Sourceforge on Jan. 28, 2014 and to date has had over 900 downloads

- TASC's background documentation:

  - Allen, P.A. and Wells, D.N., *Interpolation Methodology for Elastic-Plastic J-Integral Solutions for Surface Cracked Plates in Tension*, Engineering Fracture Mechanics 119, 2014, pp 173-201.
  - Allen, P.A. and Wells, D.N., *Applications of Automation Methods for Nonlinear Fracture Test Analysis, ASTM STP1571 on Sixth Symposium on Application of Automation Technology in Fatigue and Fracture Testing and Analysis*, Accepted for publication Nov. 2013.
  - Allen PA, Wells DN. *Elastic-Plastic J-Integral Solutions for Surface Cracks in Tension Using an Interpolation Methodology*. NASA MSFC; 2013. NASA/TM-2013-217480.

TASC Solution – US Units

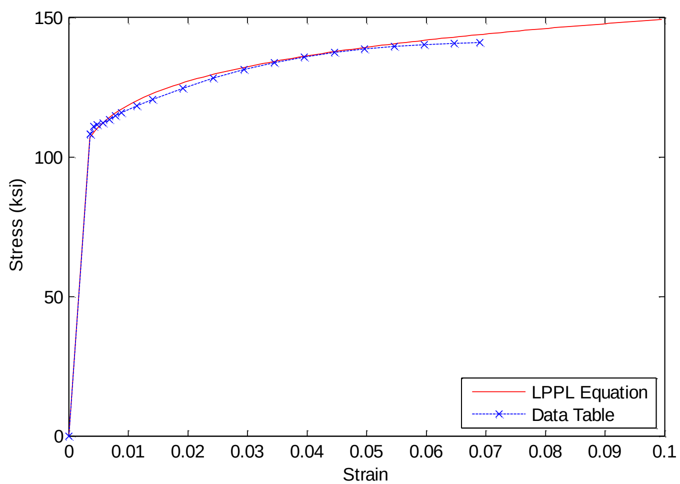

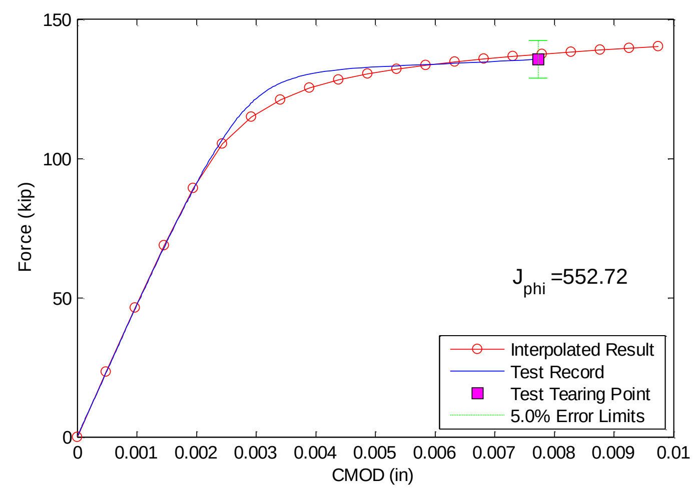

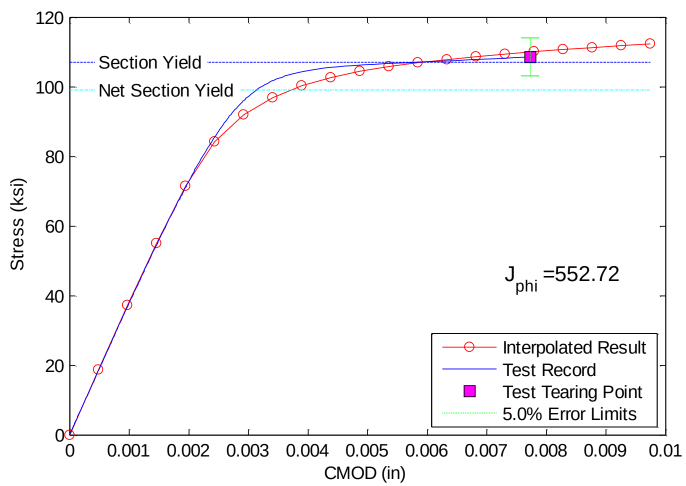

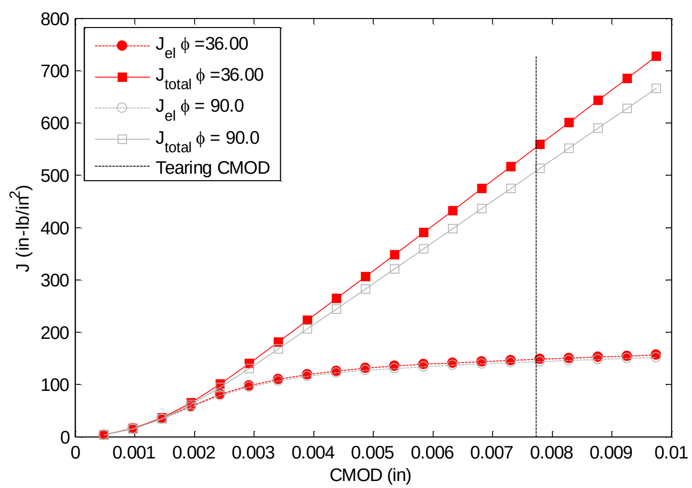

TASC Solution – US Units

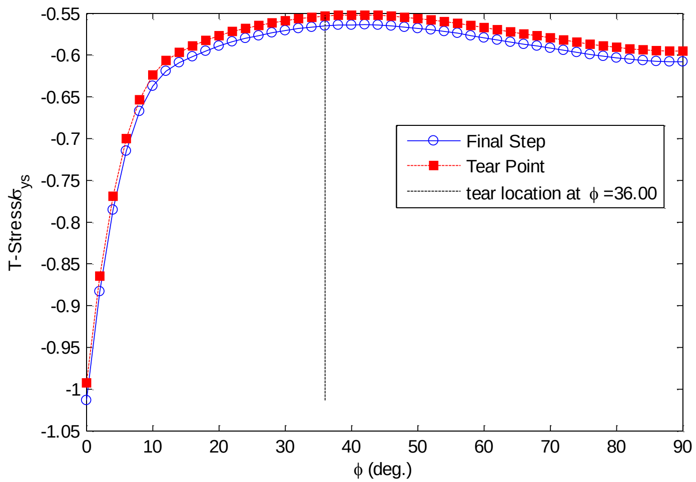

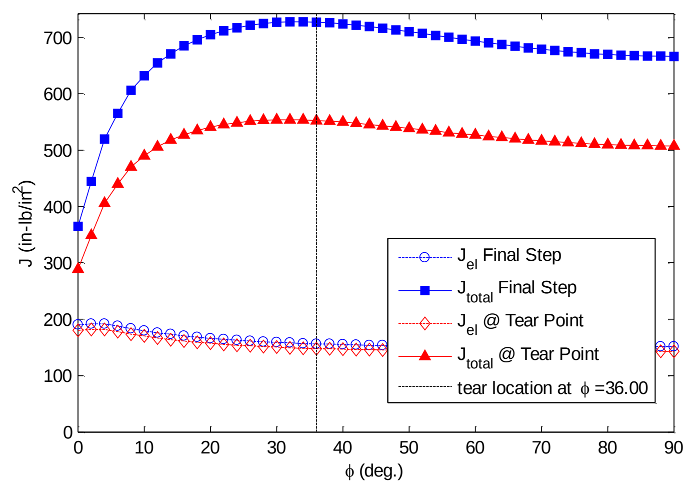

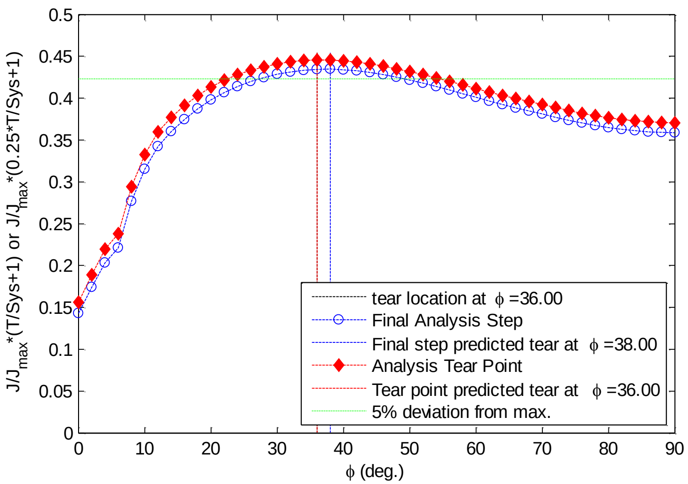

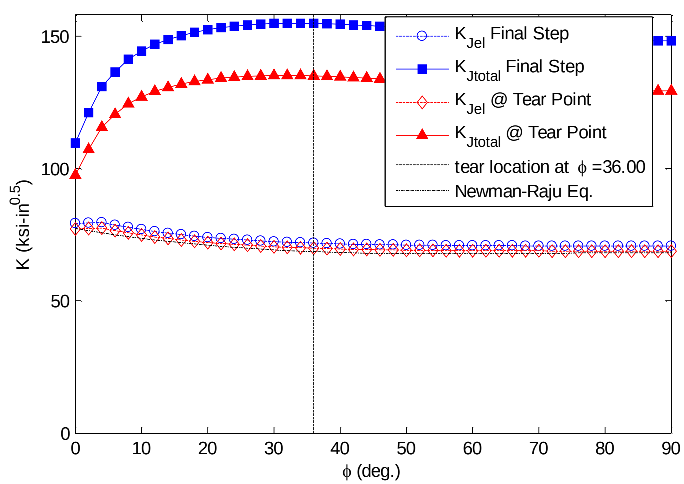

TASC Solution – US Units

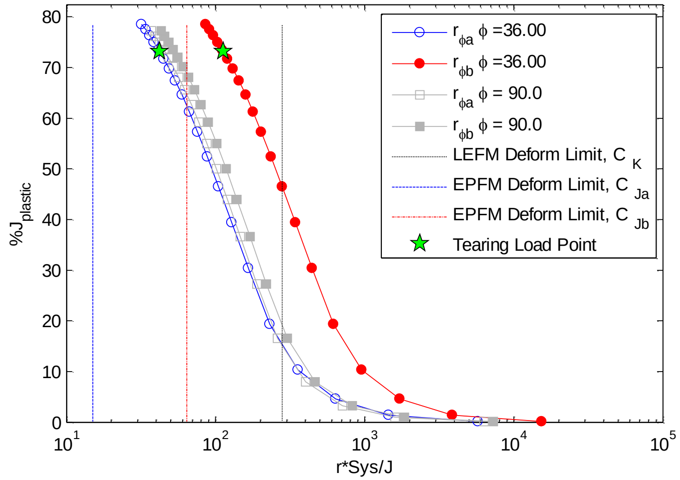

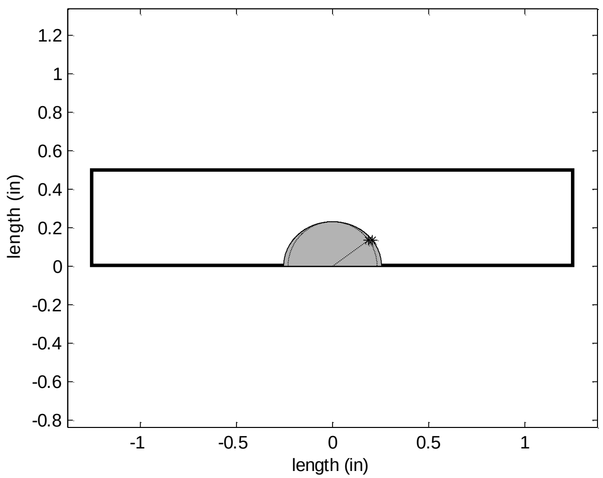

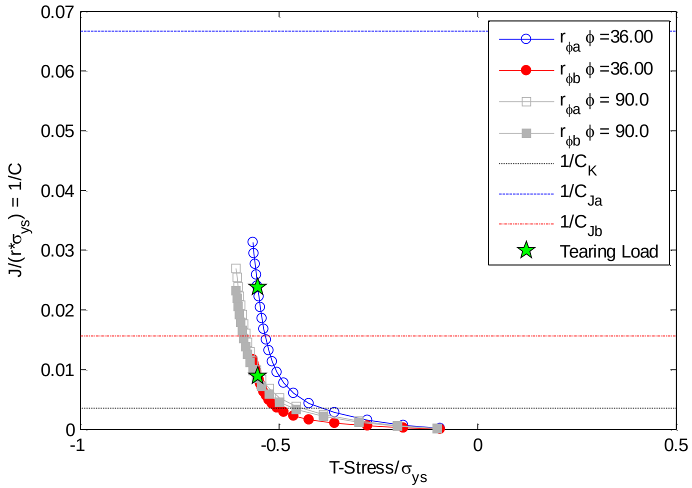

TASC Solution – SI Units

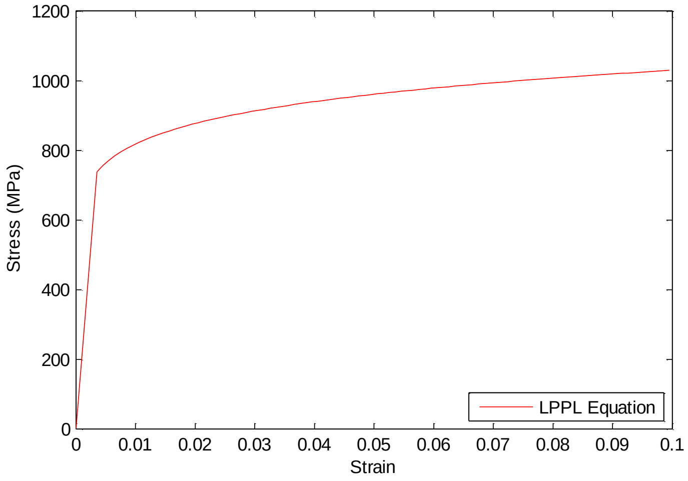

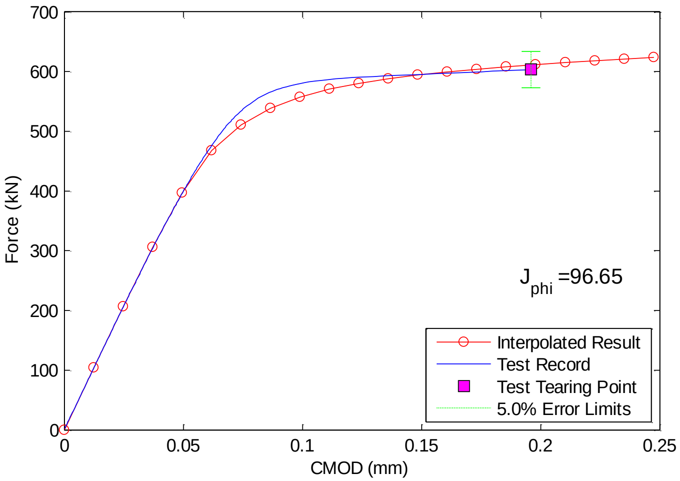

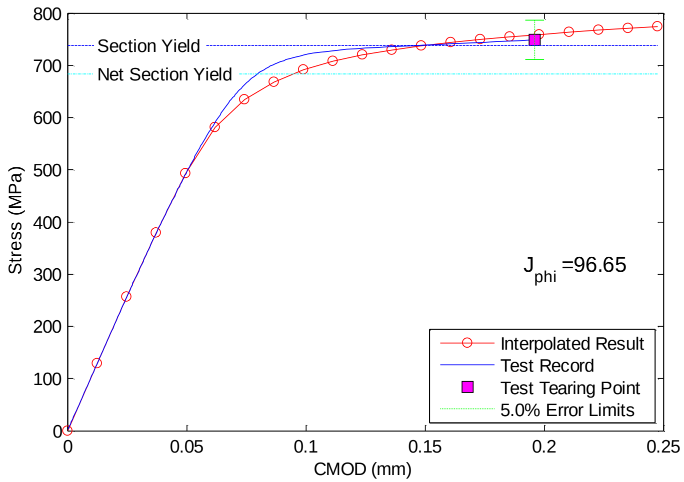

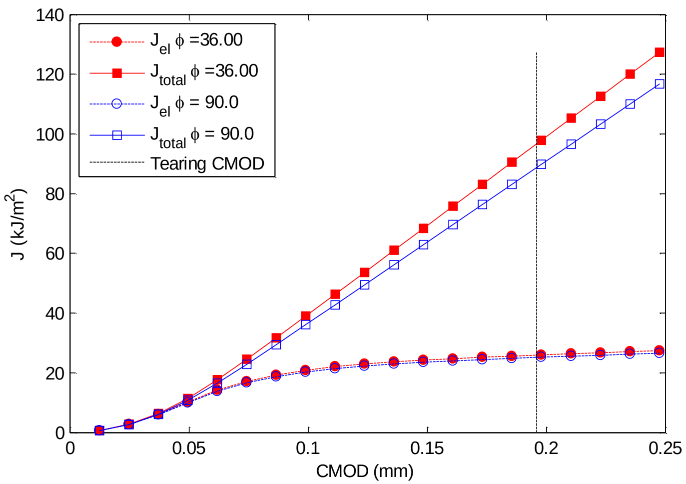

TASC Solution – SI Units

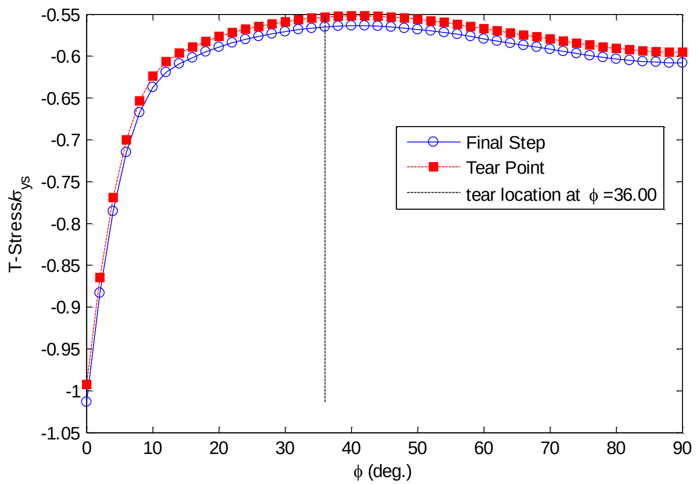

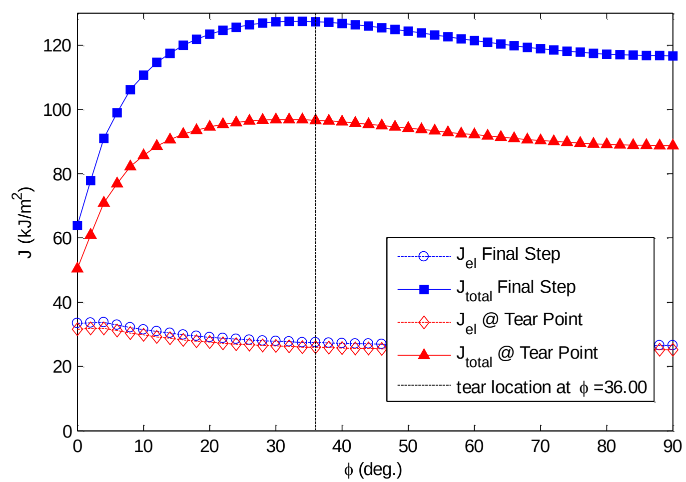

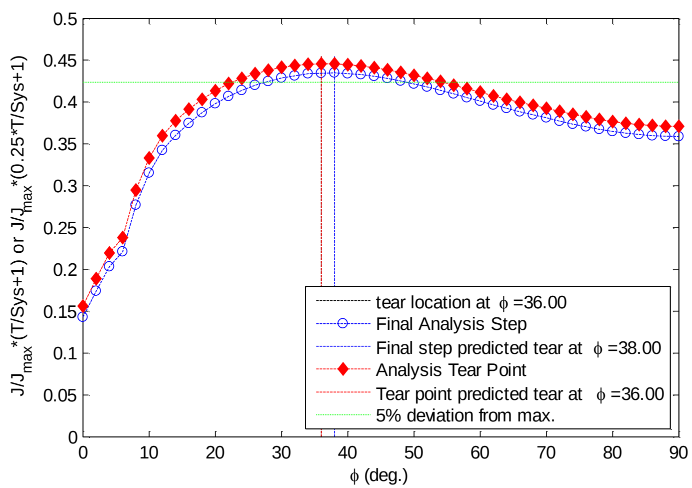

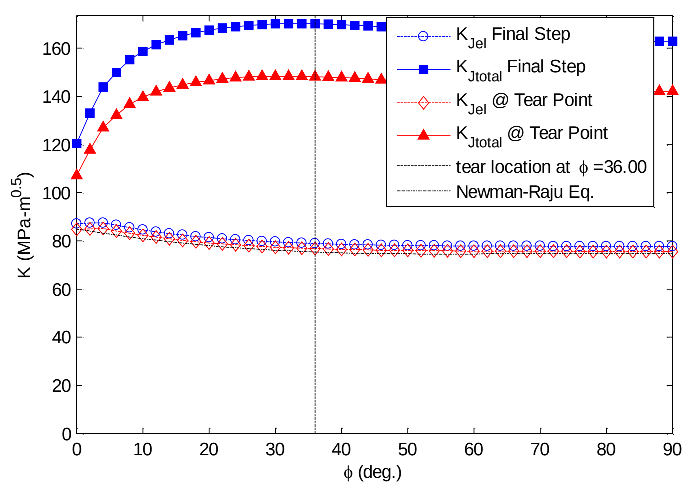

TASC Solution – SI Units

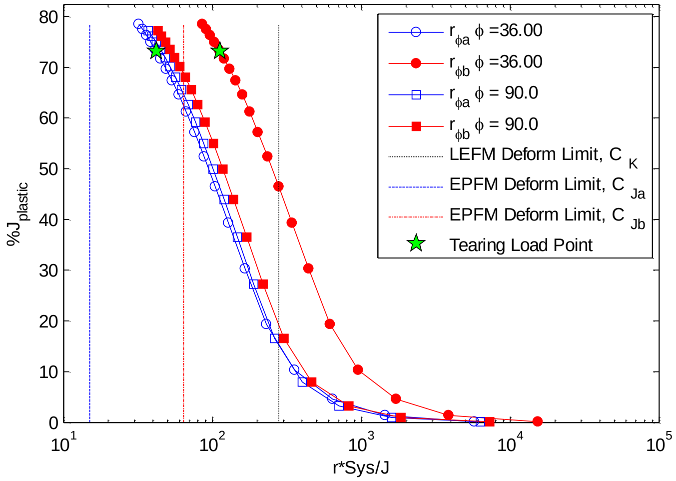

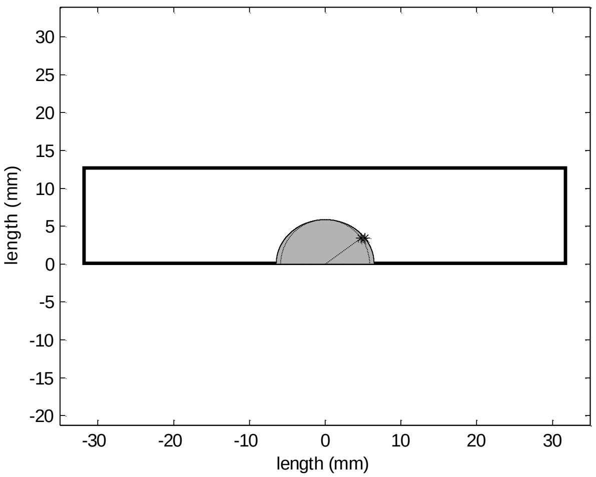

NIST
National Institute of Standards and Technology

Addition of SINTAP Lower-Tail Method as a Inhomogeneity Screening Criterion in ASTM E1921 (Appendices X5 and X6)

E. Lucon - NIST, Boulder CO (USA)

ASTM E08.07.06 Task Group on Ductile-to-Brittle Transition

San Antonio TX, 3rd May 2016

Proposed E1921 new Appendix X5 – *Inhomogeneity Screening Criterion*

- Purpose: establish whether a material is macroscopically homogeneous.
- Preamble: reference temperature $T_{0(step1)}$ calculated under the assumption of homogeneous material behaviour.
- Lower-Tail Estimation
  a. All K_{Jc} values exceeding

$$K_{CENS} = 30 + 70 \cdot \exp\left[0.019\left(T - T_{o(step1)}\right)\right]$$

  shall be censored and replaced by K_{CENS} $\rightarrow$ "upper-tail" censored data set.

  b. A revised reference temperature $T_{0(step2)}$ is obtained and compared to $T_{0(step1)}$.

  c. If $T_{0(step2)} > T_{0(step1)}$, repeat the upper-tail censoring procedure until a constant or maximum value of $T_{0(step2)}$ is obtained.

Proposed E1921 new Appendix
X5 – *Inhomogeneity Screening Criterion*

- <u>Screening Criterion</u>

a. The material is considered macroscopically <u>homogeneous</u> if:

$$T_{o(step2)} - T_{o(step1)} \le 1.44\sqrt{\frac{\beta^2}{r_{step1}}}$$

where β = sample size uncertainty factor (X4.2) and r_{step1} is the number of non-censored data used to calculate $T_{O(step1)}$.

b. The material is considered macroscopically <u>inhomogeneous</u> if:

$$T_{o(step2)} - T_{o(step1)} > 1.44\sqrt{\frac{\beta^2}{r_{step1}}}$$

and the data set shall be analyzed using the procedures of Appendix X6 (*Treatment of data sets from macroscopically inhomogeneous materials*).

Proposed E1921 new Appendix X5 – *Inhomogeneity Screening Criterion*

Additional Statements

a) The screening criterion works well for materials with multimodal distribution of macroscopic inhomogeneities and bimodal distribution with approximately equal contents of brittle and ductile constituents.

b) Bimodal materials with a small portion of brittle constituent cannot be assessed by the screening criterion, unless at least 18 K_{Jc} values are available.

c) When a material results macroscopically inhomogeneous based on the screening criterion, it cannot be predicted whether its distribution is bimodal or multimodal.

Appendix X6 - *Treatment of data sets from macroscopically inhomogeneous materials*

- For small data sets (N < 18), SINTAP provides a conservative estimate of T_o.

SINTAP estimation procedure

1) Determine values $T_{o(step1)}$ and $T_{o(step2)}$ according to X5.
2) For every non-censored $K_{Jc,i}$ value, calculate the single-data reference temperature:

$$T_{o,i} = \frac{1}{0.019} \ln \left[\frac{\left(K_{Jc,i} - 20\right)\left(\frac{N}{\ln 2}\right)^{0.25} - 11}{77} \right]$$

3) The maximum value of T_o for the data set, $T_{o(max)}$, is:

$$T_{o(max)} = \max \left| T_i - T_{o,i} \right|$$

Appendix X6 - *Treatment of data sets from macroscopically inhomogeneous materials*

4) If: $T_{o(max)} - T_{o(step2)} > 8\ ^{\circ}\mathrm{C}$

$T_{o(max)}$ shall be taken as the reference temperature for the test material.

5) If: $T_{o(max)} - T_{o(step2)} \leq 8\ ^{\circ}\mathrm{C}$

a reliable T_o cannot be estimated using SINTAP and the number of tests shall be increased to a minimum of 18.

References

- Wallin, K., Nevasmaa, P., Laukkanen A., and Planman, T., "Master Curve analysis of inhomogeneous ferritic steels," *Engineering Fracture Mechanics,* Volume 71, Issues 16-17, November 2004, pp. 2329-2346.
- Wallin, K., "Inhomogeneity Screening Criterion for the ASTM E1921 T_o Estimate Based on the SINTAP Lower-Tail Methodology," *Journal of Testing and Evaluation*, Vol. 40, No. 6, 2012.

INHOMOGENEITY SCREENING CRITERION FOR THE ASTM E1921 T_0 ESTIMATE BASED ON THE SINTAP LOWER-TAIL METHODOLOGY

ASTM E08.07.06 San Antonio 05/03/2016

Kim Wallin

Background

- ASTM E1921 is based on a theoretical scatter and size effect assumption and makes use of a maximum likelihood estimation method to determine the fracture toughness transition temperature T_0.
- The estimation method in E1921 is valid only for macroscopically homogeneous steels.
- If the steel is inhomogeneous, the maximum likelihood method applied in E1921 becomes unreliable.
- A simple screening criterion, based on the SINTAP lower-tail estimation method, is proposed
- The efficiency and limitations of the criterion is shown for a variety of different types of inhomogeneity

Inhomogeneous Master Curve analysis

- Bimodal MC $$P_f = 1 - p_a \cdot \exp\left\{-\left(\frac{K_{JC} - K_{min}}{K_{0a} - K_{min}}\right)^4\right\} - (1 - p_a) \cdot \exp\left\{-\left(\frac{K_{JC} - K_{min}}{K_{0b} - K_{min}}\right)^4\right\}$$

- Multimodal MM $$f\left(T_{0i}\right) = \frac{e^{-\frac{\left(T_{0i} - T_{0ave}\right)^2}{2 \cdot \sigma T_0^2}}}{\sigma T_0 \cdot \sqrt{2\pi}}$$

Inhomogeneous Master Curve analysis

- The use of the inhomogeneity analysis methods require, a minimum of 20 to 30 test results
- The standard assessment only requires between 6…9 test results to provide a valid T_0 estimate.
- This raises the problem of how to decide whether a material is homogeneous or heterogeneous.
- A solution for this problem would be the use of a simple inhomogeneity screening criterion to decide if the material is homogeneous or inhomogeneous.

Screening criterion

- It should be such that the probability of falsely recognizing a homogeneous material as inhomogeneous is sufficiently small.
- It should also be able to recognize materials with a significant inhomogeneity with a high probability.
- At the same time, the probability that a T_0 value resulting from an inhomogeneous material, falsely recognized as homogeneous, is not significantly un-conservative with respect to a T_0 value that would be descriptive of the material.

T_0 value descriptive of an inhomogeneous material

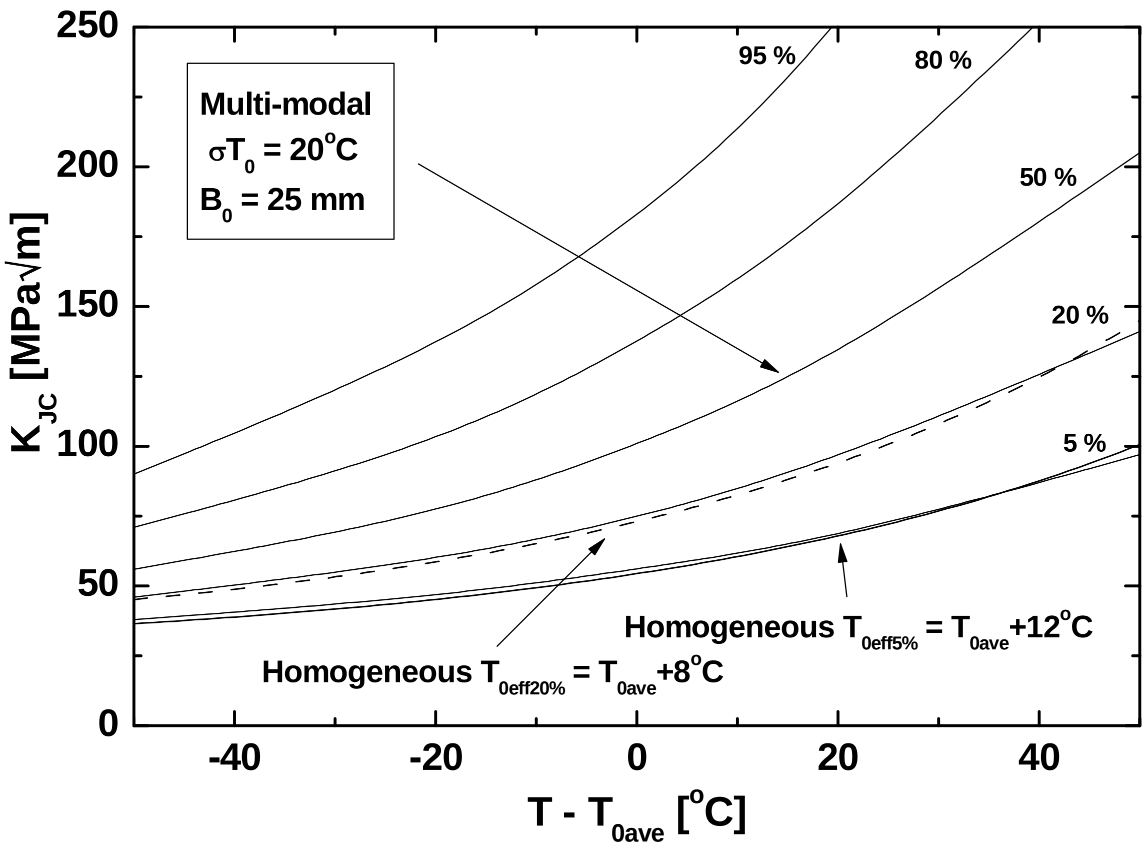

Type	ΔT_{0ab} °C	p_a	σT_0 °C	T_{0ref}	$T_{01921}-T_{0ref}$ °C	$T_{0eff20\%}-T_{0ref}$ °C	$T_{0eff5\%}-T_{0ref}$ °C
Homog.	0	0	0	T_0	0-1	0	0
BM	20	0.5		T_{0b}	7	12	13
BM	20	0.25		T_{0b}	3	7	8
BM	20	0.1		T_{0b}	1	3	3
BM	40	0.5		T_{0b}	9	29	30
BM	40	0.25		T_{0b}	3	18	19
BM	40	0.1		T_{0b}	1	7	11
BM	60	0.5		T_{0b}	11	47	49
BM	60	0.25		T_{0b}	5	32	38
BM	60	0.1		T_{0b}	1	9	24
MM			10	T_{0ave}	-4	4	5
MM			20	T_{0ave}	-15	8	12
MM			30	T_{0ave}	-25	14	20
MM			40	T_{0ave}	-37	21	30

The SINTAP Lower-Tail Analysis Method

- The SINTAP method is intended for the analysis of small data sets, where the uncertainty related to the data set size becomes an important factor.
- It is intended to give representative lower bound estimates suitable for structural integrity analysis purposes.
- It is not intended to be used e.g. to determine transition temperature shifts or in other cases where the average fracture toughness is of interest.
- For a homogeneous material, the SINTAP method provides on the average a 10% lower fracture toughness estimate than the standard Master Curve.
- The SINTAP lower-tail analysis contains three steps.

SINTAP Step 1

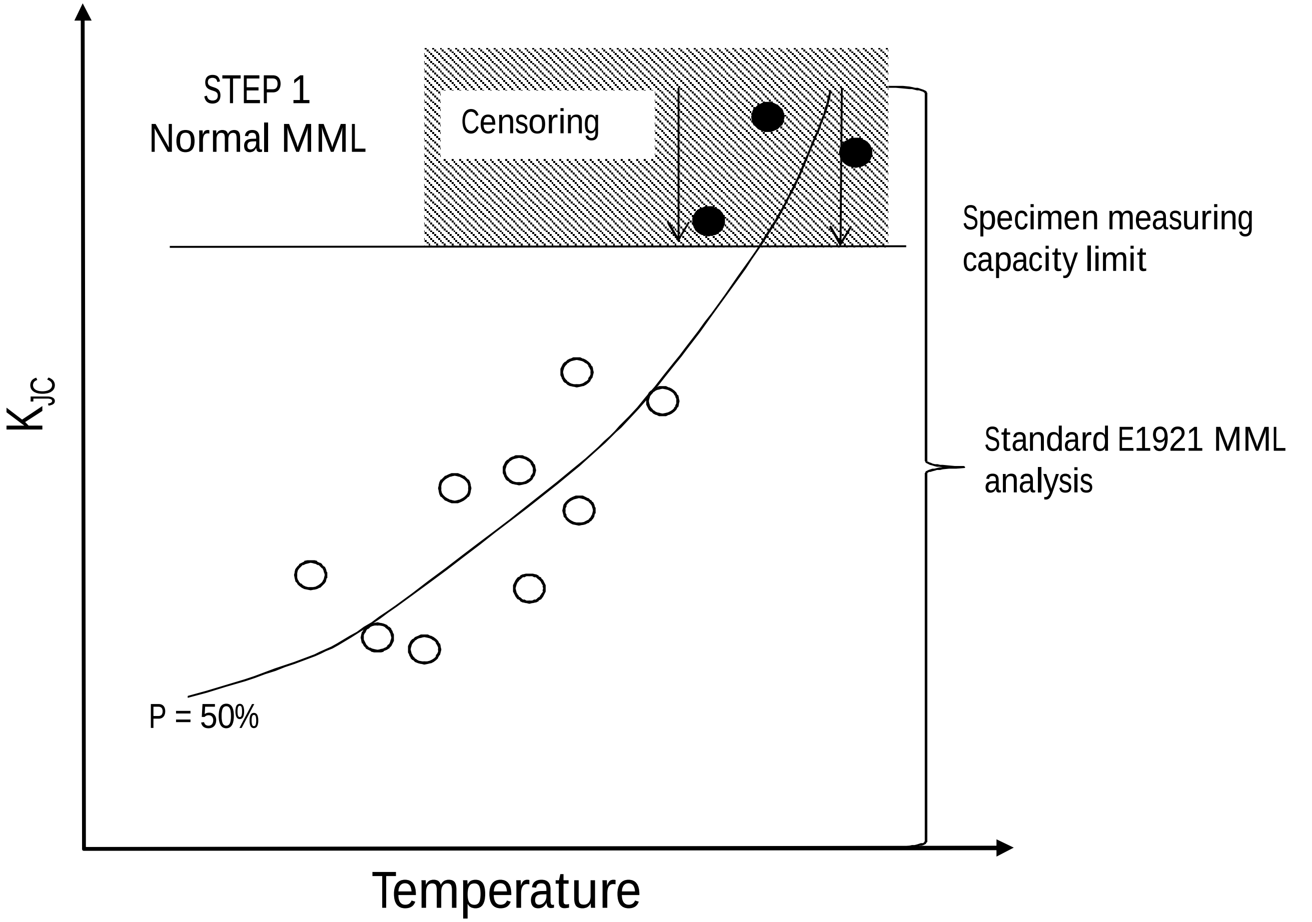

SINTAP Step 2

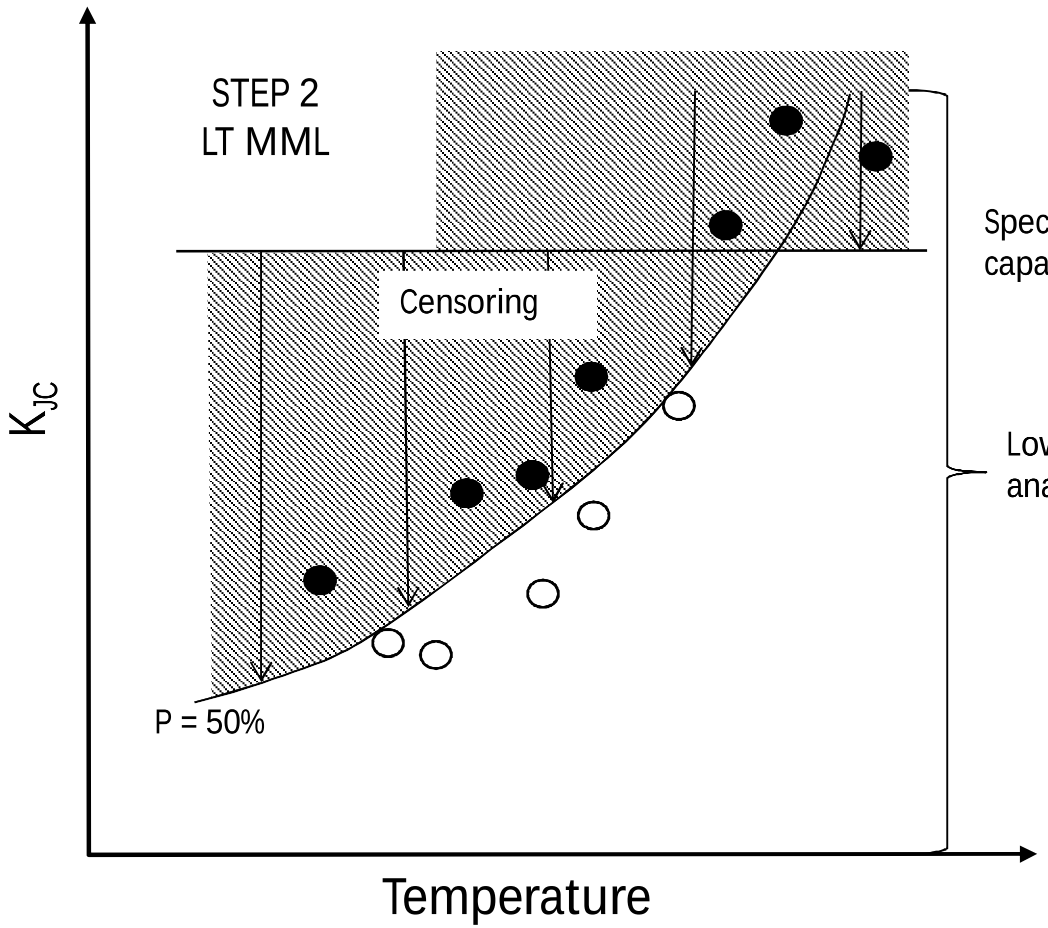

SINTAP Step 3

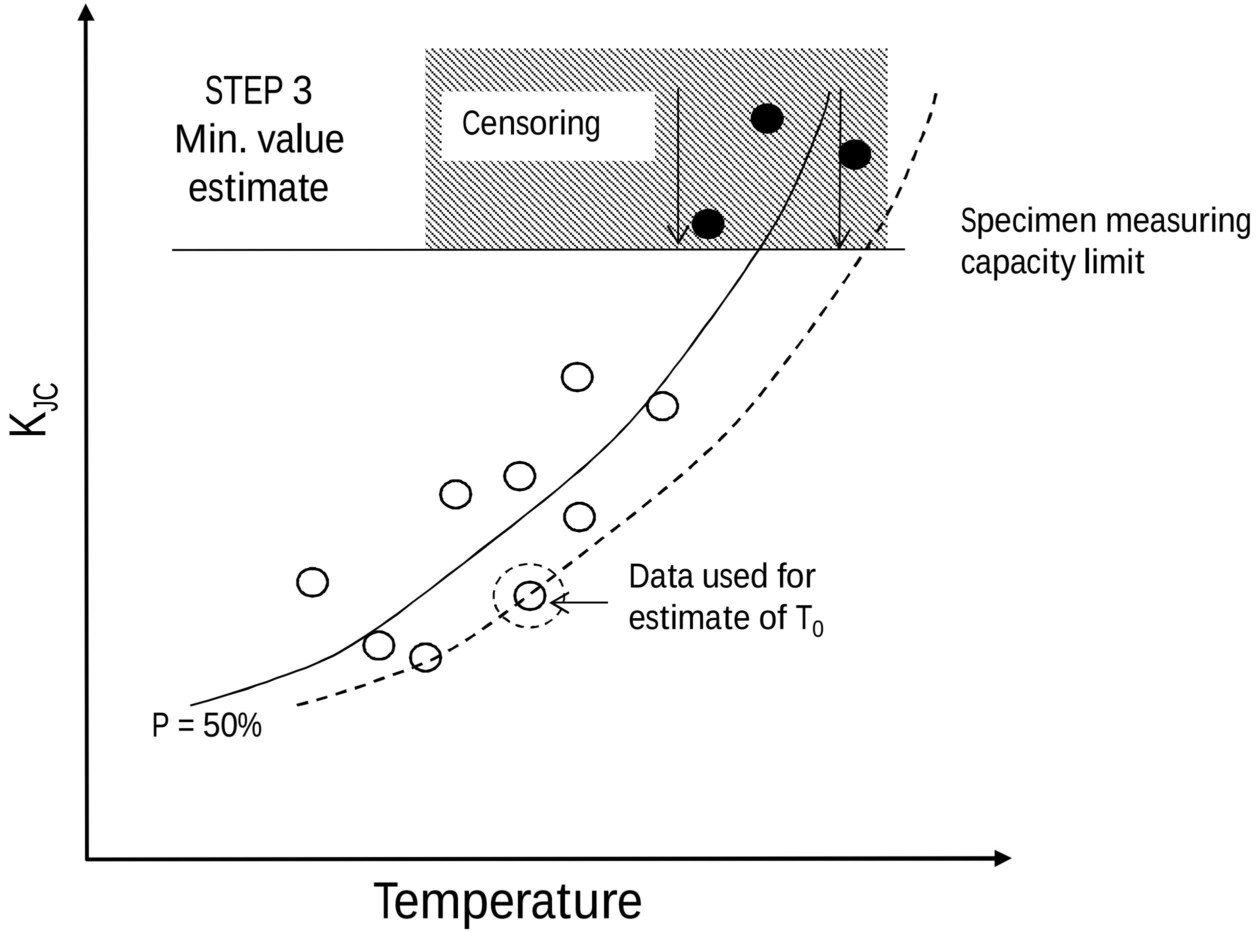

Step 3 is employed when the number of tests to be analysed is between 3 and 9

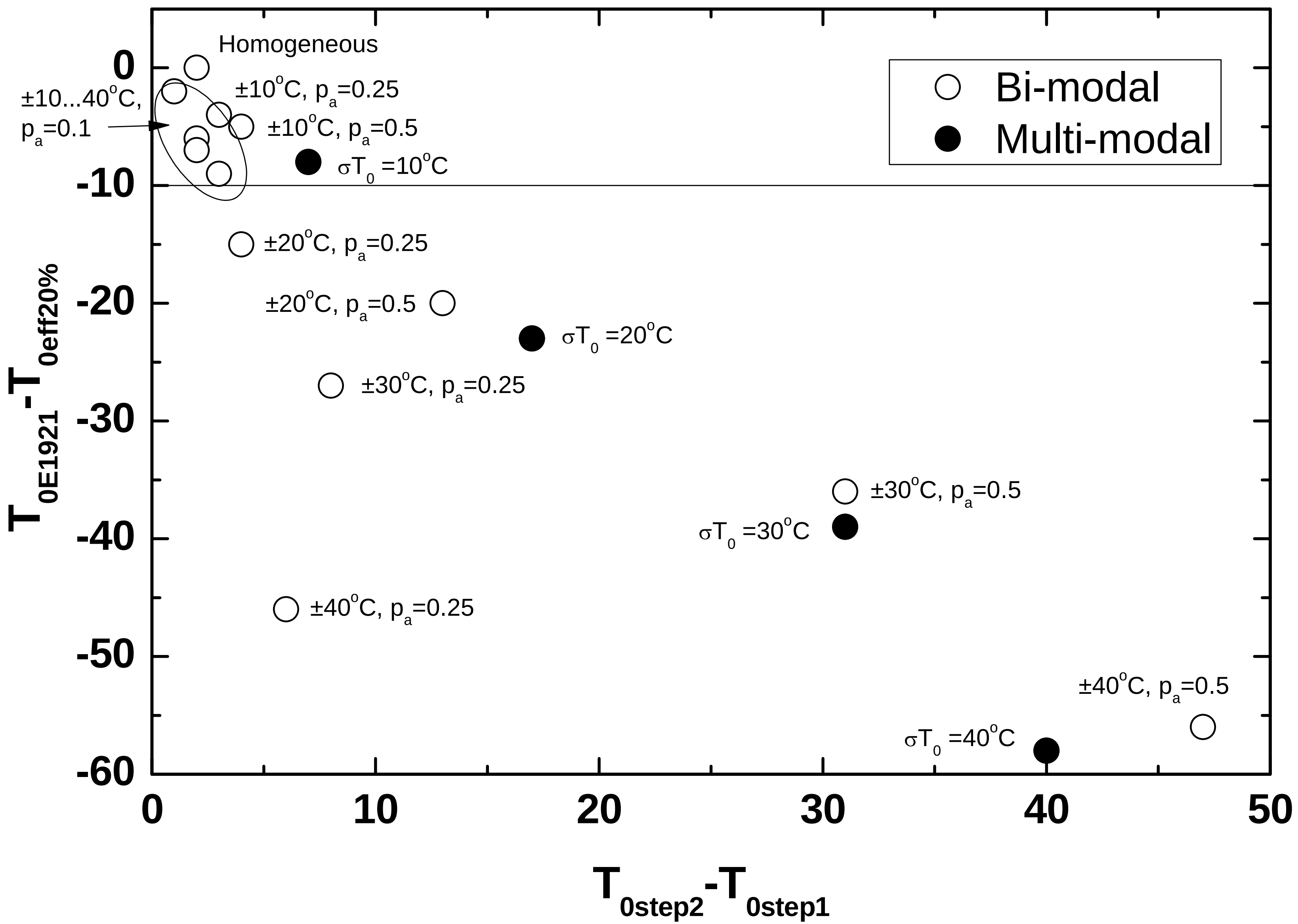
Homogeneous
±10...40°C, p_a=0.1
±10°C, p_a=0.25
±10°C, p_a=0.5
σT_0 =10°C
±20°C, p_a=0.25
±20°C, p_a=0.5
σT_0 =20°C
±30°C, p_a=0.25
±30°C, p_a=0.5
σT_0 =30°C
±40°C, p_a=0.25
±40°C, p_a=0.5
σT_0 =40°C
Bi-modal
Multi-modal
T_0E1921-T_0eff20%
T_0step2-T_0step1
0
-10
-20
-30
-40
-50
-60
0
10
20
30
40
50

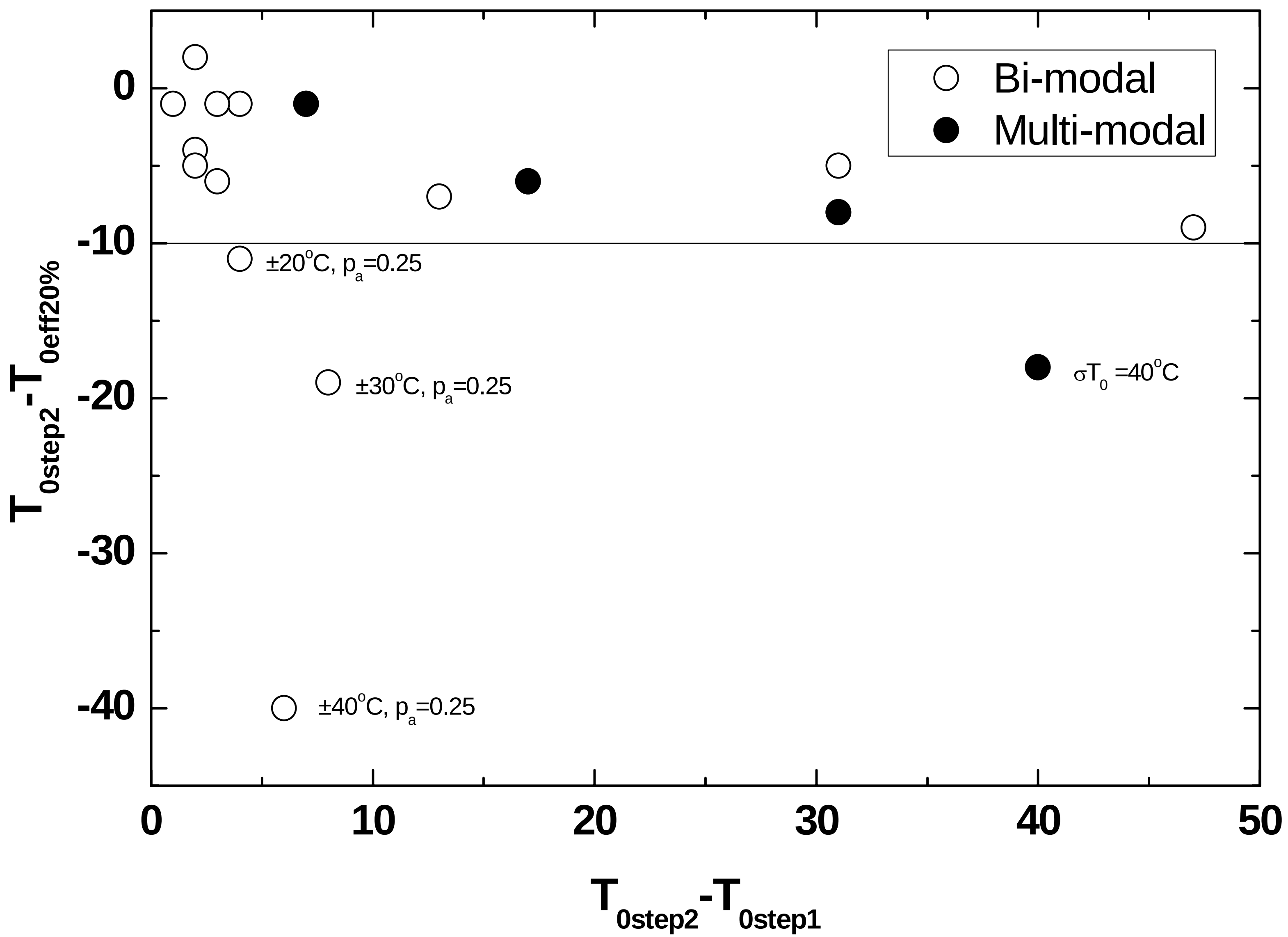
Bi-modal
Multi-modal
±20°C, pa=0.25
±30°C, pa=0.25
±40°C, pa=0.25
σT0 =40°C
T0step2-T0eff20%
T0step2-T0step1
0
-10
-20
-30
-40
0
10
20
30
40
50

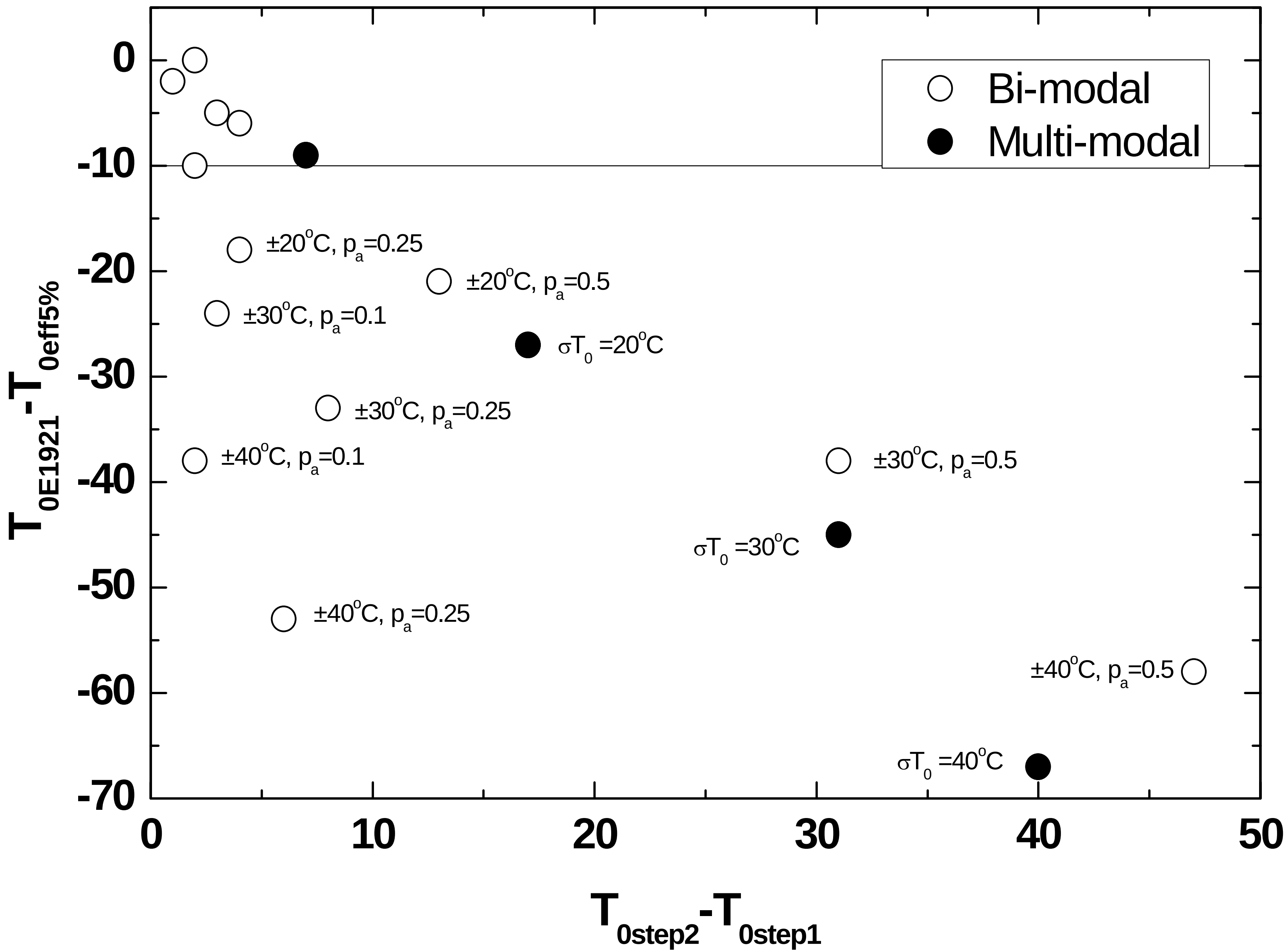

Bi-modal
Multi-modal
±20°C, pa=0.25
±20°C, pa=0.5
±30°C, pa=0.1
σT0 =20°C
±30°C, pa=0.25
±40°C, pa=0.1
±30°C, pa=0.5
σT0 =30°C
±40°C, pa=0.25
±40°C, pa=0.5
σT0 =40°C
T0E1921-T0eff5%
T0step2-T0step1
0
-10
-20
-30
-40
-50
-60
-70
0
10
20
30
40
50

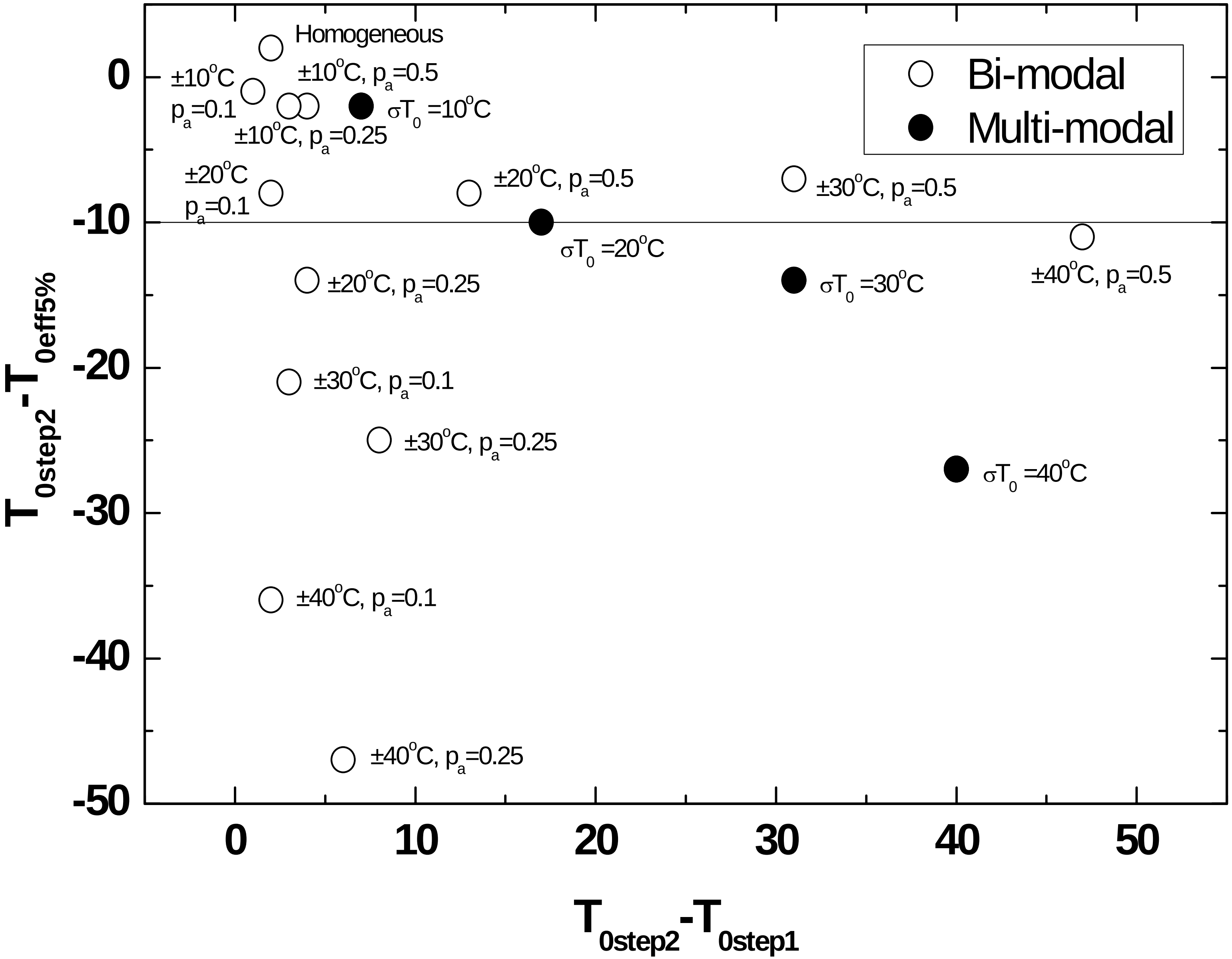

Homogeneous
±10°C
p_a=0.1
±10°C, p_a=0.5
±10°C, p_a=0.25
σT_0 =10°C
±20°C
p_a=0.1
±20°C, p_a=0.5
σT_0 =20°C
±30°C, p_a=0.5
σT_0 =30°C
±40°C, p_a=0.5
±20°C, p_a=0.25
±30°C, p_a=0.1
±30°C, p_a=0.25
σT_0 =40°C
±40°C, p_a=0.1
±40°C, p_a=0.25
Bi-modal
Multi-modal
0
-10
-20
-30
-40
-50
0
10
20
30
40
50
T0step2-T0eff5%
T0step2-T0step1

Inhomogeneity Screening Criterion

- The inhomogeneity screening criterion is based on a comparison of the difference between the SINTAP step 2 T_0 and the standard ASTM E1921 T_0 (or SINTAP step 1).
- ASTM E1921 contains an expression for margin adjustment of T_0 accounting for the uncertainty in T_0 that is associated with the use of only a few specimens to establish T_0. The margin expression for an 85 % two-tail confidence has the form

$$\Delta T_0 = \sigma\left(Z_{85}\right) = 1.44 \cdot \sqrt{\frac{\beta^2}{r} + \sigma_{\exp}^2}$$

- The screening criterion becomes simply as

$$T_{0step2} - T_{0step1} \leq 1.44 \cdot \sqrt{\frac{\beta^2}{r}} \Rightarrow \text{homogenous}$$

$$T_{0step2} - T_{0step1} > 1.44 \cdot \sqrt{\frac{\beta^2}{r}} \Rightarrow \text{inhomogenous}$$

Verification

- The screening criterion was tested on different types of inhomogeneities, using Monte Carlo simulation.
- This consisted of defining different distributions with varying amounts of inhomogeneity and randomly generating virtual fracture toughness values from them.
- Nine evenly spaced temperatures covering ± 40°C from T_{0ave} or from $(T_{0a}+T_{0b})/2$ were used.
- Two different realistic data set sizes were examined, n = 9 and n = 18, so that the smaller set had one value per temperature and the larges set had two.
- The smaller data set was selected because it has a realistic size and is the largest data set, still making use of step 3 in the SINTAP method.
- The larger data set represents a size that is realistic, if some inhomogeneity in the material is expected.

Probability of a false screening

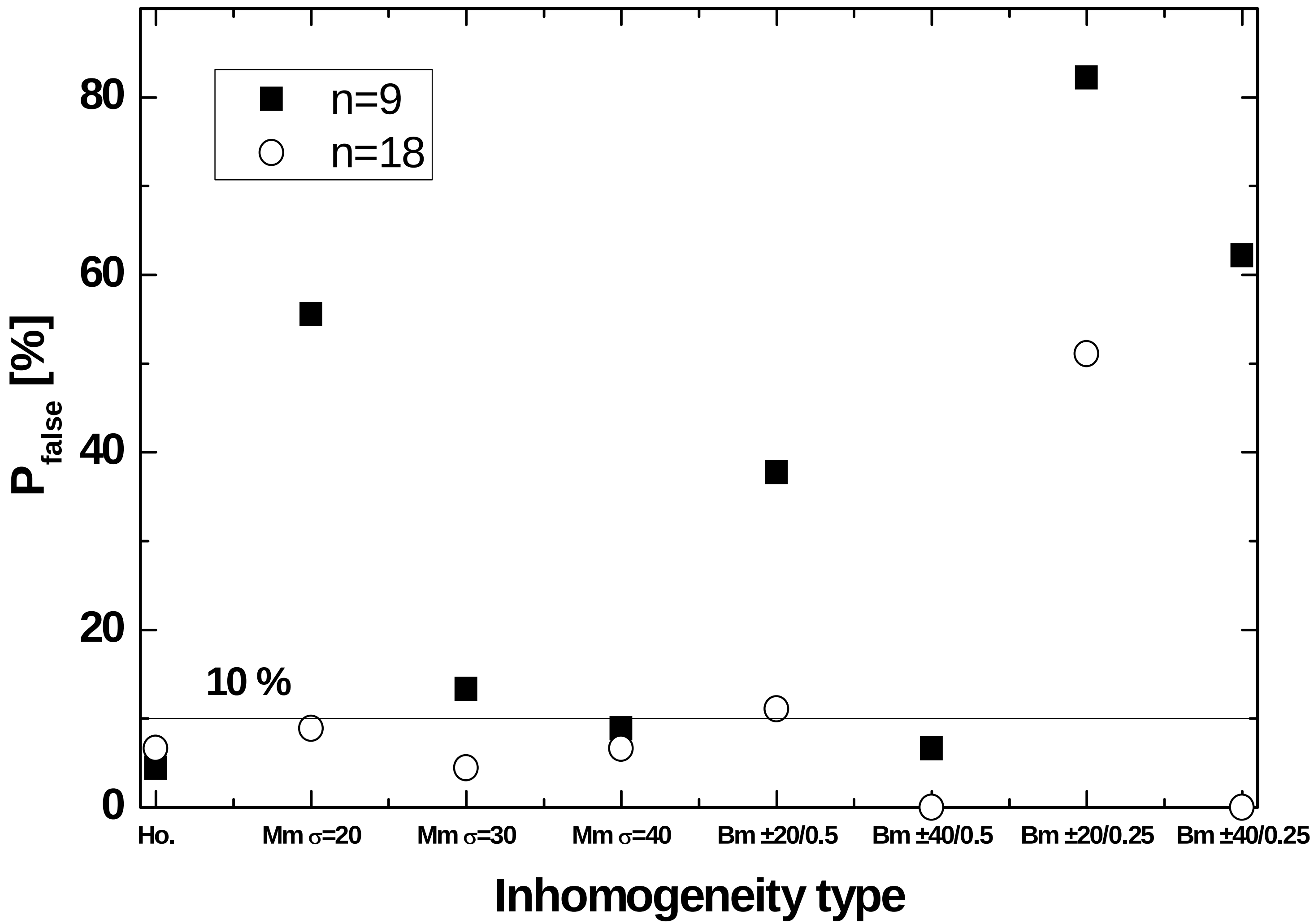

Probability of unconservative false screening

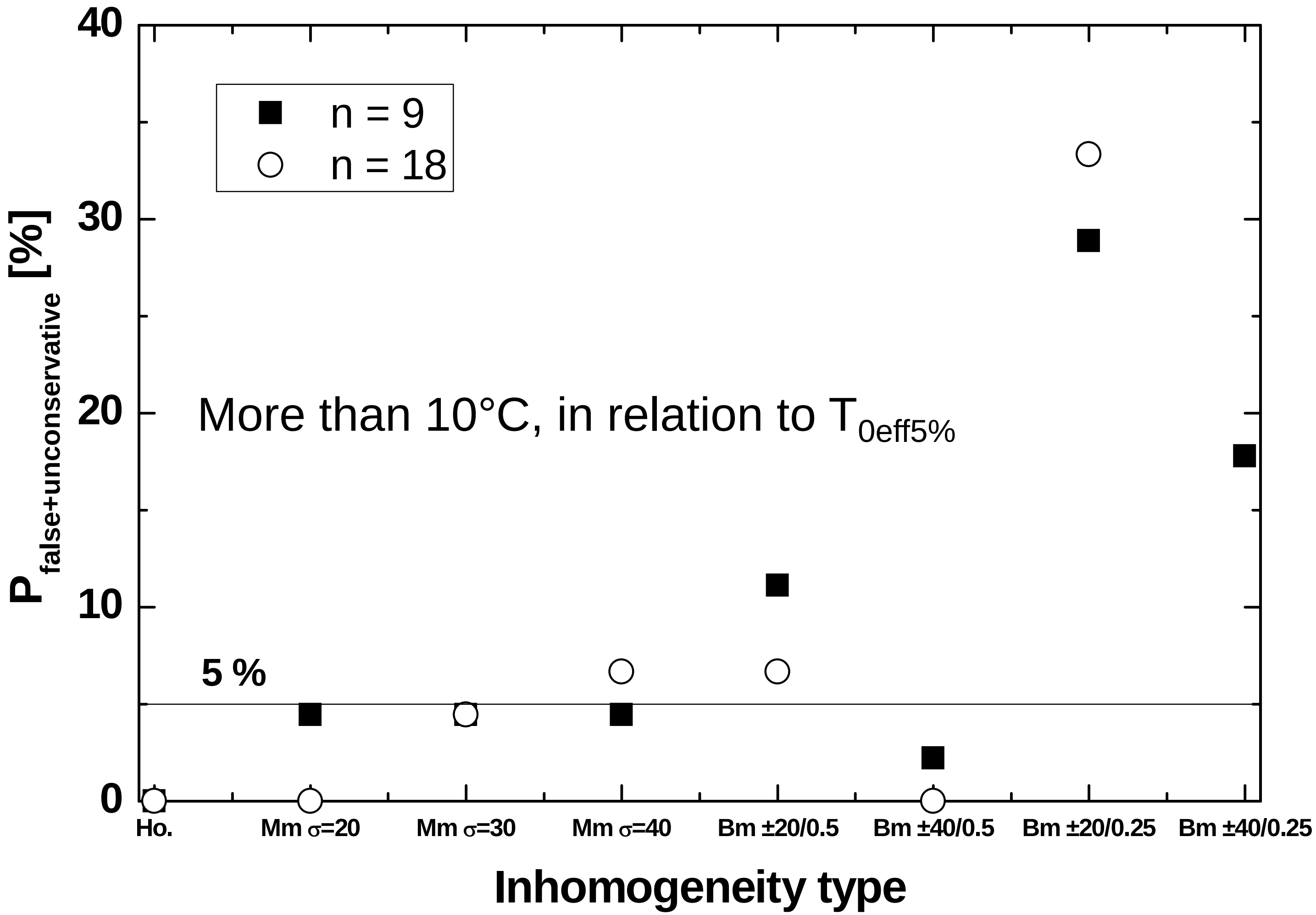

Bias on T_0, introduced by using SINTAP lower-tail assessment method for a data set size that includes step 3

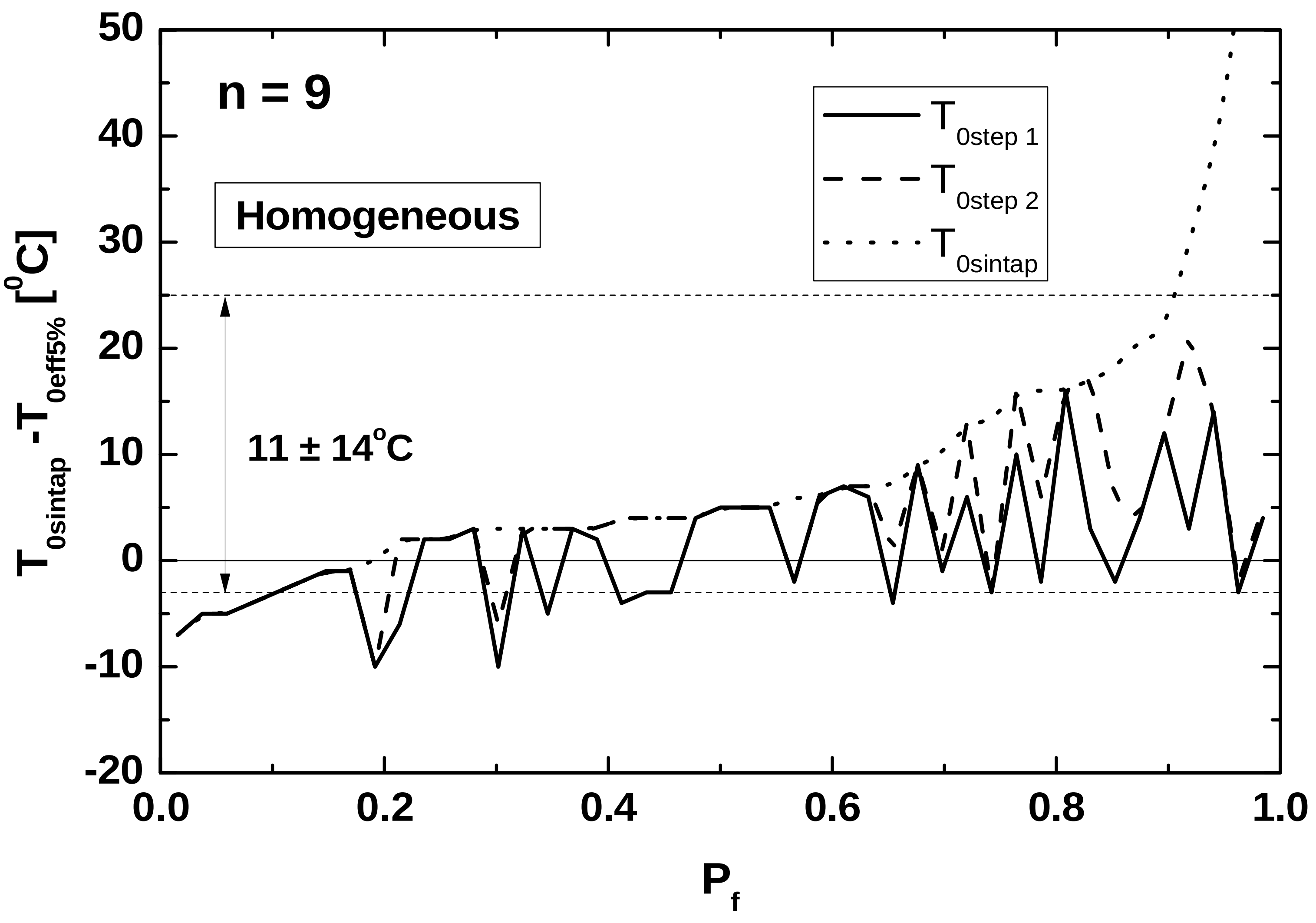

Bias on T_0, introduced by using SINTAP lower-tail assessment method for a data set size that excludes step 3

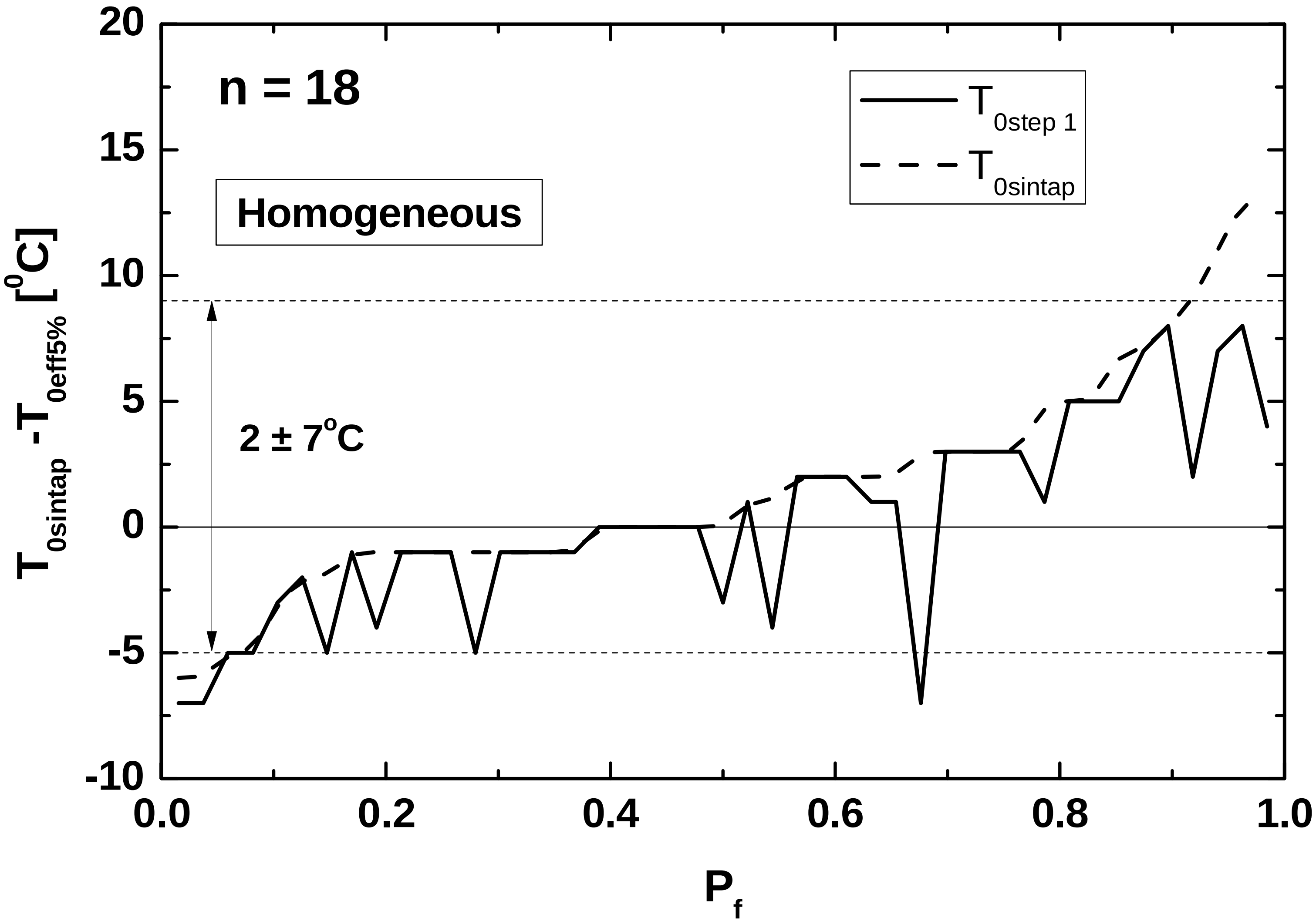

Conclusions

- The screening criterion works well for multimodal inhomogeneities and bimodal inhomogeneities with close to equal amounts of ductile and brittle constituents.
- When combined with the SINTAP T_0 estimate, the probability of falsely judging an inhomogeneous material as homogenous and making more than a 10°C error in the descriptive T_0 value is only approximately 5 %.
- The probability of falsely judging a homogeneous material as being inhomogeneous is also only approximately 5 %.
- Bimodal inhomogeneities, containing only a small portion of brittle constituent can never be reliably assessed with small data sets, since the inhomogeneities act as outliers. For such materials the screening criterion is ineffective.


VTT
TECHNOLOGY FOR BUSINESS

Research Report

Inter-laboratory Study to Establish Precision Statements for ASTM E-3039 Standard Test Method for Determination of Crack-Tip-Opening Angle of Pipe Steels using DWTT Specimens

Dr. Su Xu, Dr. W. R. Tyson and Dr. E. Lucon

Introduction

An Inter-laboratory Study (ILS) was conducted to establish a precision statement for Standard Test Method for Determination of Crack-Tip-Opening Angle of Pipe Steels Using DWTT Specimens.

The ILS also serves the purpose to further evaluate and improve the test method. The report summarizes the details and results of the ILS.

Participating Laboratories

The following laboratories participated in this Inter-laboratory Study:

1. CanmetMATERIALS, Natural Resources Canada, Canada L8P 0A5
   Drs. S. Xu and W.R. Tyson
2. CSM--Centro Sviluppo Materiali, Roma, Italy
   Drs. Andrea Fonzo and Gianluca Mannucci
3. Salzgitter Mannesmann Research, Duisburg, Germany
   Drs. Marion Erdelen-Peppler and Andreas Liessem
4. DRDC Atlantic Dockyard Laboratory Pacific, CFB Esquimalt, Canada V9A 7N2
   Dr. Christopher Bayley
5. Research and Development Centre, Regina, Saskatchewan, Canada S4P 3C7
   Drs. Muhammad Rashid and Laurie Collins
6. Technical Development Bureau, Nippon Steel Corporation, Chiba, Japan
   Mr. Takuya Hara and Dr. Taishi Fujishiro
7. Steel Research Laboratory, JFE Steel Corporation, Chiba , Japan
   Dr. Satoshi

Material

An electric-resistance-welded (ERW) X70 pipe was provided by one of the participants.

The composition was obtained from spectrum analyses and the material is a typical low-C, low-impurity, Mn-containing, micro-alloyed pipe steels.

Pipe Type	API L Grade	D (mm)	t (mm)	D/t	Year Manufactured
UOE	X70	609.6	12.7	48	~2012

Chemical composition of pipe steel (wt %)

C	Mn	Si	Al	Nb	Ti	Cu	Cr	Ni
0.036	1.47	0.13	0.037	0.069	0.019	0.21	0.072	0.083

P	S	Mo	Ca	Sn	B	V
0.0070	0.0026	0.17	<0.005	0.0085	<0.005	0.0040

Microstructure of through-thickness section parallel to the pipe axial direction at one-quarter plate thickness

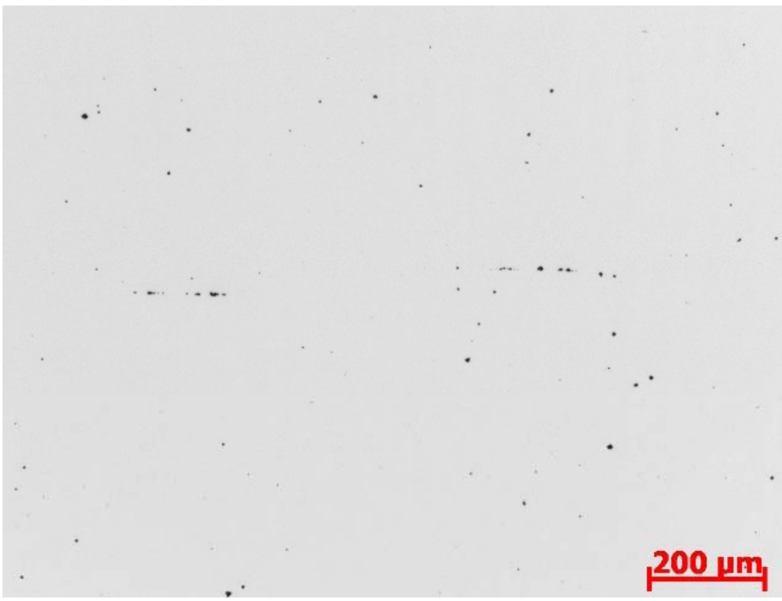

(a) As-polished

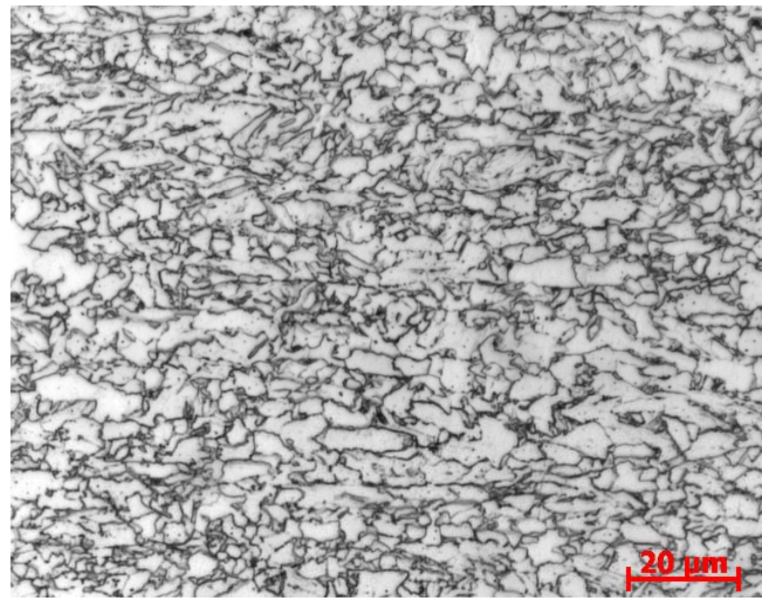

(b) Etched

Average transverse tensile and Charpy properties of pipe steel at 24°C

YS (MPa)	UTS (MPa)	Elongation (%)	YS/UTS	Charpy absorbed energy (J)
564	687	32.7	0.82	247

Location of pipe section and DWTT specimen

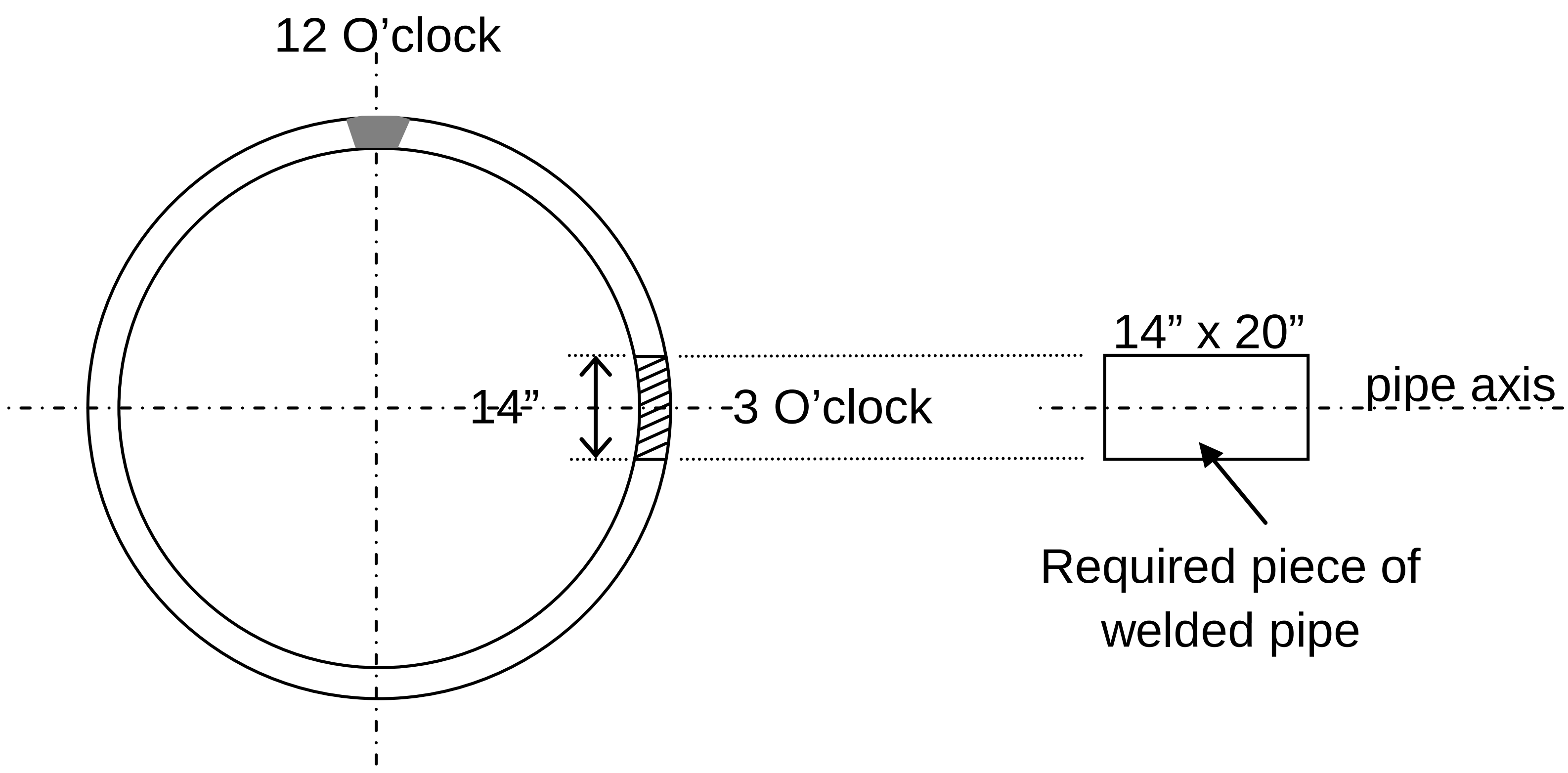

DWTT specimen location and orientation

A pipe section (the pipe axial direction is horizontal)

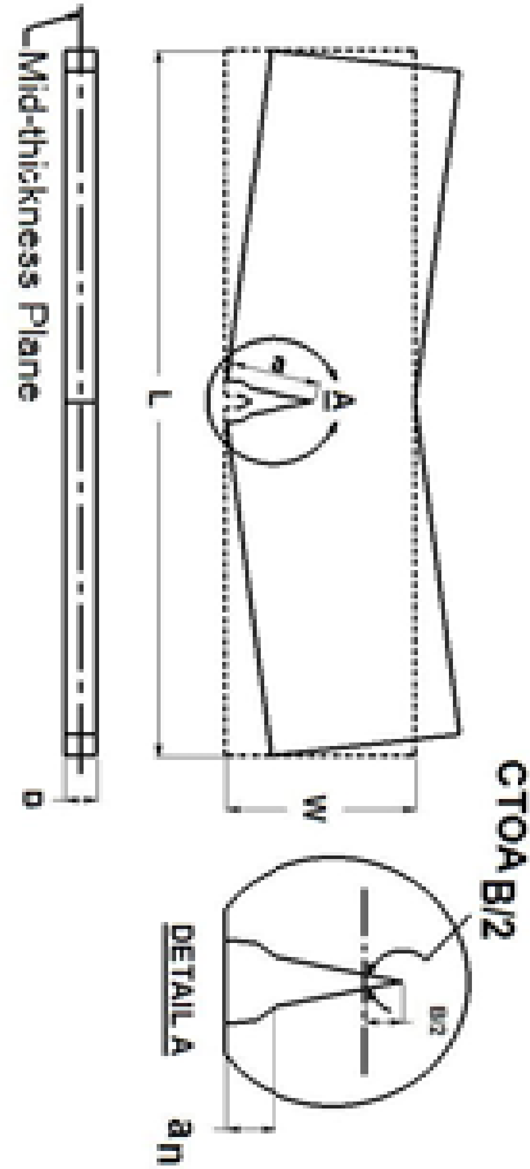

DWTT specimen orientation

Some of the DWTT machines used in the ILS

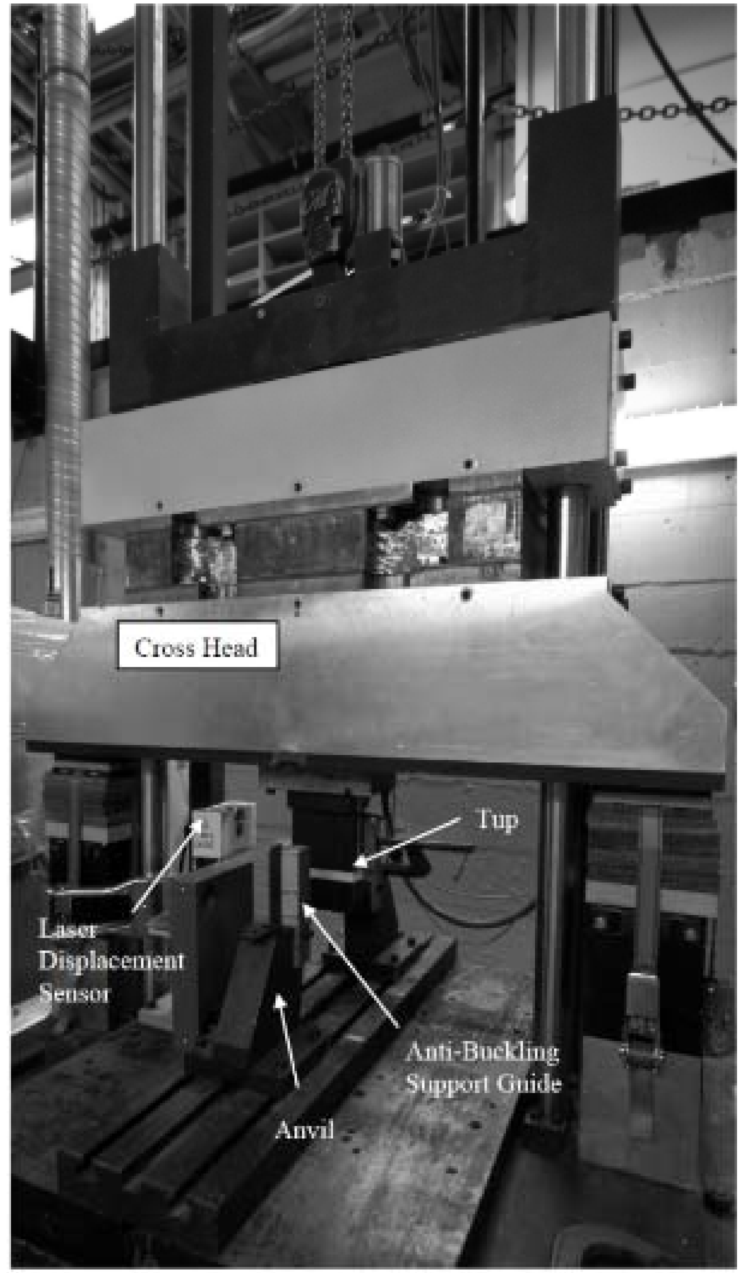

$CTOA_{B/2}$ values of the ILS

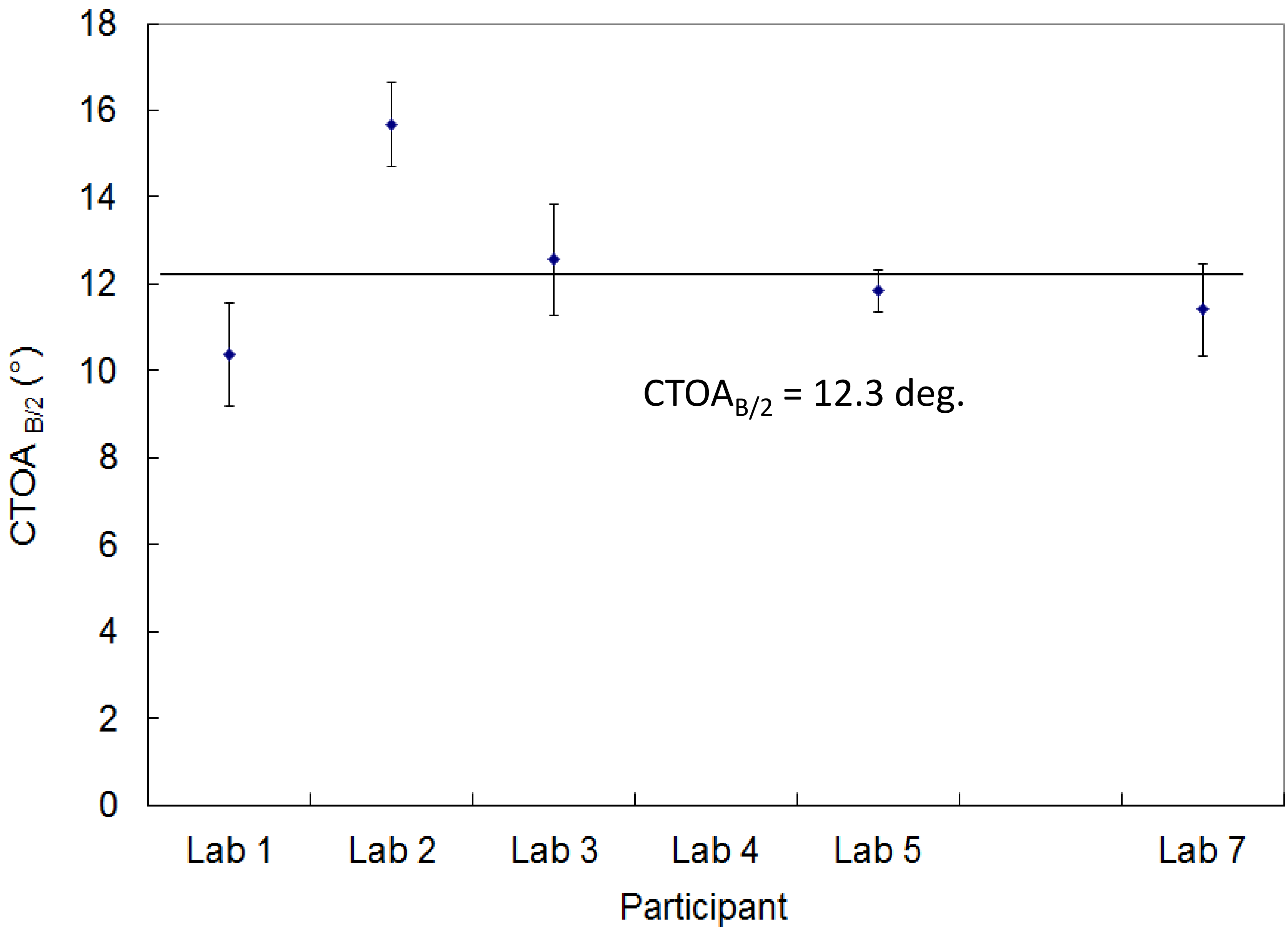

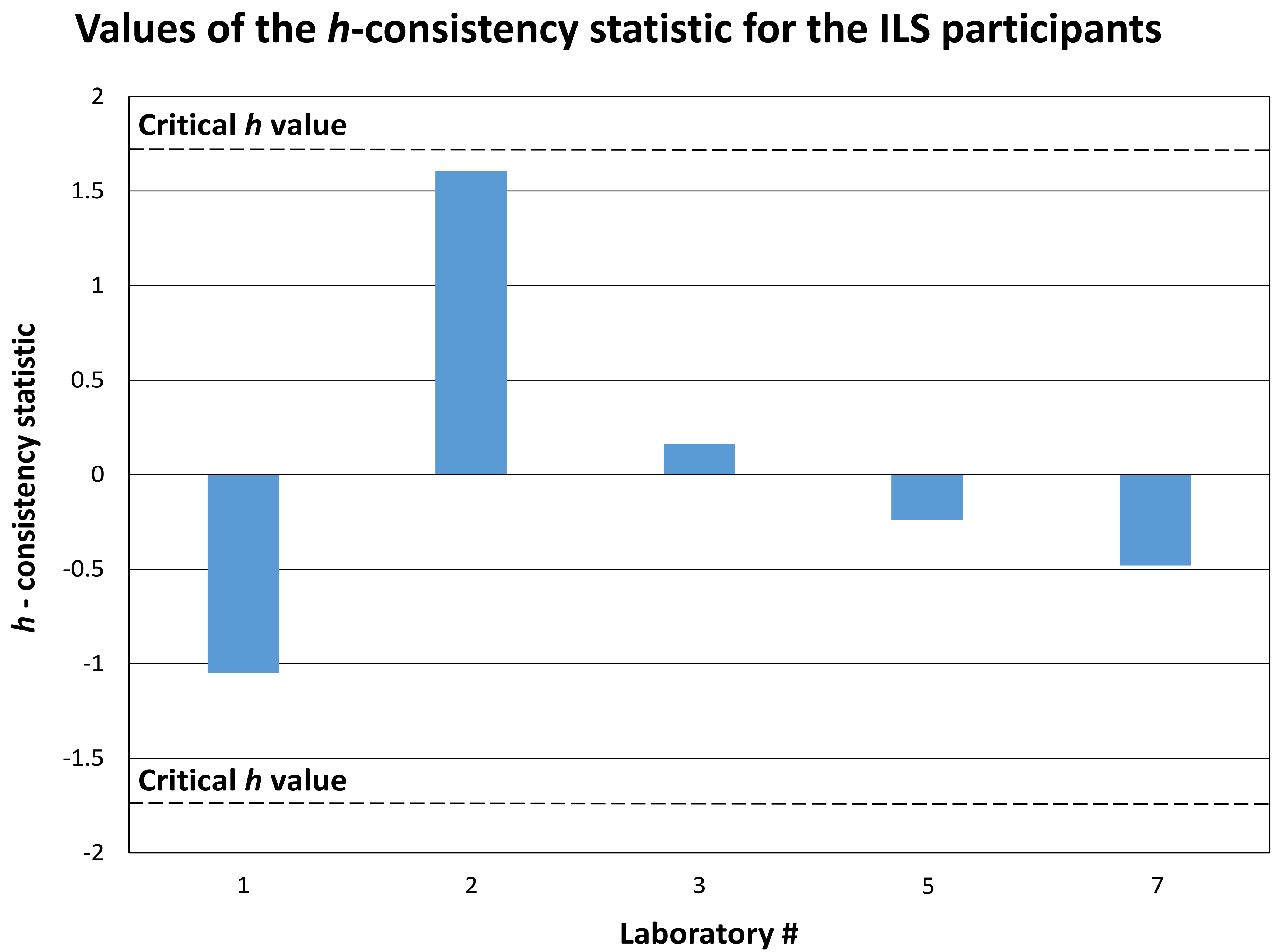

Values of the h-consistency statistic for the ILS participants
Critical h value
Critical h value
2
1.5
1
0.5
0
-0.5
-1
-1.5
-2
h - consistency statistic
1
2
3
5
7
Laboratory #

Typical Results from One of the Laboratories on the DWTT Tests

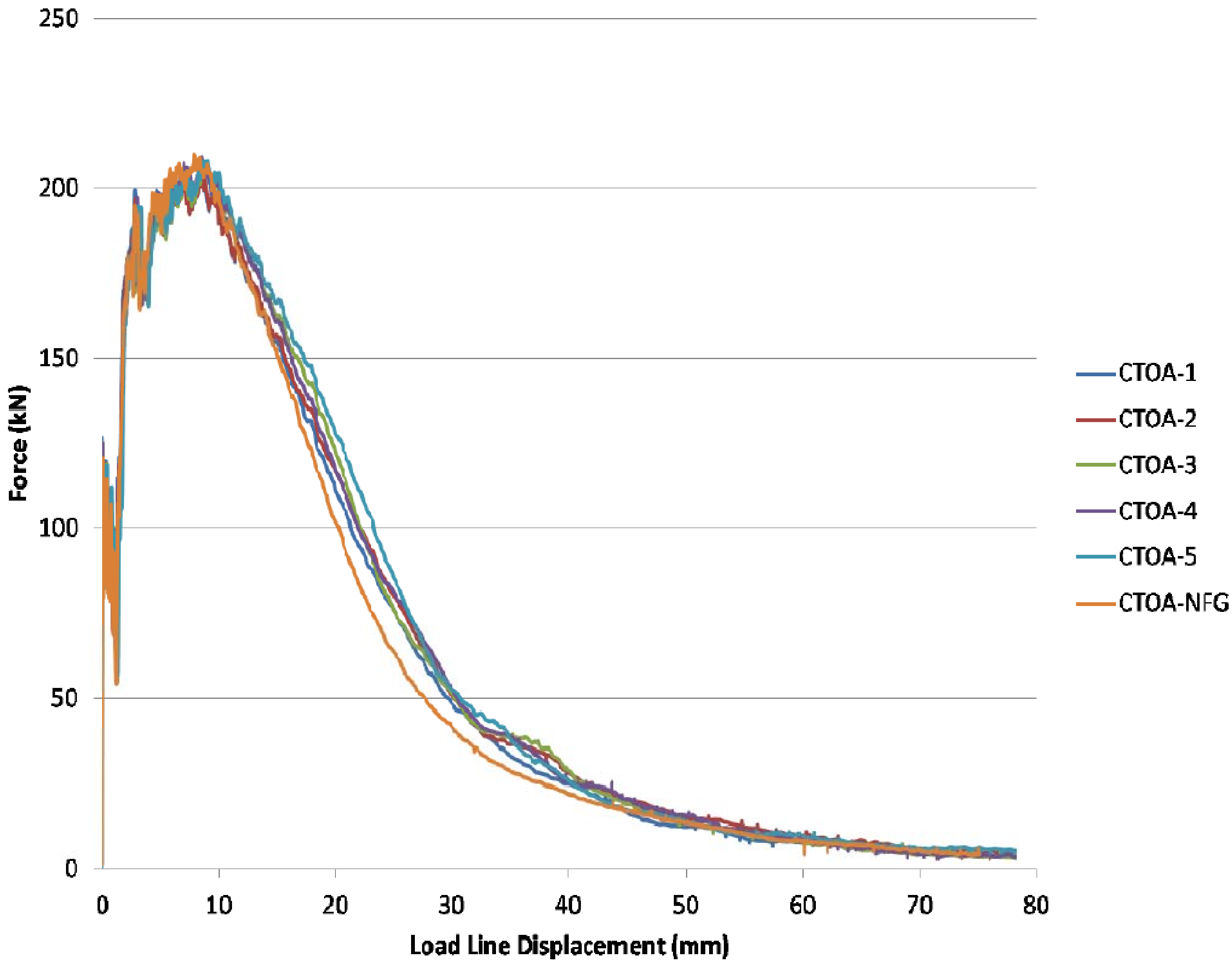

Precision and Bias Statement

Precision—Values of *CTOA* measured from an X70 pipe steel of thickness t = 12.7 mm reported in the framework of an inter-laboratory study (ILS) using a draft recommended practice have been analyzed in accordance with Practice E691 in order to establish the precision of the test method. The terms repeatability limit and reproducibility limit are used as specified in Practice E177. The inter-laboratory study involved five laboratories. Each laboratory provided between three and five $CTOA_{B/2}$ test results. The results of the statistical analysis are summarized in Table 4.

Parameter	Average	Repeat-ability Standard Deviation	Repro-ducibility Standard Deviation	Repeat-ability Limit	Repro-ducibility Limit
CTOA, °	12.3	0.9	2.0	2.6	5.6

Bias—Since there is no accepted reference material, method, or laboratory suitable for determining the bias in $CTOA_{B/2}$ using the procedure in this test method, no statement of bias is being made.

Identification of the onset of crack extension from dcpd data

Kevin Nibur

Hy-Performance Materials Testing, LLC.

Bend OR

Nov. 16 2015 ASTM E08 dcpd discussion

HY-PERFORMANCE

MATERIAL TESTING LLC

Bend, Oregon

How to identify onset of crack extension from dcpd results from ductile materials using interrupted testing

- Example at right is a low alloy QT steel

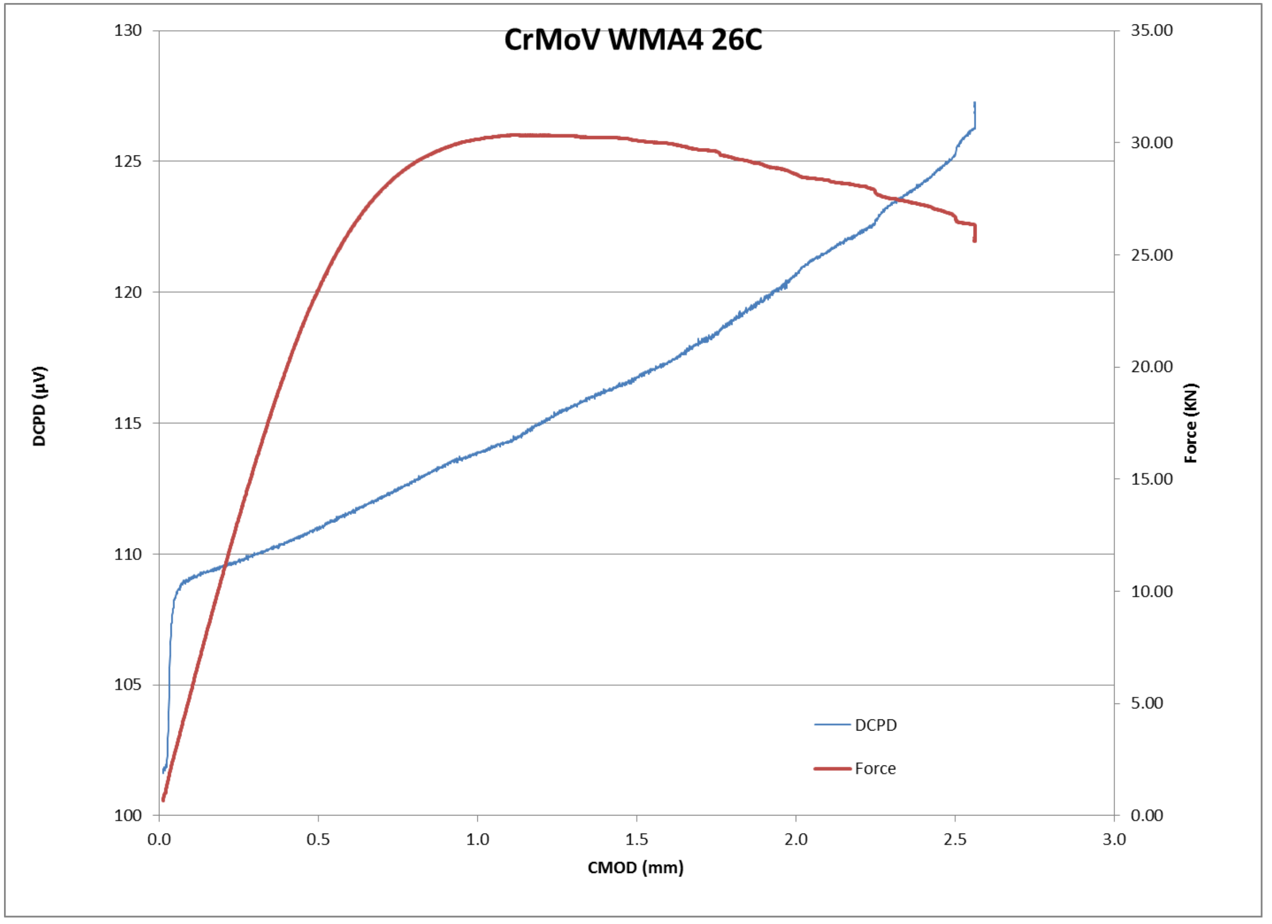

Examine dcpd vs displacement in detail

- Identify likely indications of crack extension –if possible from multiple specimens
- Plan interrupted experiments to stop before and after suspected crack extension

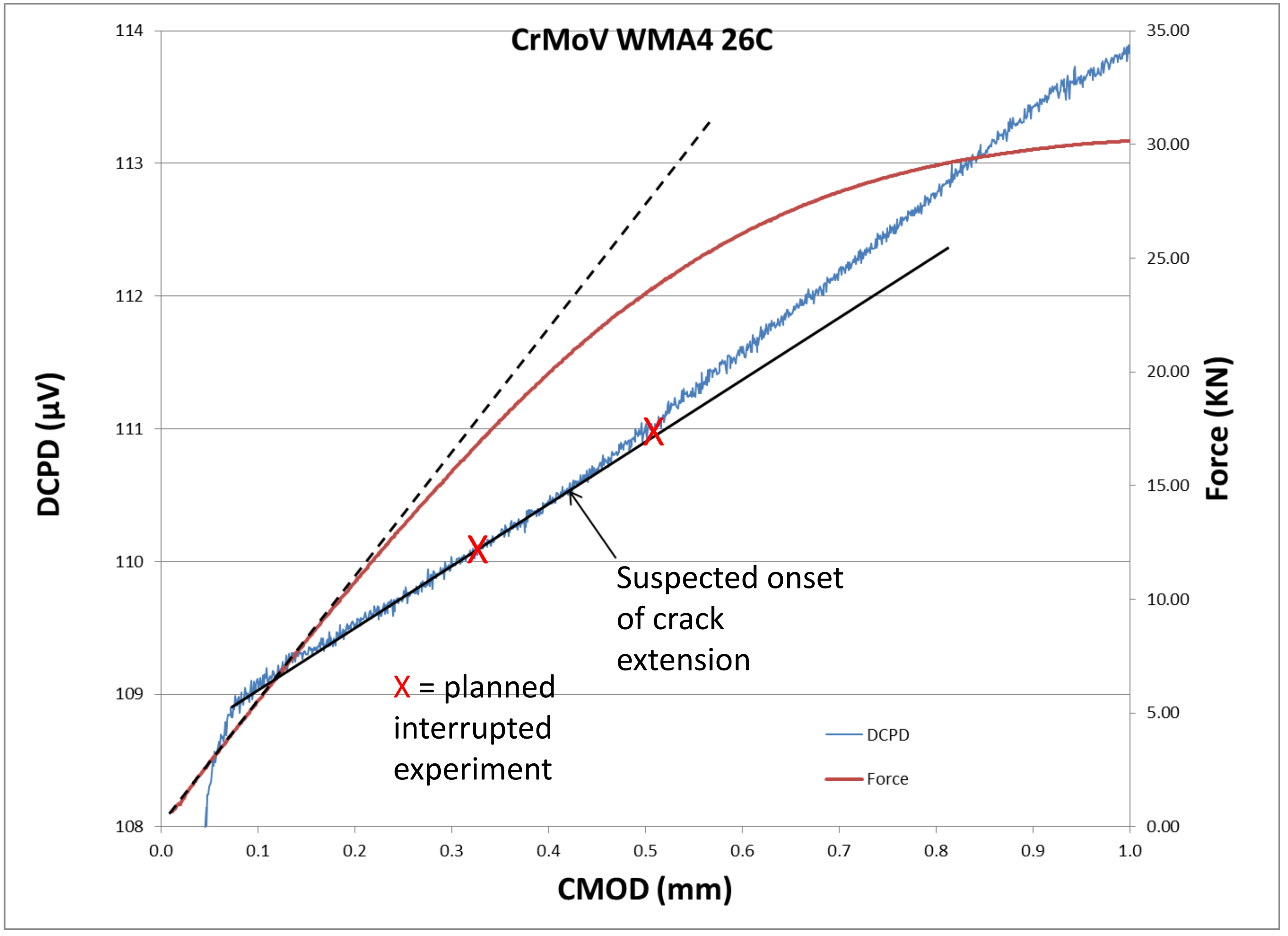

On separate specimens, stop tests <u>before</u> and after suspected indications of crack extension

cleave specimens (for steels) or generate a fatigue marker and break open specimen

Examine fracture surface for indications of ductile crack extension

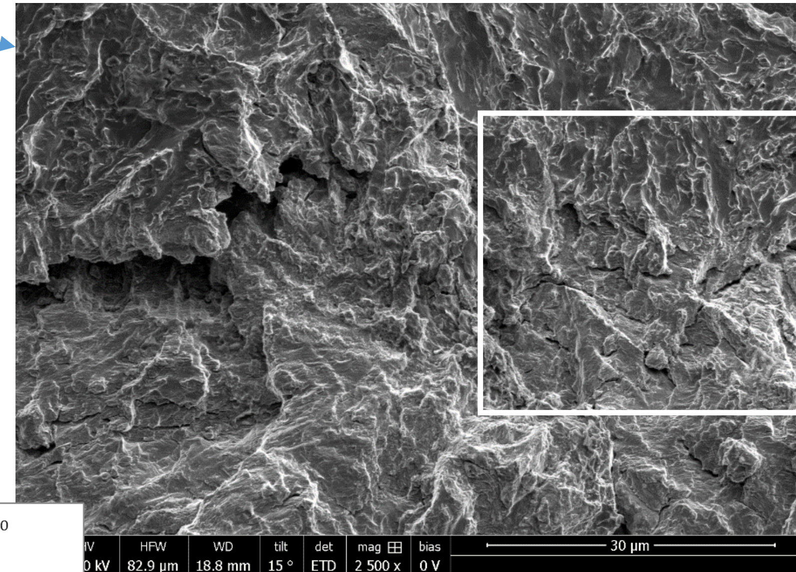

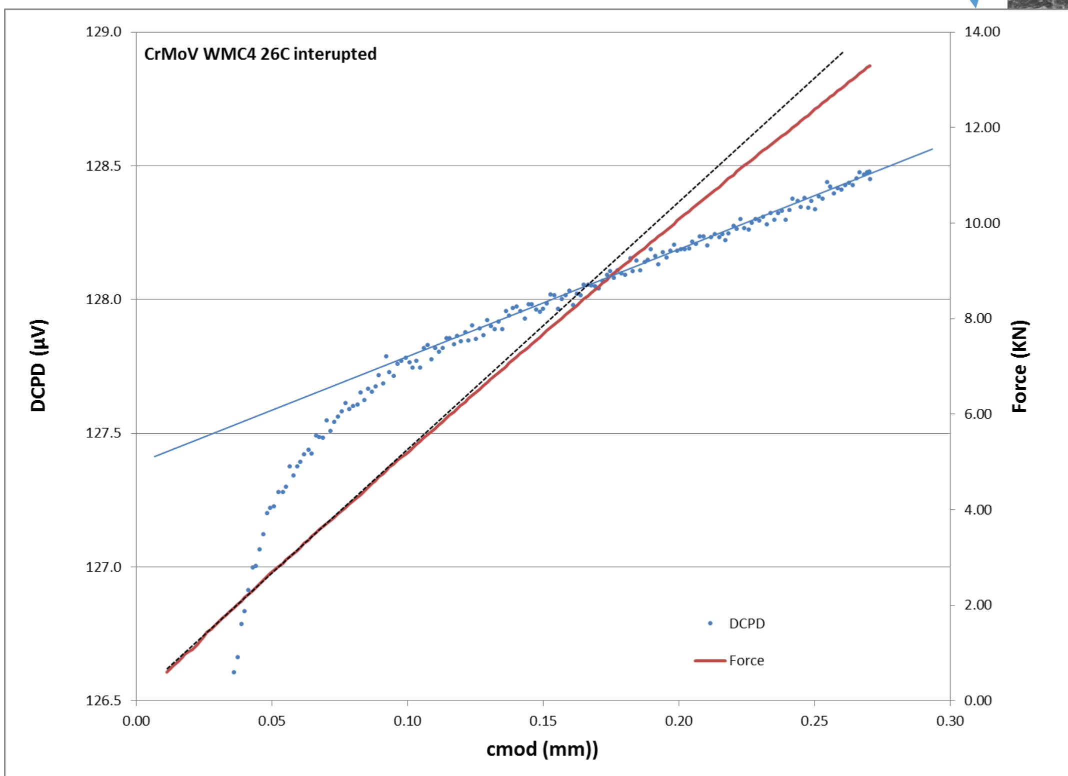

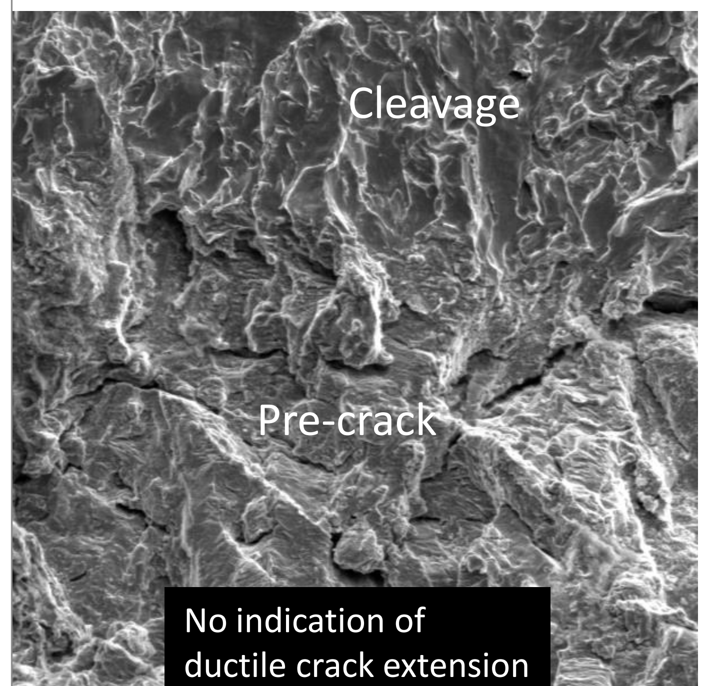

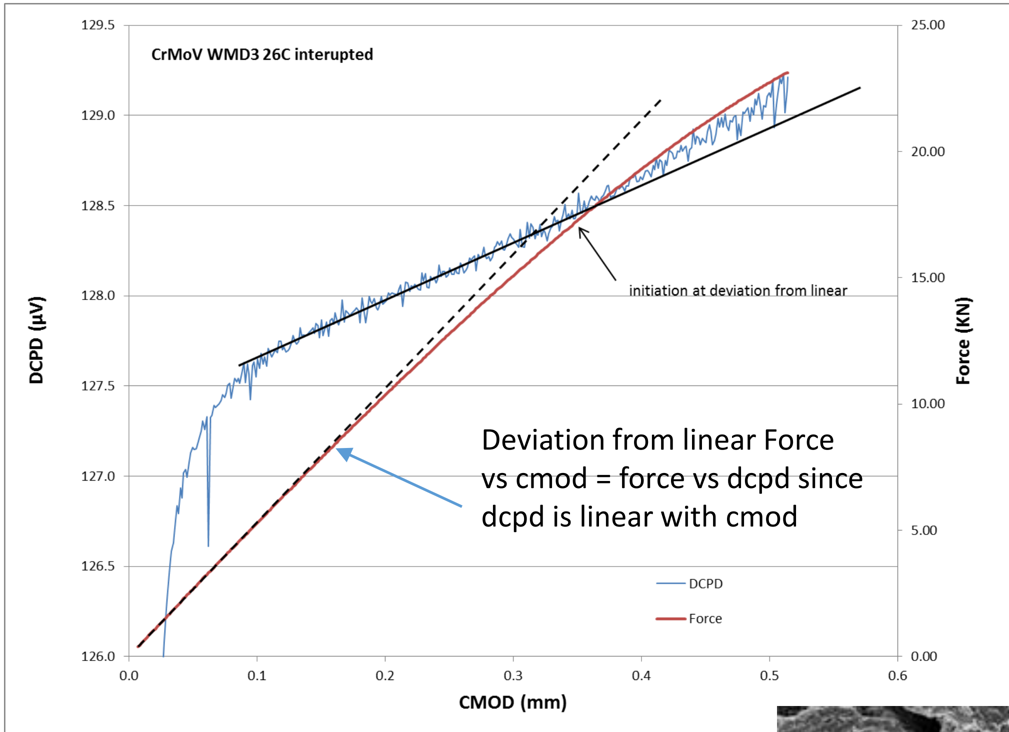

Interrupted test stopped after suspected onset of crack extension confirms correct interpretation of dcpd data

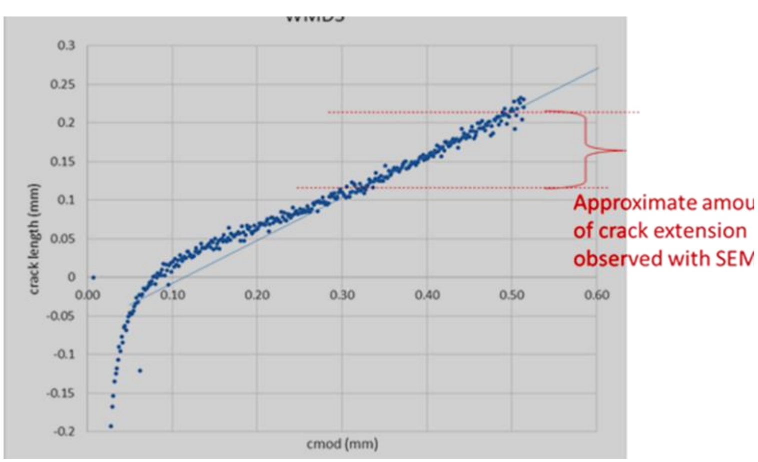

Johnson’s eqn. Predicts
~100 µm of crack extension

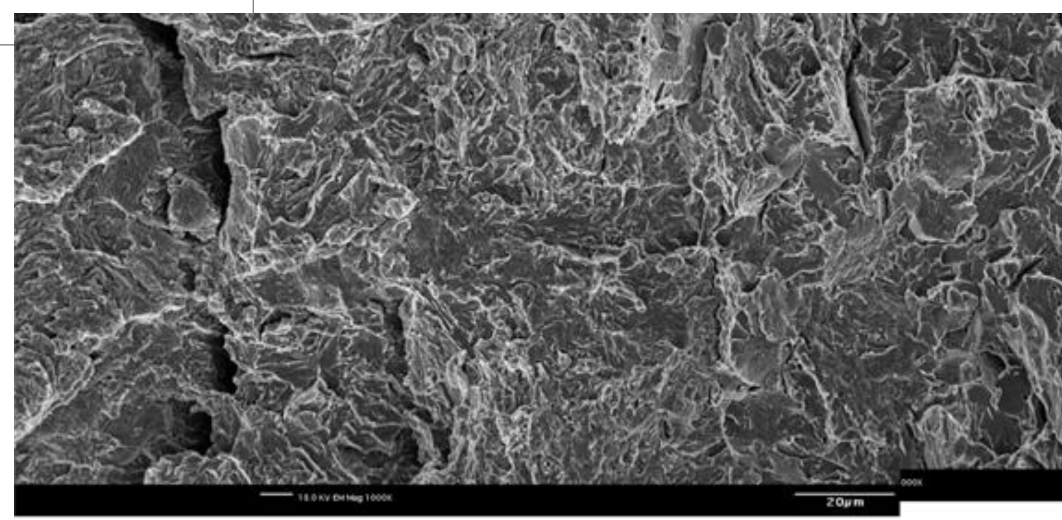

Precrack

IHAC

Low temperature cleavage

~100 µm

Example 1. Changing hydrogen boundary conditions alters onset of stable crack extension with little change in load – displacement curve

- CrMo low alloy QT steel
- **Arrows mark onset of crack extension as <u>confirmed</u> from interrupted test results**
- First deviation from linear DCPD vs cmod relationship usually correlated with onset of crack extension

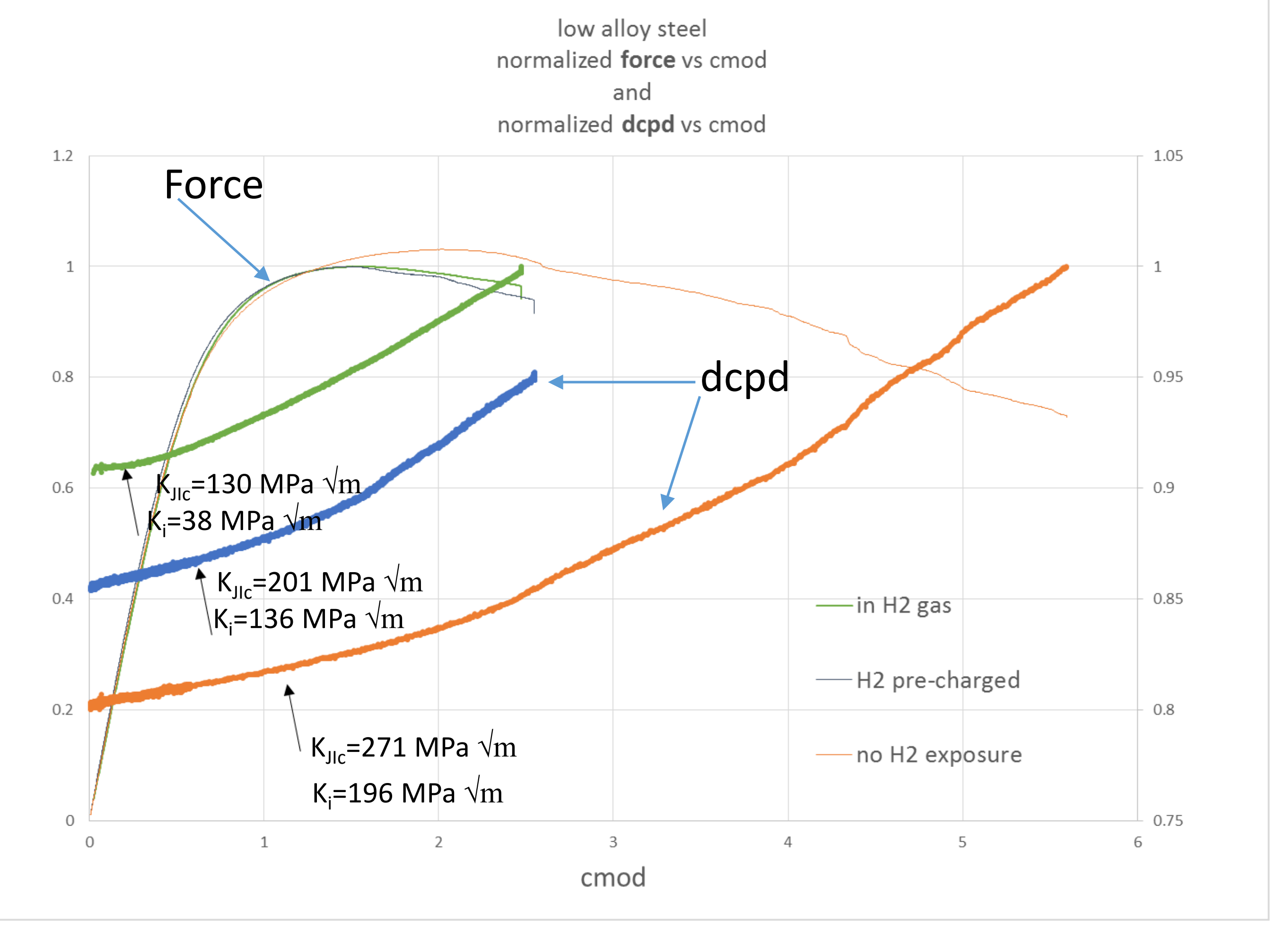

Example 2. Interrupted test result from a ductile austenitic steel

<u>Use of force vs dcpd method would greatly under-predict the onset of crack extension</u>

- 21Cr-6Ni-9Mn SS forging (~Nitronic 40)
- **Extreme example showing onset of crack extension much later than onset of blunting**
- Nitrogen strengthened austenitic SS
  - σ_y=646 MPa
  - $J_Q \approx 1430$ kJ/m^2 (K_{JQ} ~570 MPa $\sqrt{m}$)
  - Crack tip stretch zone on order of 1mm
- First deviation from linear DCPD vs cmod relationship consistently correlated with crack initiation
- **<u>Note orange force vs cmod curve</u>**: cmod is linear with dcpd, so force vs dcpd would look the same
  - **<u>No crack extension occurred in this specimen!</u>**

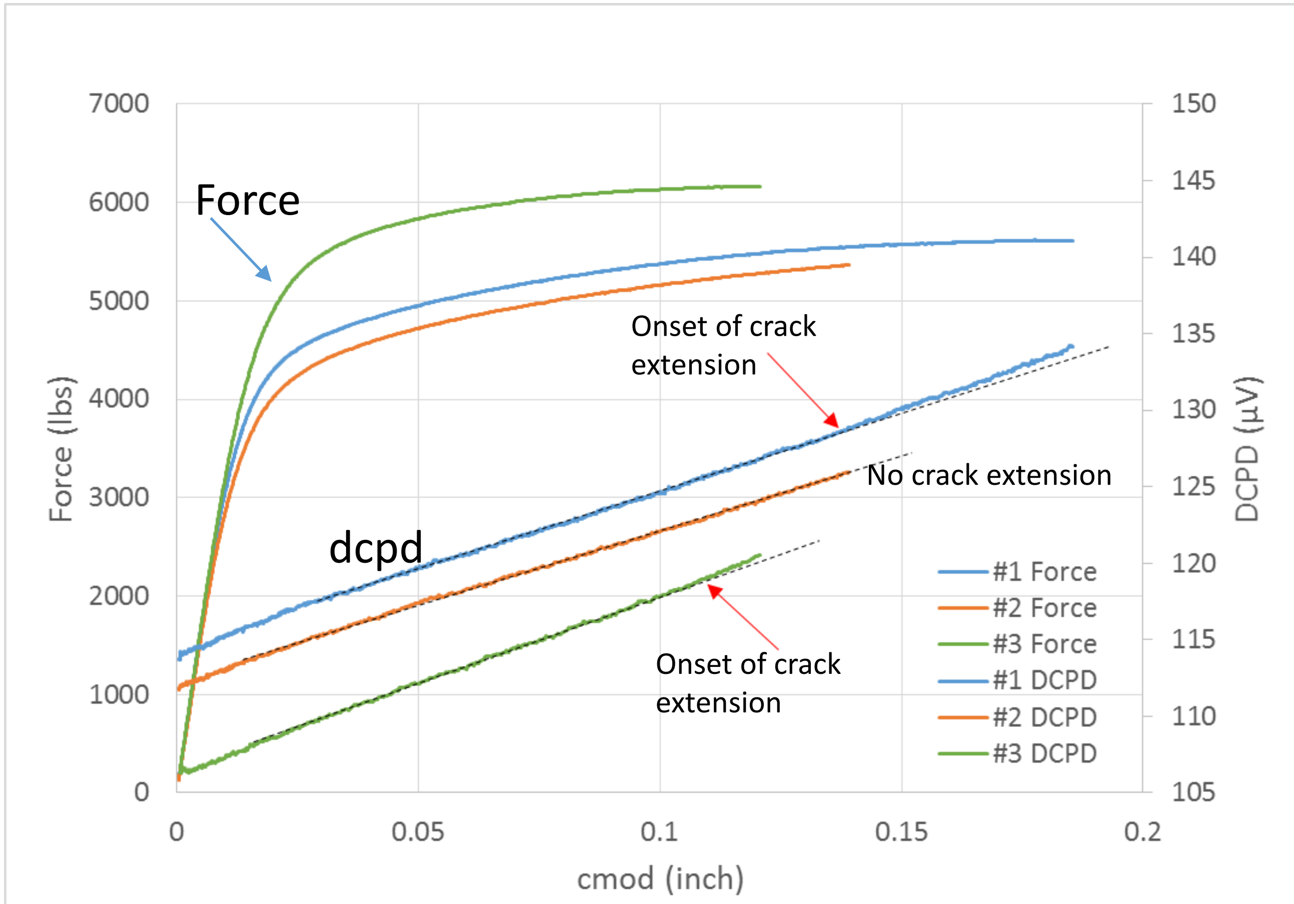

Deflection of force vs dcpd curve reflects onset of blunting, not onset of crack extension

HY-PERFORMANCE
MATERIAL TESTING LLC
Bend, Oregon

Interpreting PD Data For E1820

Keith Tarnowski
2nd May 2016

Imperial College London

Contents

- Influence of strain on PD
- Interpreting PD Data
- Review of the ‘Load’ Method
- Review of the ‘COD’ Method
- Conclusions

Imperial College London

Contents

- **Influence of strain on PD**
- Interpreting PD Data
- Review of the ‘Load’ Method
- Review of the ‘COD’ Method
- Conclusions

Imperial College London

Experimental Setup

- Range of PD configurations
- a/W = 0.45 and 0.55
- EDM Pre-crack
- Type 316H Stainless Steel
- Monotonic Loading
    - Stopped prior to stable tearing

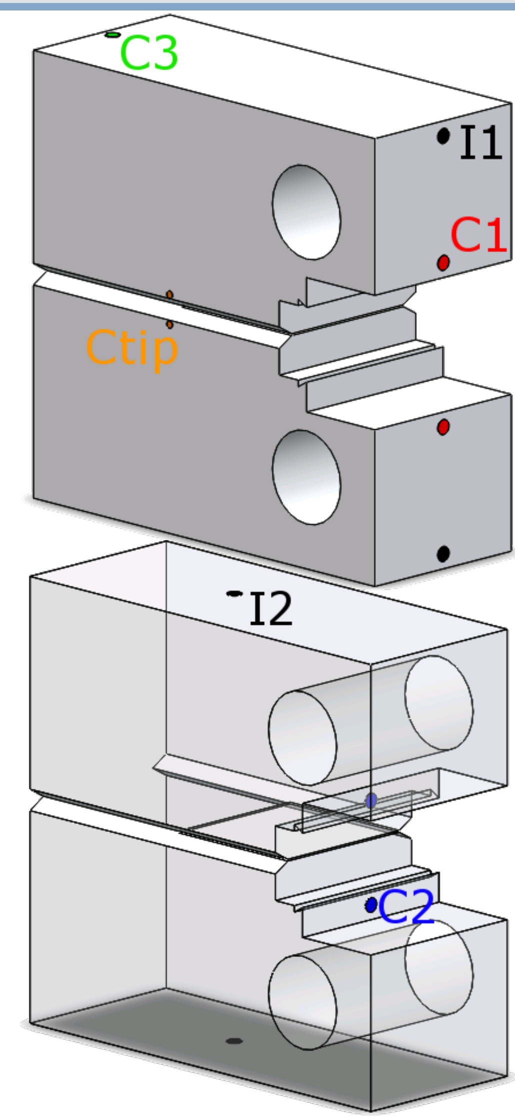

Influence of Strain

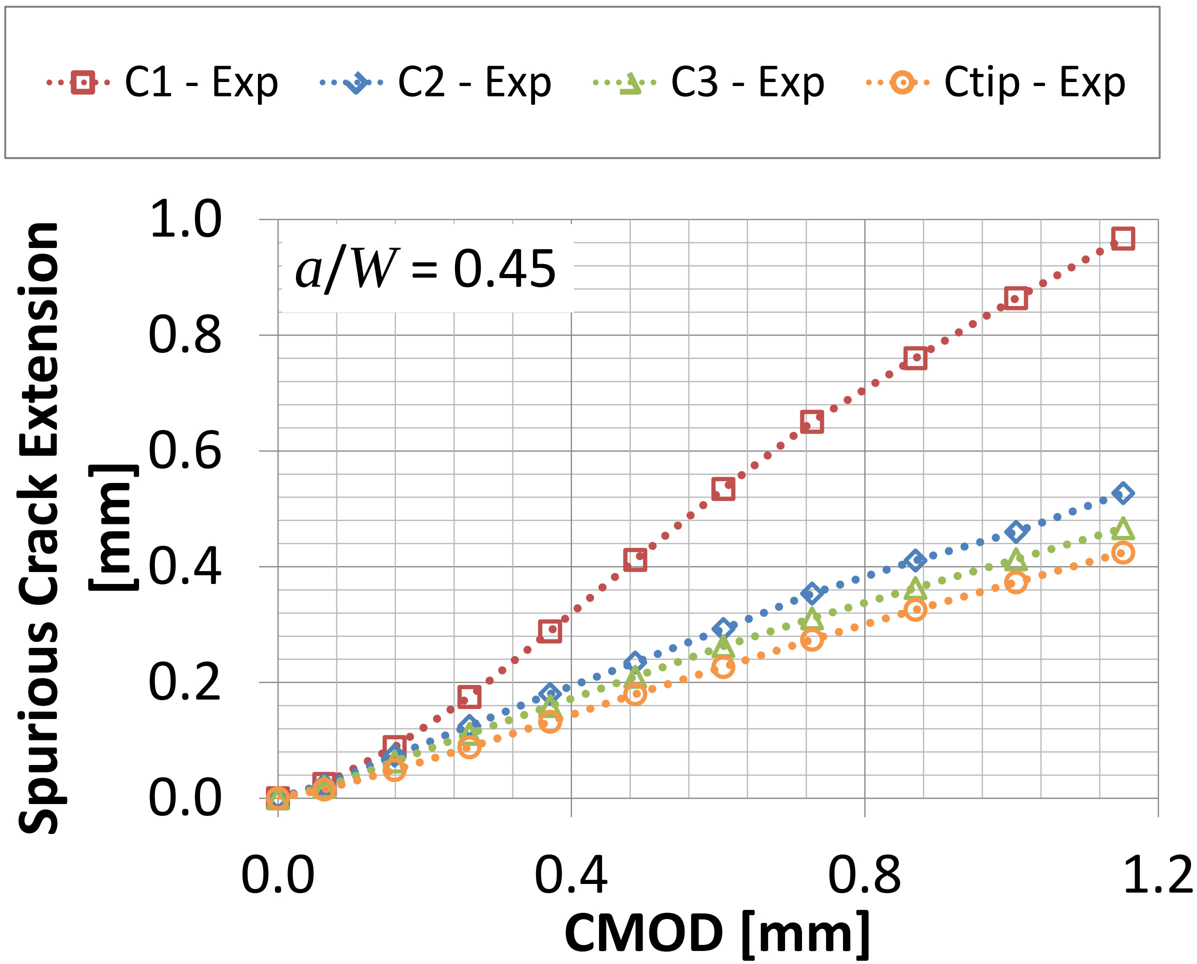

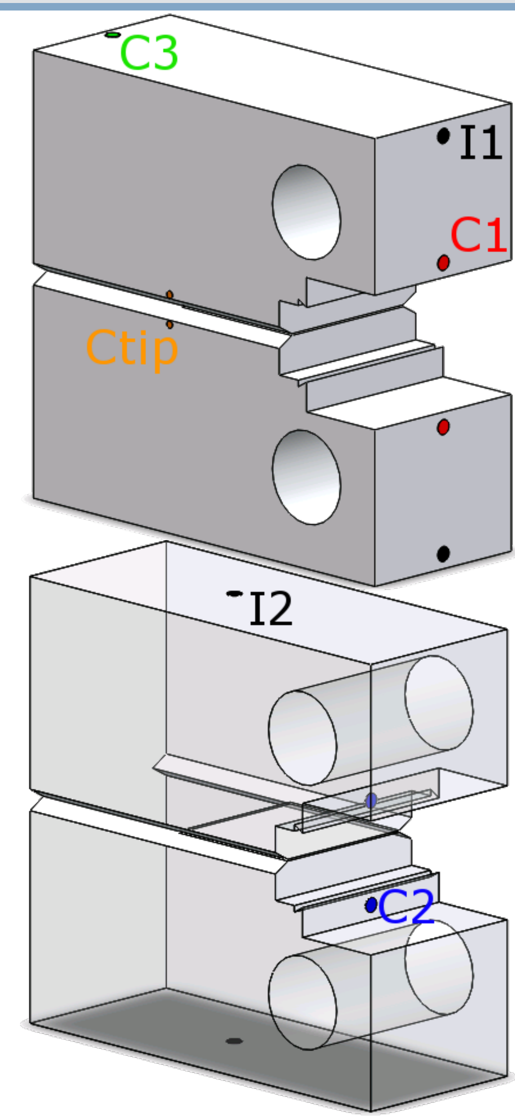

Imperial College London

Influence of Strain

- Strain affects PD in two ways:
  - Geometric
  - Material
- Elastic Strain:
  - Geometric > Material
- Plastic Strain:
  - Geometric >> Material

A simple sequentially coupled structural-electrical FE model can be used to predict the influence of strain.

FE Models

- ¼ 3D Abaqus models
  - Stationary Crack
- Pin Explicitly Modelled

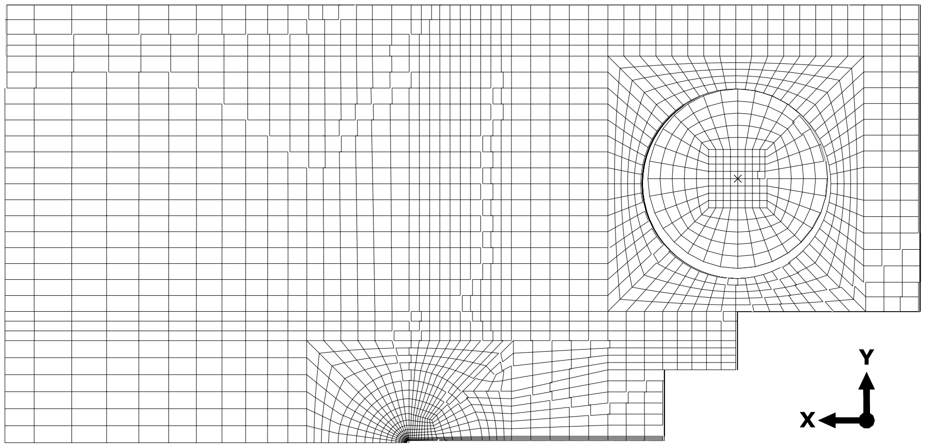

Electrical Analysis 1 – Undeformed Specimen

↓

Structural Analysis

↓

Electrical Analysis 2 – Deformed Specimen

↓

Compare Electrical Analyses 1 & 2

Imperial College London

Influence of Strain

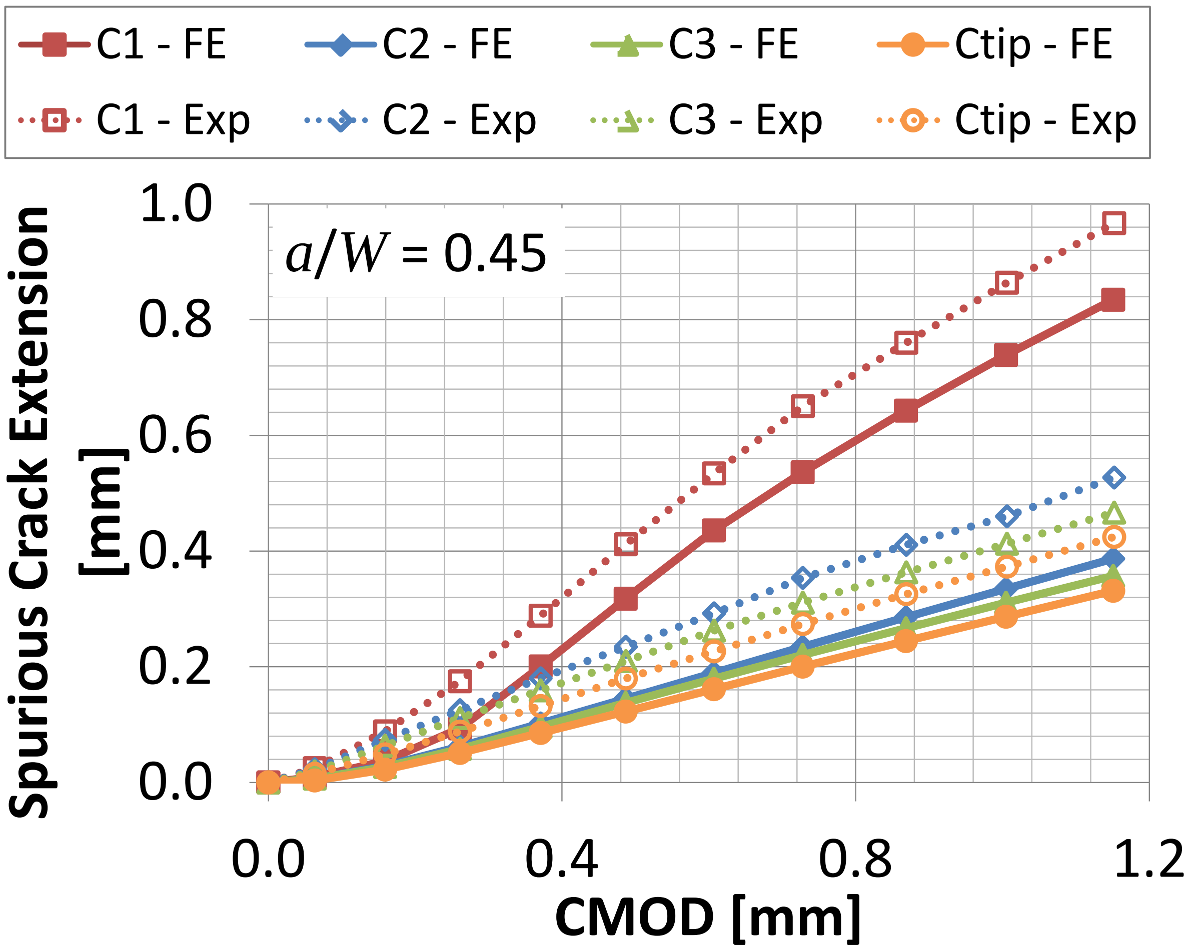

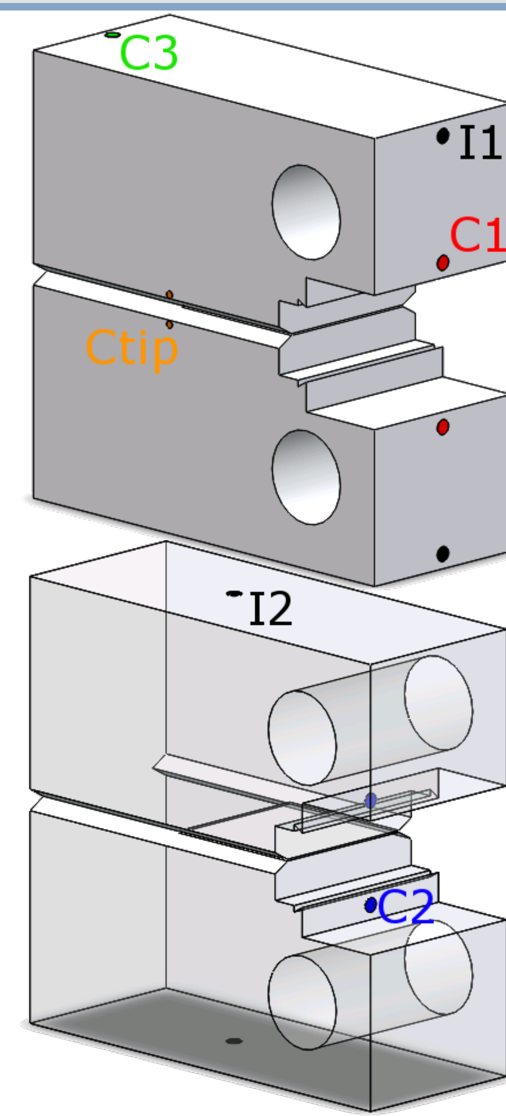

Imperial College London

Contents

Interpreting PD Data

- Two methods in ISO 12135:2002 & ESIS P2-92
- Typical Calibration: $a/W = f((V_0+\Delta V)/V_0)$

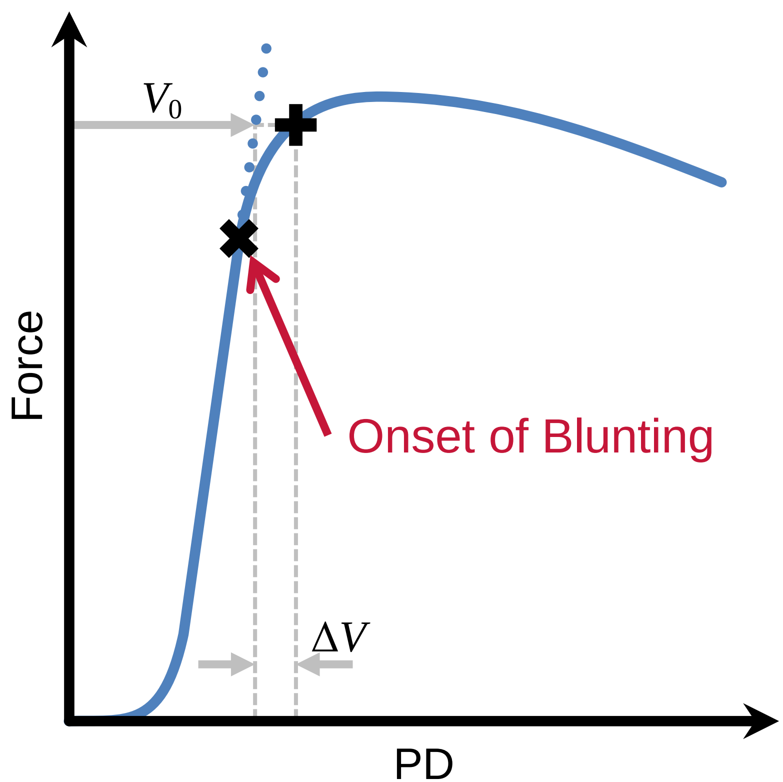

'Load' Method

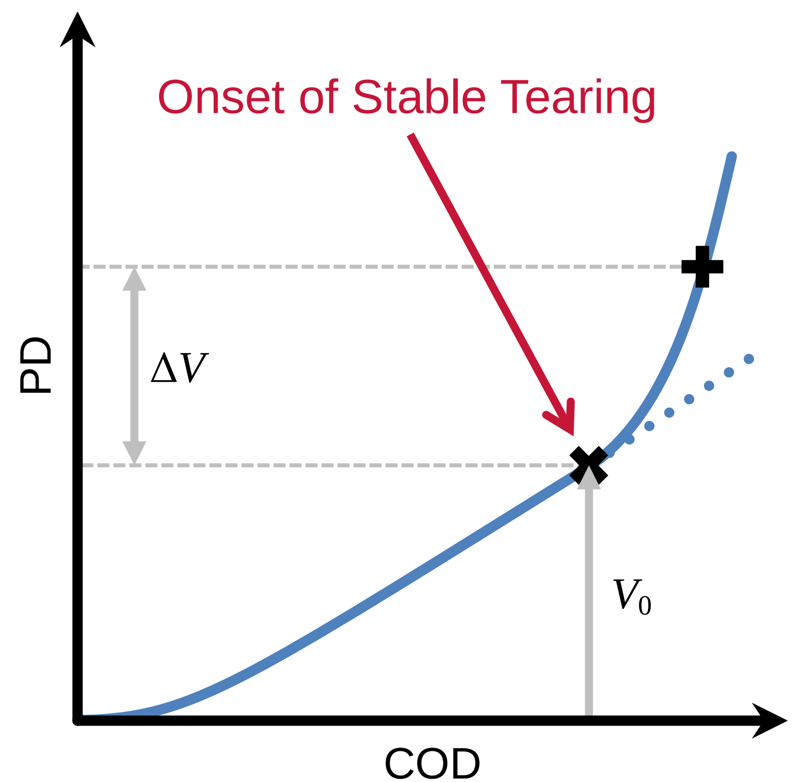

'COD' Method

Imperial College London

Interpreting PD Data

	'Load' Method	'COD' Method
Blunting Measurement	PD	SEM
Stable Tearing Measurement	PD	PD
Value of V_0	Load dependent	Fixed
Known Problems	Can underestimate $J_{0.2}$ [1,2,3]	Can be difficult to identify point of inflection [1]

[1] Bicego, V. et al., ASTM STP 1092

[2] Bakker, A., ASTM STP 856

[3] Hollstein, T. et al., ASTM STP 856

Contents

- Influence of strain on PD
- Interpreting PD Data
- **Review of the ‘Load’ Method**
- Review of the ‘COD’ Method
- Conclusions

Measuring Blunting

- PD configuration ‘C2’
- Blunting obtained from FE:
  - PD (‘Load’ Method)
  - Displacement field
- Compared with Blunting Lines:
  - ASTM E1820-13
  - ISO 12135:2002
- Type 316H known to agree with ISO 12135 [1]

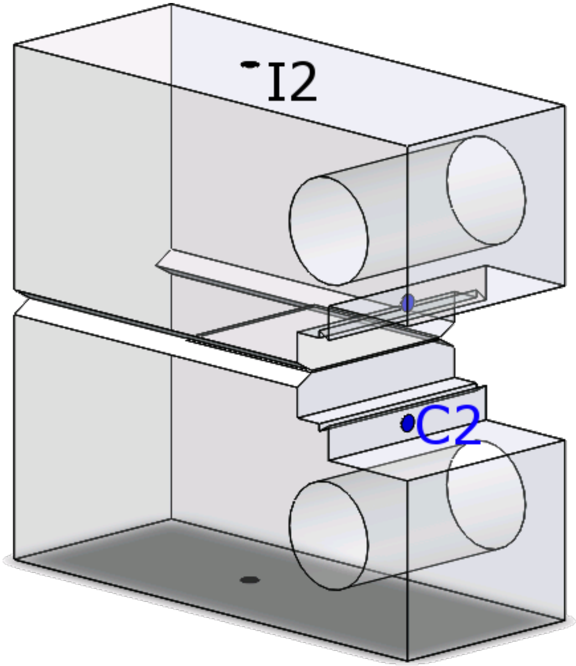

[1] Mills, W.J., International Materials Reviews, 1997

Measuring Blunting: PD

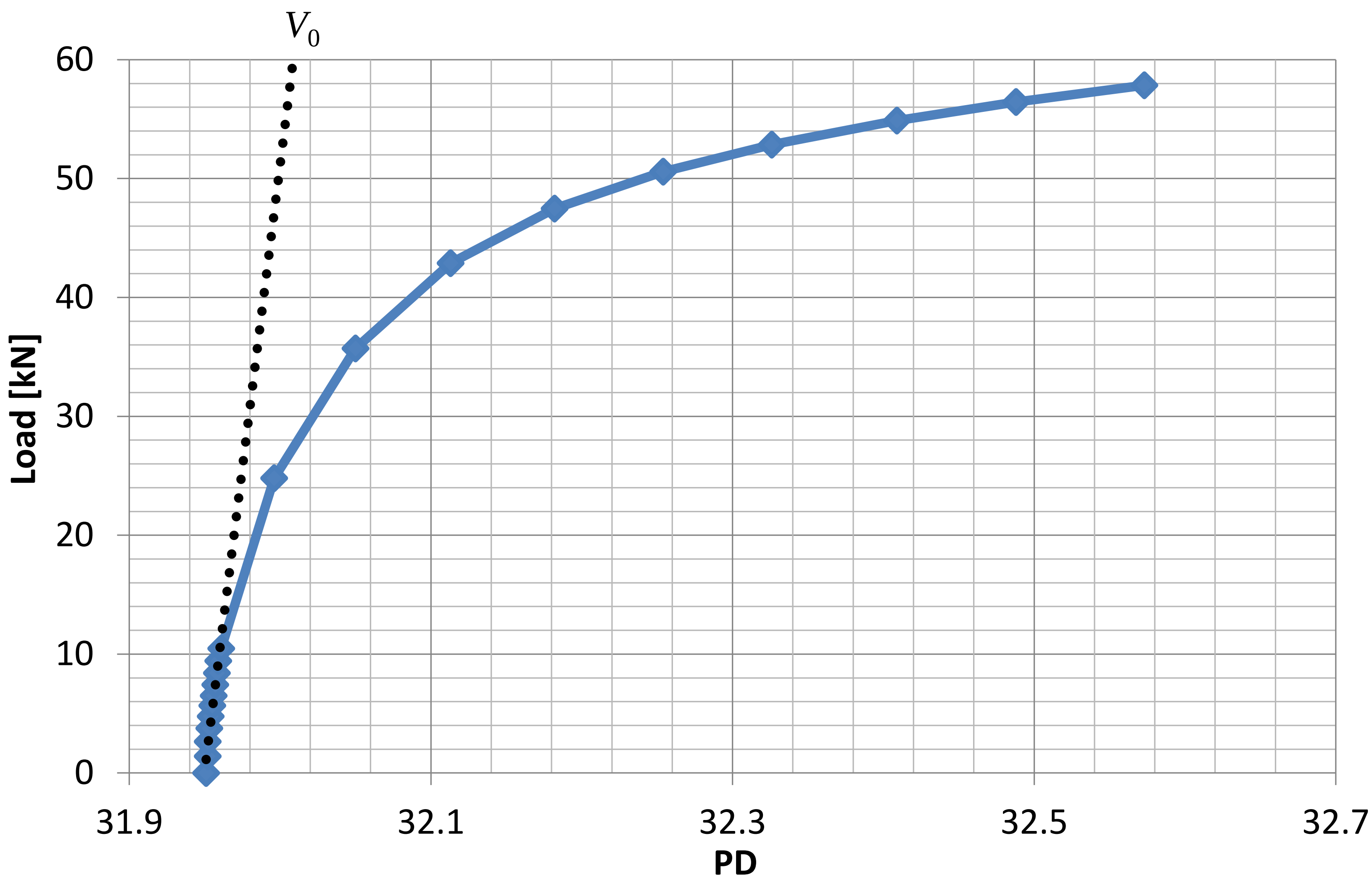

Imperial College London

Measuring Blunting: Displacement

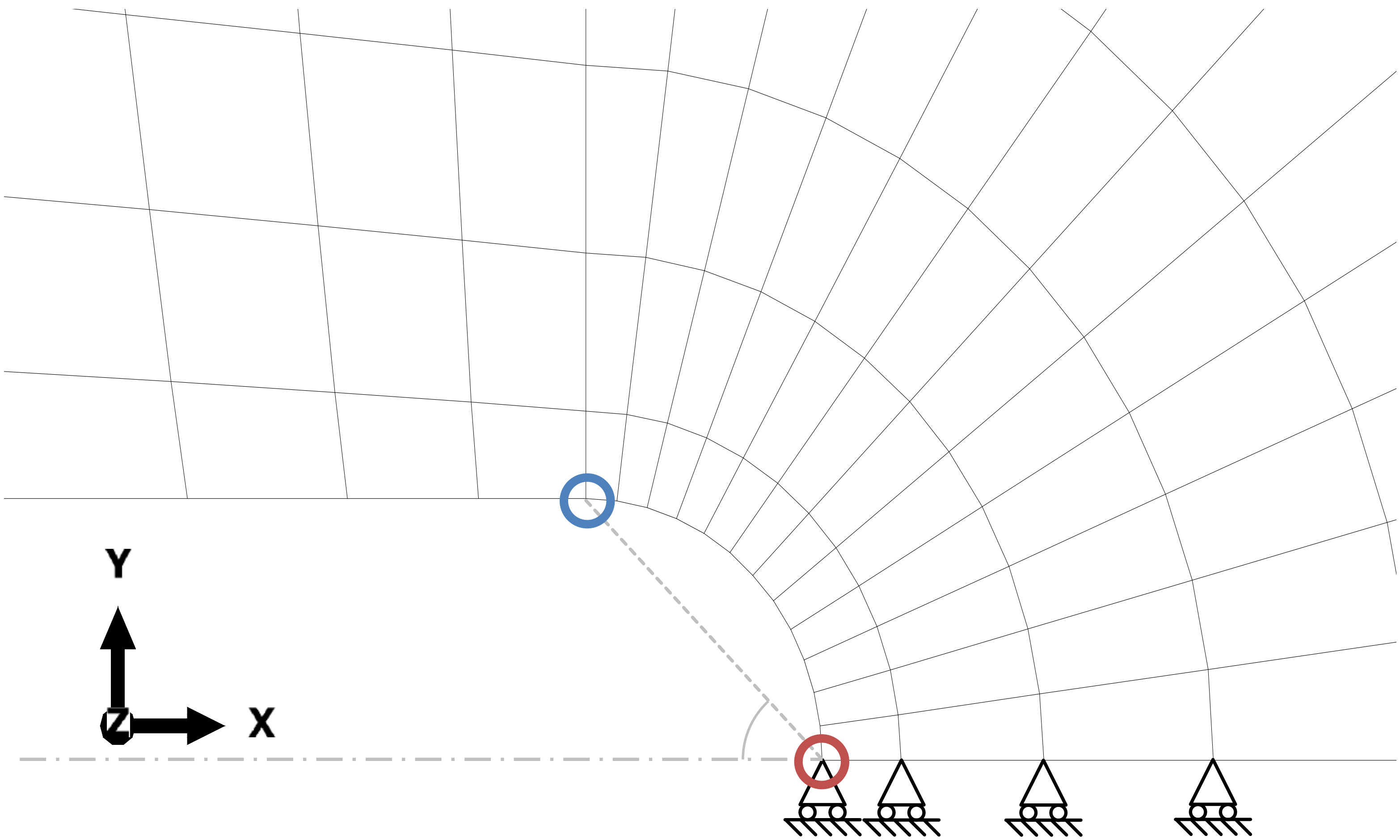

Imperial College London

Measuring Blunting: Comparison

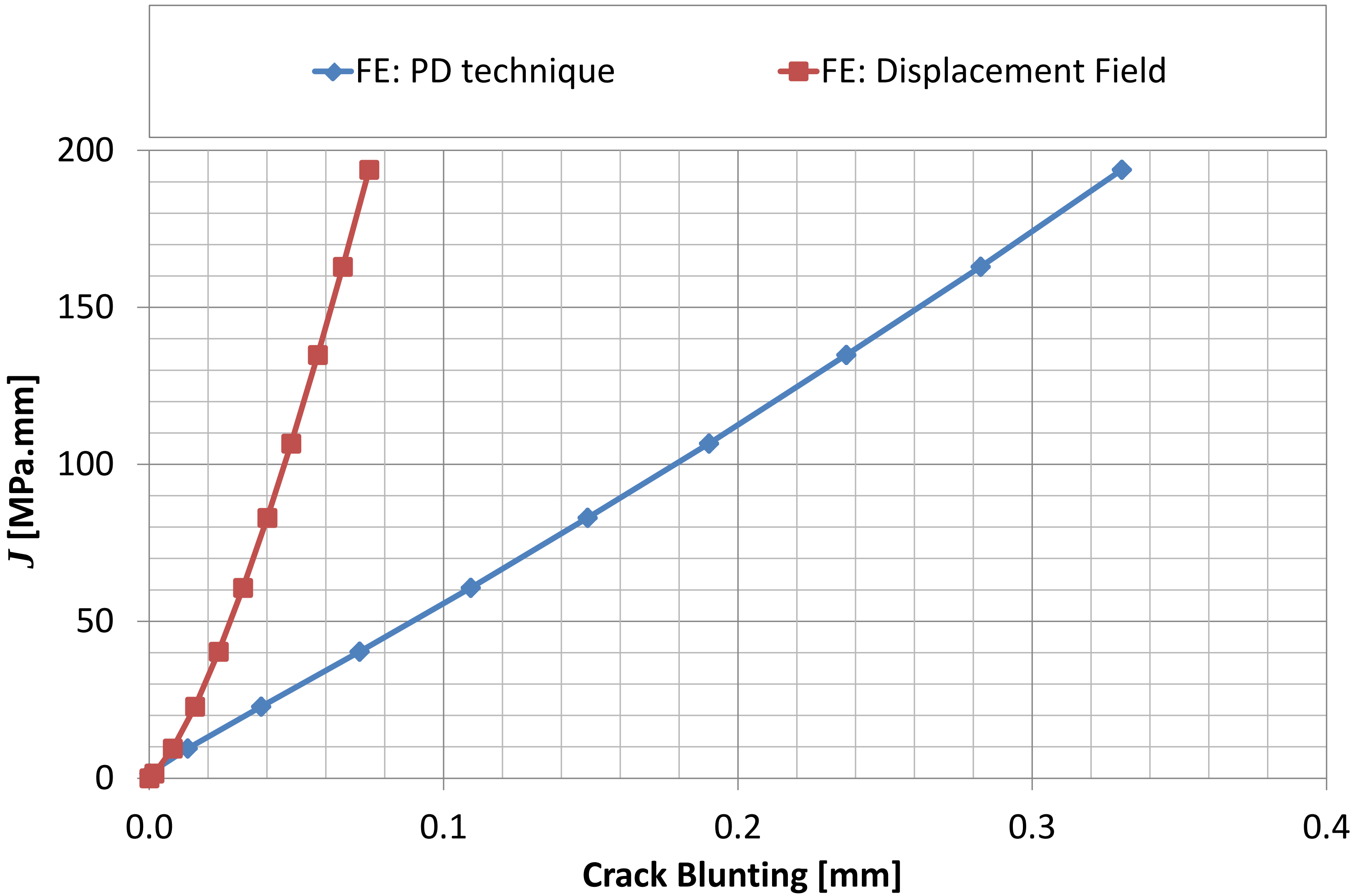

Imperial College London

Measuring Blunting: Comparison

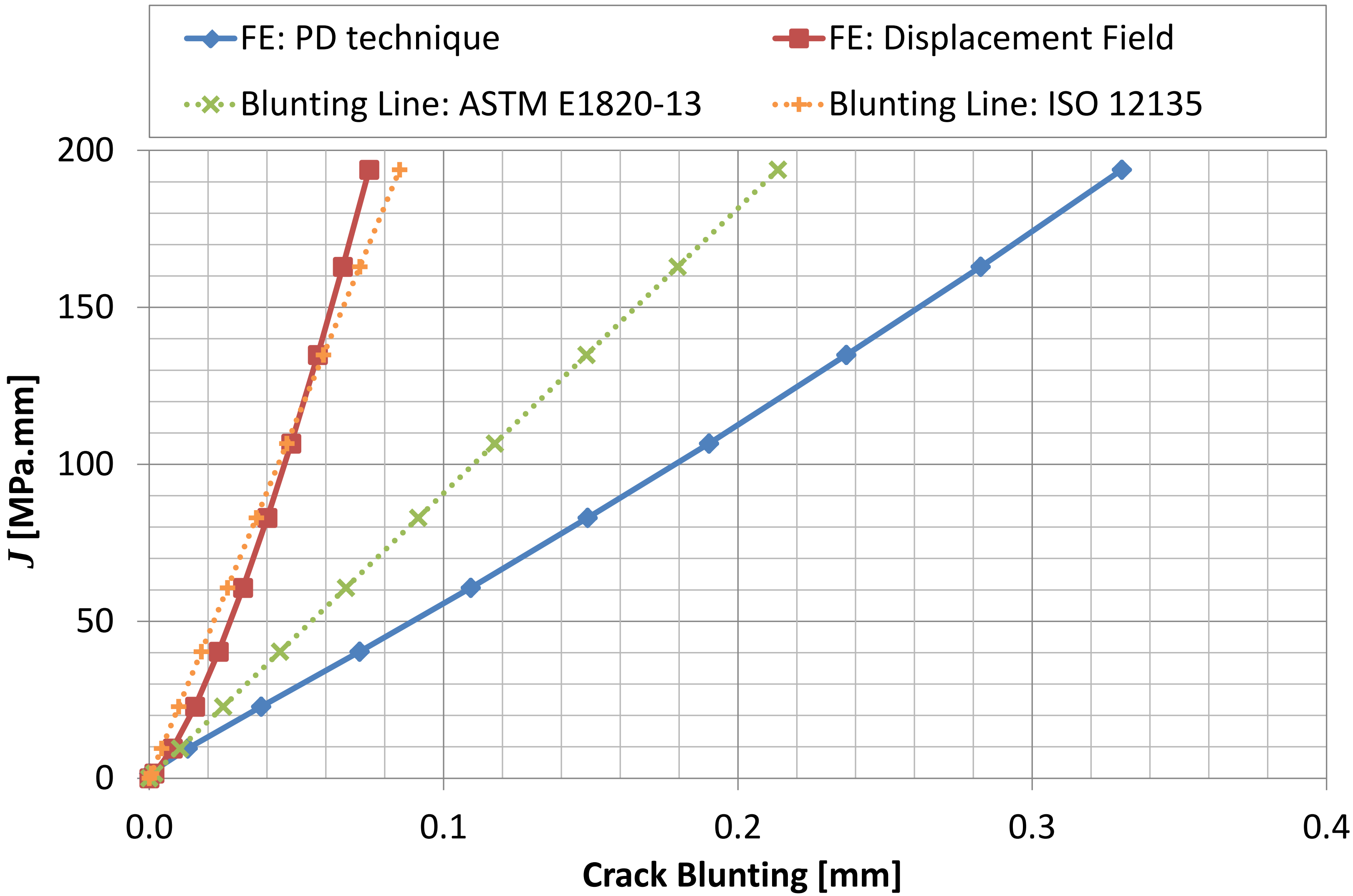

Imperial College London

Interpreting PD Data

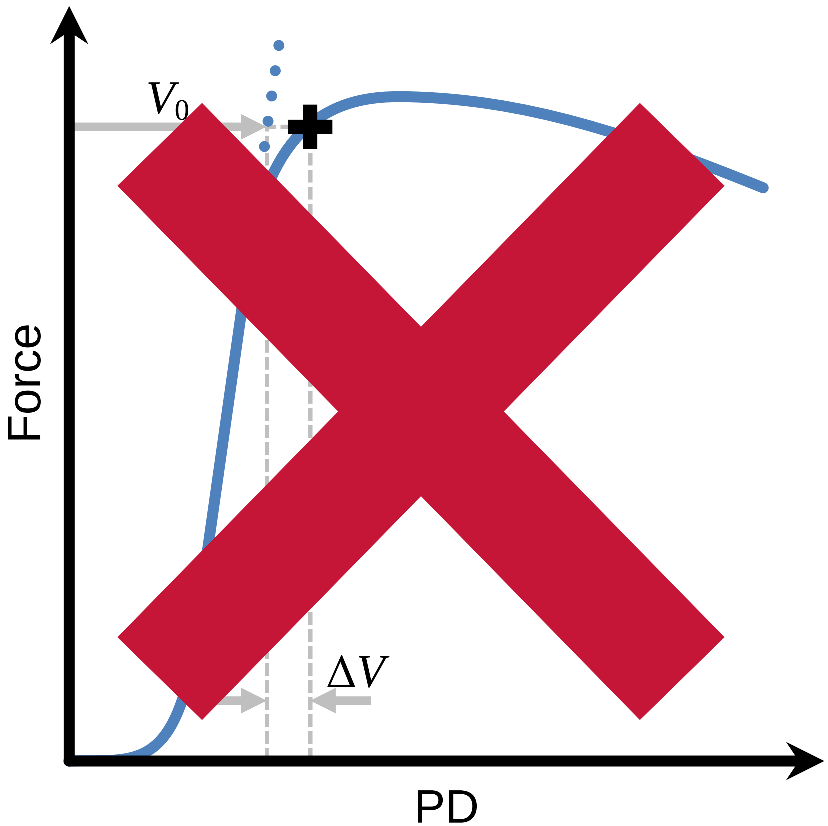

'Load' Method

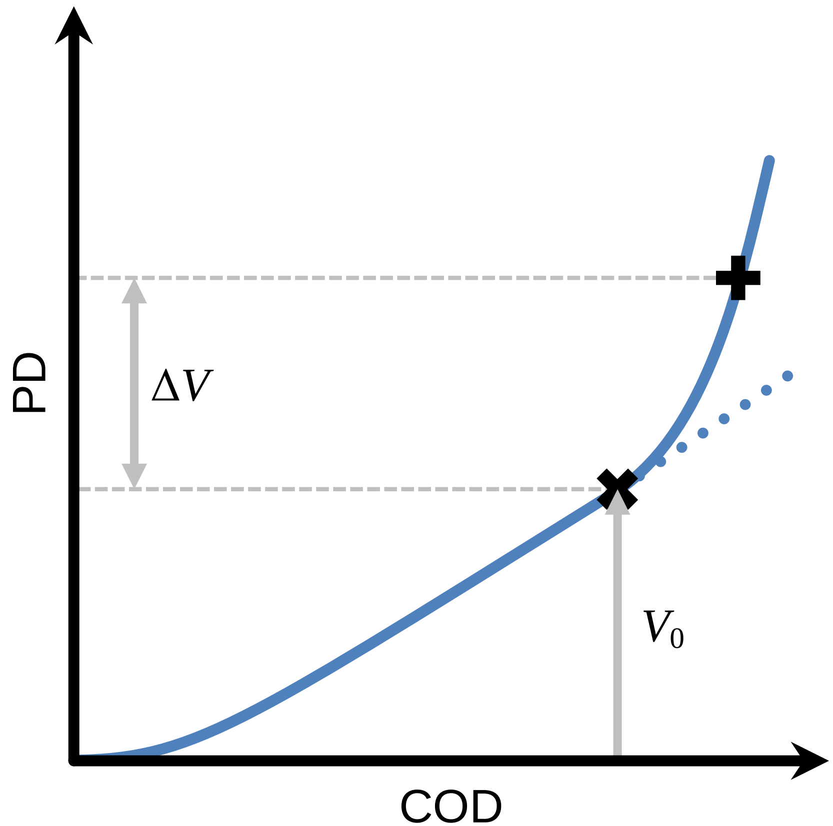

'COD' Method

Imperial College London

Contents

- Influence of strain on PD
- Interpreting PD Data
- Review of the ‘Load’ Method
- **Review of the ‘COD’ Method**
- Conclusions

Review of the 'COD' Method

- Can be difficult to identify point of inflection:
  - High strain hardening
  - High toughness
  - High tearing modulus

- FE Study:
  - 0.2 mm crack growth (node release)
  - σ_{ref} at onset of crack growth:
    - » $0.75\sigma_y$, $1.00\sigma_y$, $1.25\sigma_y$ & $1.50\sigma_y$
  - Crack growth at constant load

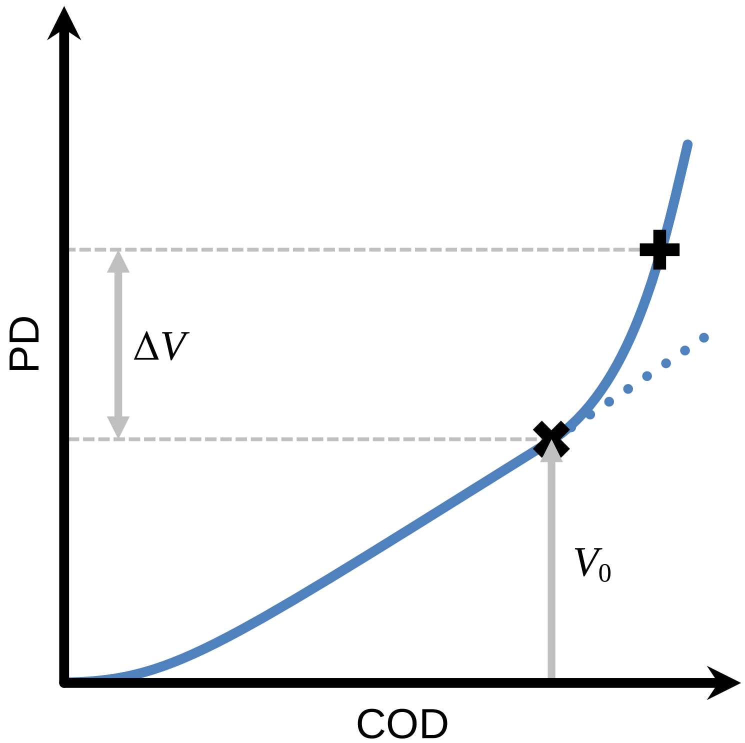

'COD' Method

Imperial College London

Review of the 'COD' Method

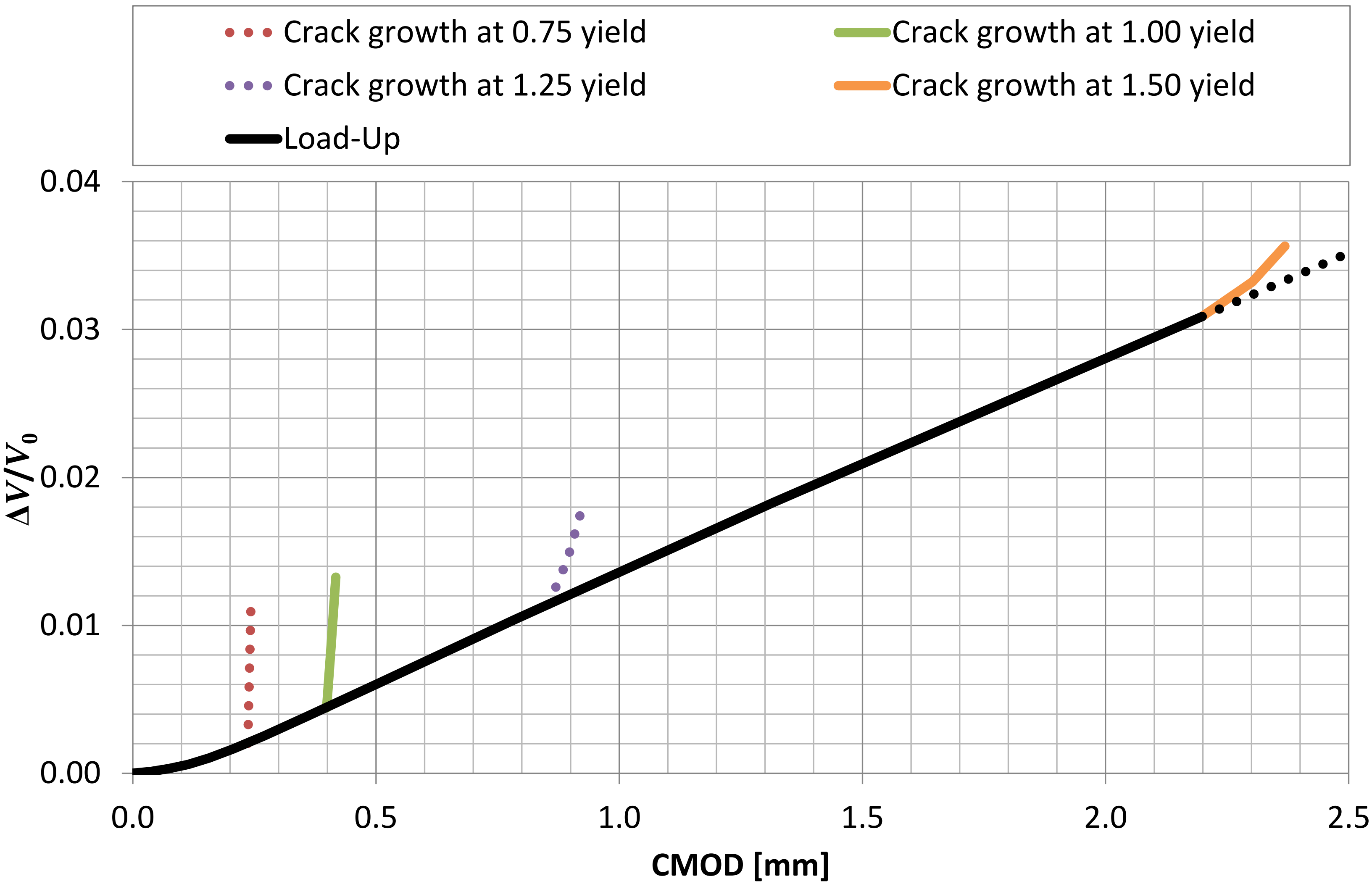

Review of the 'COD' Method

- Mitigating actions:
  - Suitable PD configuration
  - Reduce PD noise
  - Reference Measurement

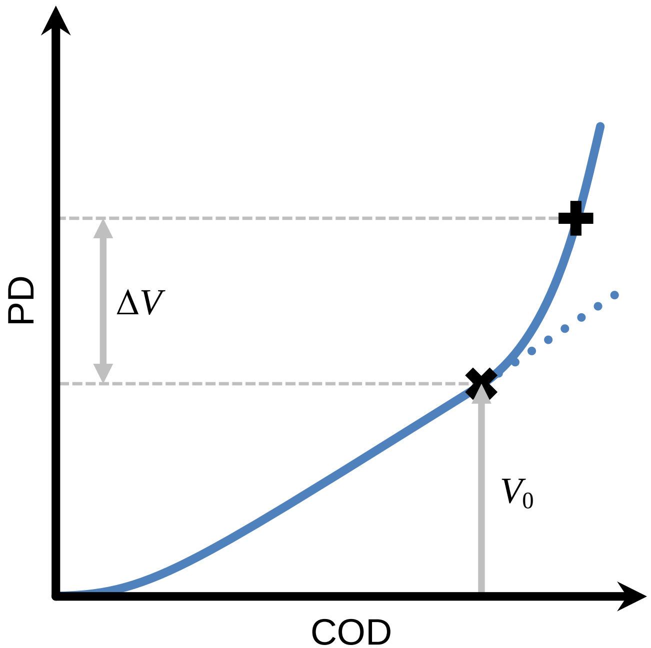

'COD' Method

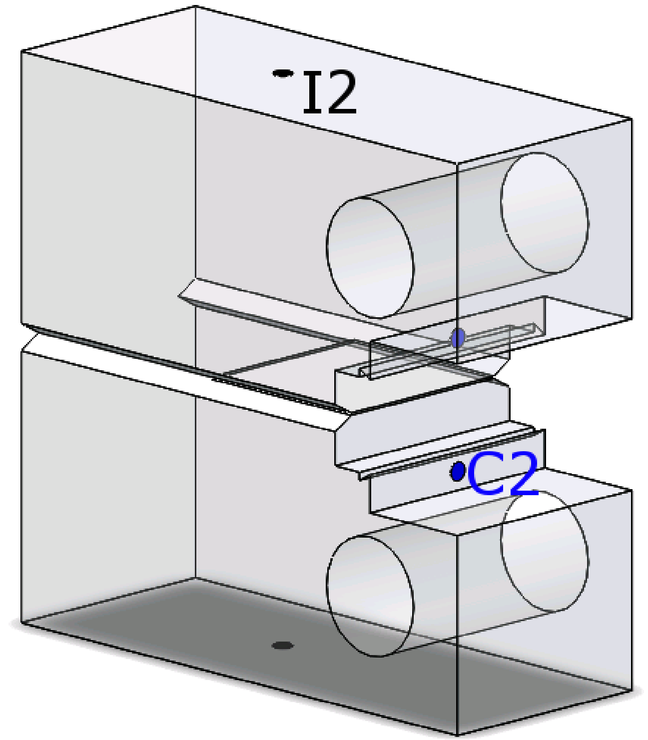

Imperial College London

Contents

- Influence of strain on PD
- Interpreting PD Data
- Review of the ‘Load’ Method
- Review of the ‘COD’ Method
- **Conclusions**

Imperial College London

Conclusions

- ‘Load’ Method:
  - PD not suitable for measuring blunting

- ‘COD’ method:
  - Requires an alternative blunting measurement:
    - » SEM
    - » Blunting line?
  - Can be difficult of identify point of inflection
    - » Suitable PD configuration
    - » Reduce PD noise
    - » Reference Measurement

Imperial College London

Influence of Pin Hole Strain

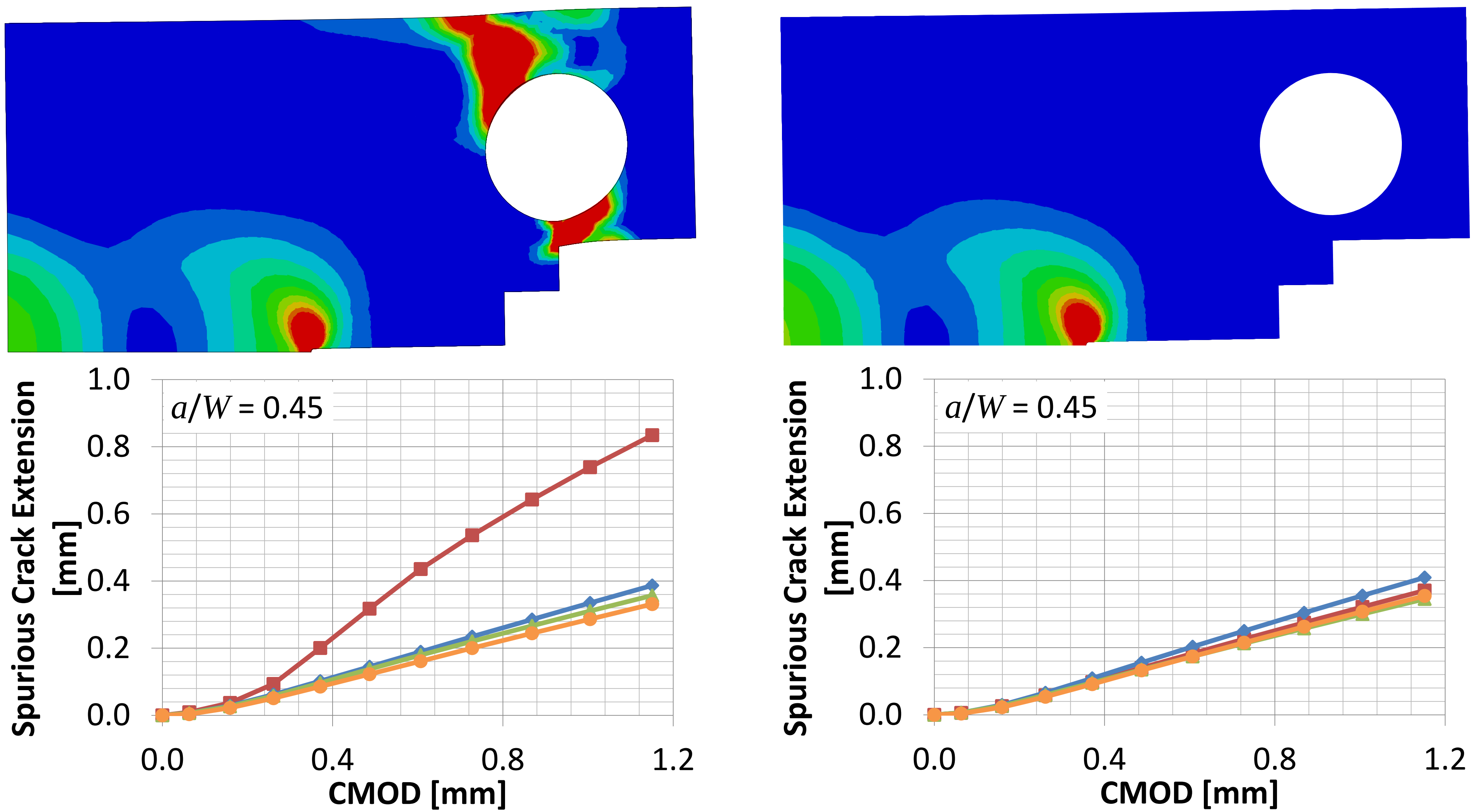

ASTM E08 meeting, May. 2016

Proposal of mitigation in dimensional tolerance requirements in ASTM E1921
Proposal of change in mechanical notch requirement in ASTM E1820 and E1921

Masato Yamamoto, CRIEPI

Kim Wallin, VTT

Naoki Miura, CRIEPI

CRIEPI
Central Research Institute of Electric Power Industry

Background

- Master Curve approach using **Mini-C(T)** specimens (4 mm-thickness) is promising method
  - Can be taken from broken halves of Charpy specimens used for surveillance program
  - Some of current dimensional requirements are severer for smaller specimens

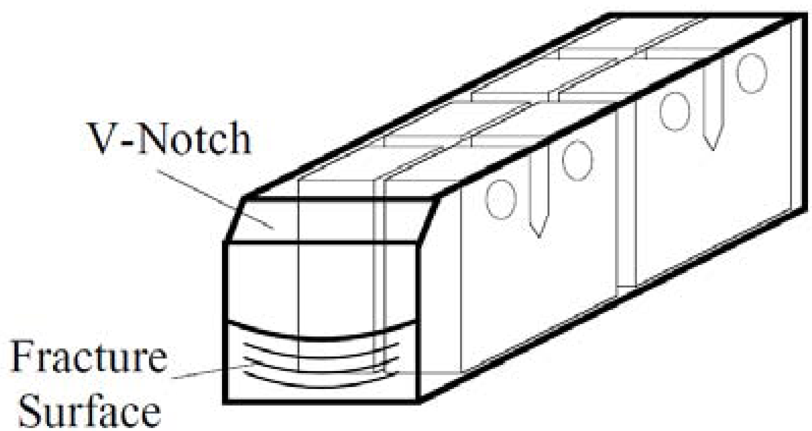

Outline of proposal

- Mitigation in dimensional tolerance requirements for C(T) specimens

- Change in specification of mechanical notch shape and dimension requirement C(T) specimens

  - Nov. 2015 meeting : presentation at E08.07.06
  - May 2016 meeting : presentation at E08.07.05

MITIGATION OF TOLERANCE

Requirements of dimensional tolerances

- ASTM E1820 and E1921 gives dimensional tolerances of C(T) specimens as **relative values**
  - Those requirements were set assuming larger (1inch-T) specimens, considering available machining and measurement preciseness.

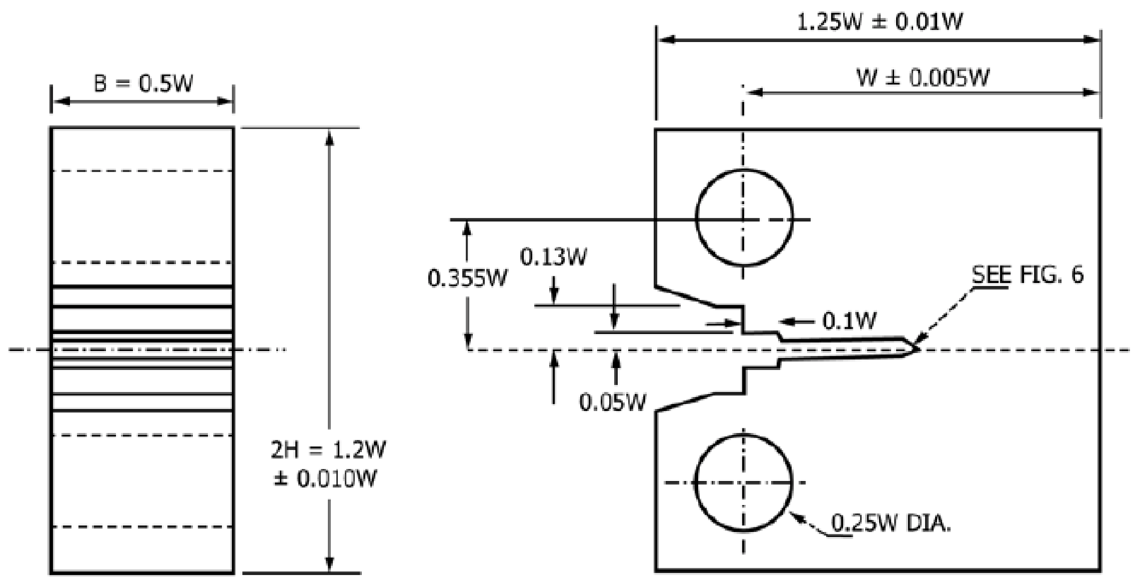

COMPACT TEST SPECIMEN FOR PIN OF 0.24W (+0.000W/−0.005W) DIAMETER

PVP 2015-45505

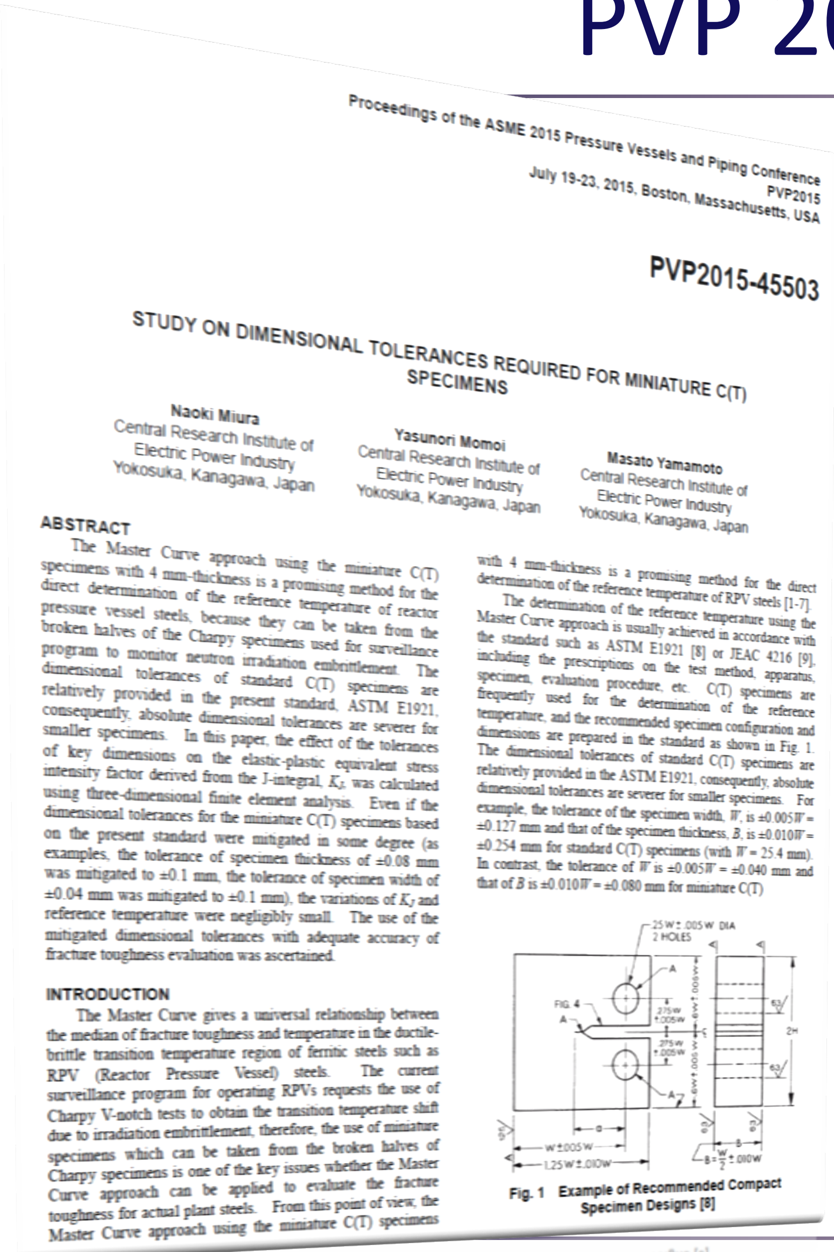
Proceedings of the ASME 2015 Pressure Vessels and Piping Conference
PVP2015
July 19-23, 2015, Boston, Massachusetts, USA

PVP2015-45503

STUDY ON DIMENSIONAL TOLERANCES REQUIRED FOR MINIATURE C(T) SPECIMENS

Naoki Miura
Central Research Institute of Electric Power Industry
Yokosuka, Kanagawa, Japan

Yasunori Momoi
Central Research Institute of Electric Power Industry
Yokosuka, Kanagawa, Japan

Masato Yamamoto
Central Research Institute of Electric Power Industry
Yokosuka, Kanagawa, Japan

ABSTRACT
The Master Curve approach using the miniature C(T) specimens with 4 mm-thickness is a promising method for the direct determination of the reference temperature of reactor pressure vessel steels, because they can be taken from the broken halves of the Charpy specimens used for surveillance program to monitor neutron irradiation embrittlement. The dimensional tolerances of standard C(T) specimens are relatively provided in the present standard, ASTM E1921, consequently, absolute dimensional tolerances are severer for smaller specimens. In this paper, the effect of the tolerances of key dimensions on the elastic-plastic equivalent stress intensity factor derived from the J-integral, K_J, was calculated using three-dimensional finite element analysis. Even if the dimensional tolerances for the miniature C(T) specimens based on the present standard were mitigated in some degree (as examples, the tolerance of specimen thickness of ±0.08 mm was mitigated to ±0.1 mm, the tolerance of specimen width of ±0.04 mm was mitigated to ±0.1 mm), the variations of K_J and reference temperature were negligibly small. The use of the mitigated dimensional tolerances with adequate accuracy of fracture toughness evaluation was ascertained.

INTRODUCTION
The Master Curve gives a universal relationship between the median of fracture toughness and temperature in the ductile-brittle transition temperature region of ferritic steels such as RPV (Reactor Pressure Vessel) steels. The current surveillance program for operating RPVs requests the use of Charpy V-notch tests to obtain the transition temperature shift due to irradiation embrittlement, therefore, the use of miniature specimens which can be taken from the broken halves of Charpy specimens is one of the key issues whether the Master Curve approach can be applied to evaluate the fracture toughness for actual plant steels. From this point of view, the Master Curve approach using the miniature C(T) specimens with 4 mm-thickness is a promising method for the direct determination of the reference temperature of RPV steels [1-7].

The determination of the reference temperature using the Master Curve approach is usually achieved in accordance with the standard such as ASTM E1921 [8] or JEAC 4216 [9], including the prescriptions on the test method, apparatus, specimen, evaluation procedure, etc. C(T) specimens are frequently used for the determination of the reference temperature, and the recommended specimen configuration and dimensions are prepared in the standard as shown in Fig. 1. The dimensional tolerances of standard C(T) specimens are relatively provided in the ASTM E1921, consequently, absolute dimensional tolerances are severer for smaller specimens. For example, the tolerance of the specimen width, W, is $\pm 0.005W = \pm 0.127$ mm and that of the specimen thickness, B, is $\pm 0.010W = \pm 0.254$ mm for standard C(T) specimens (with $W = 25.4$ mm). In contrast, the tolerance of W is $\pm 0.005W = \pm 0.040$ mm and that of B is $\pm 0.010W = \pm 0.080$ mm for miniature C(T).

Fig. 1 Example of Recommended Compact Specimen Designs [8]

- Miura et. al addressed the mitigation of tolerance requirement for 4mm-T Mini- C(T) specimens
  - Change in K_J in various tolerance values was determined by 3-D finite element analyses
  - Mitigation of tolerances of **B, W, L, 2H and GL to ±0.1mm (0.0125W)** gives negligibly small change in K_J

Analysis Model

- Mini- C(T) specimens
  - Variable dimensions: *B*, a_m, *W*, *L*, *2H*, *N*, and *GL*
  - Fixed dimensions: a_f, L_D, and *D*

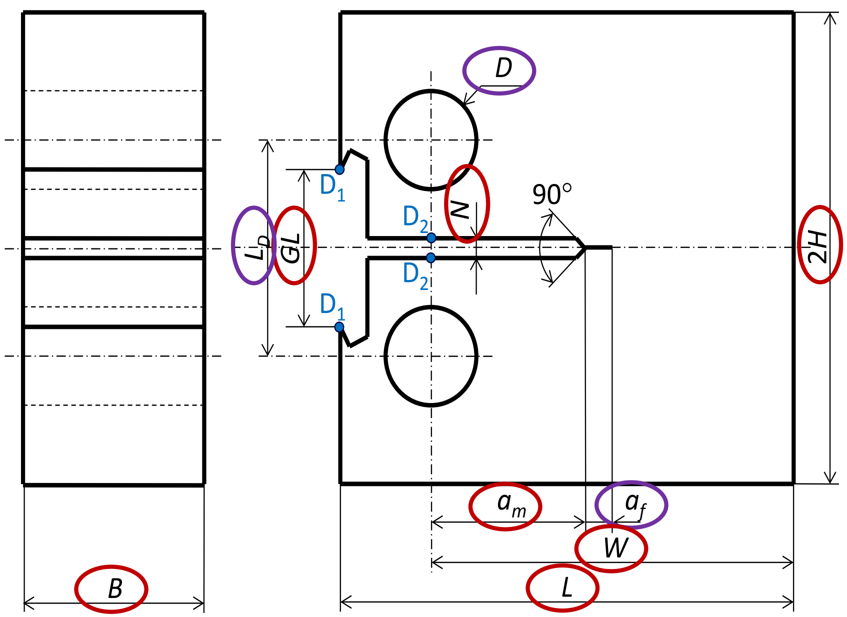

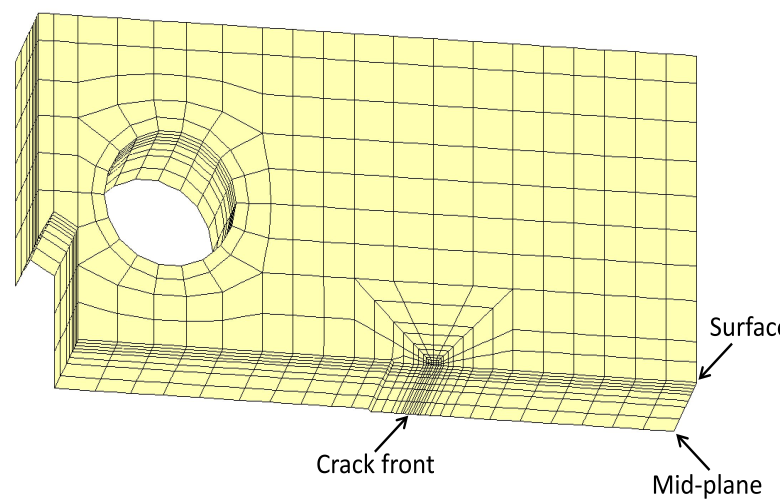

Analysis Matrix

Base case

Case No.	B, mm	a_m, mm	a_f, mm	W, mm	L, mm	$2H$, mm	N, mm	GL, mm	L_D, mm	D, mm
Std	4.0	3.4	0.6	8.0	10.0	9.6	0.08	3.0	4.4	2.0
N0	4.0	3.4	0.6	8.0	10.0	9.6	0.00	3.0	4.4	2.0
N1	4.0	3.4	0.6	8.0	10.0	9.6	0.15	[illegible]	[illegible]	[illegible]
N2	4.0	3.4	0.6	8.0	10.0	9.6	0.20	[illegible]	[illegible]	[illegible]
N3	4.0	3.4	0.6	8.0	10.0	9.6	0.25	[illegible]	[illegible]	2.0
N4	4.0	3.4	0.6	8.0	10.0	9.6	0.50	3.0	4.4	2.0
B1	3.9	[illegible]	[illegible]	[illegible]	10.0	9.6	0.20	3.0	4.4	2.0
B2	4.1	[illegible]	[illegible]	[illegible]	10.0	9.6	0.20	3.0	4.4	2.0
a1	4.0	3.0	[illegible]	[illegible]	[illegible]	9.6	0.20	3.0	4.4	2.0
a2	4.0	3.8	[illegible]	[illegible]	[illegible]	9.6	0.20	3.0	4.4	2.0
W1	4.0	3.35	0.6	7.9	[illegible]	[illegible]	[illegible]	3.0	4.4	2.0
W2	4.0	3.45	0.6	8.1	[illegible]	[illegible]	[illegible]	3.0	4.4	2.0
L1	4.0	3.4	0.6	8.0	9.9	[illegible]	[illegible]	[illegible]	4.4	2.0
L2	4.0	3.4	0.6	8.0	10.1	[illegible]	[illegible]	[illegible]	4.4	2.0
H1	4.0	3.4	0.6	8.0	10.0	9.5	[illegible]	[illegible]	[illegible]	2.0
H2	4.0	3.4	0.6	8.0	10.0	9.7	[illegible]	[illegible]	[illegible]	2.0
GL1	4.0	3.4	0.6	8.0	10.0	9.6	0.20	2.7	[illegible]	[illegible]
GL2	4.0	3.4	0.6	8.0	10.0	9.6	0.20	3.3	[illegible]	[illegible]

Effect of notch height

Effect of thickness

Effect of crack length

Effect of width

Effect of length

Effect of height

Effect of GL

0.1mm = 0.0125W

Effect of Dimensional Tolerances

- Comparison of two K_Js
  - K_0 : derived from J by finite element analysis
    - ✓ index in which **all dimensional factors are taken into account**
  - K_c : derived from J by ASTM E1921 for load vs. load-line displacement relation obtained from finite element analysis
    - ✓ can be considered as the index to judge **whether dominant dimensional factors are properly considered in ASTM E1921**

Effect of Dimensional Tolerances

- Both K_0 and K_c normalized by values for standard dimension case
- Values of K_0 and K_c where they approximately reach
  - maximum fracture toughness capacity, $K_{Jc(\text{limit})}$, J_{max}

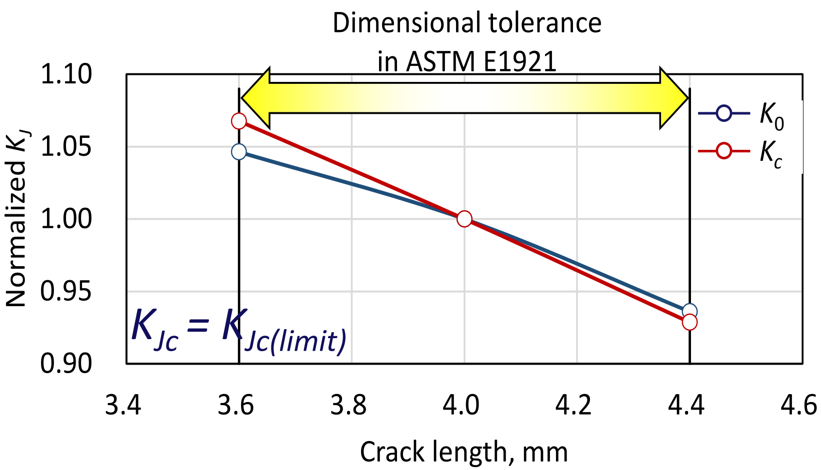

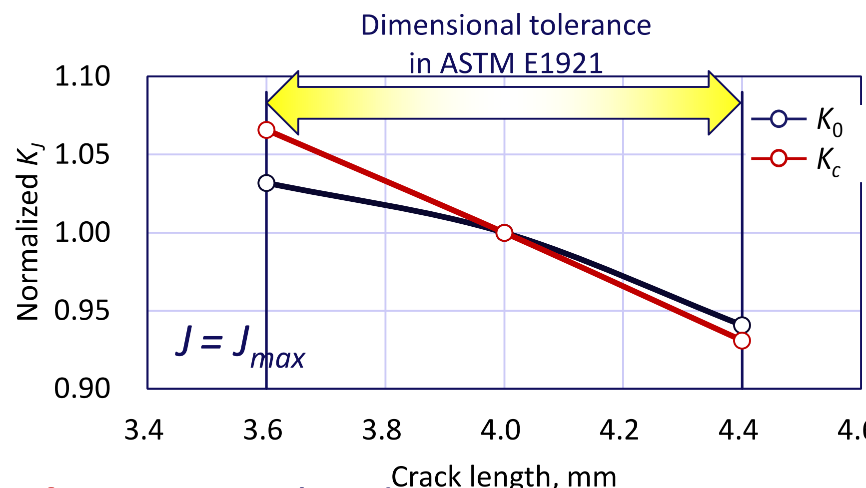

Effect of **crack length** on normalized K_J

Change of ±10% (±0.4 mm) in *a* causes approximate variation of ±5% in K_J
Trend is similar both for K_0 and K_c
a is one of dominant factors to impact on K_J, nevertheless, contribution of *a* must be properly considered in ASTM E1921

Effect of Dimensional Tolerances

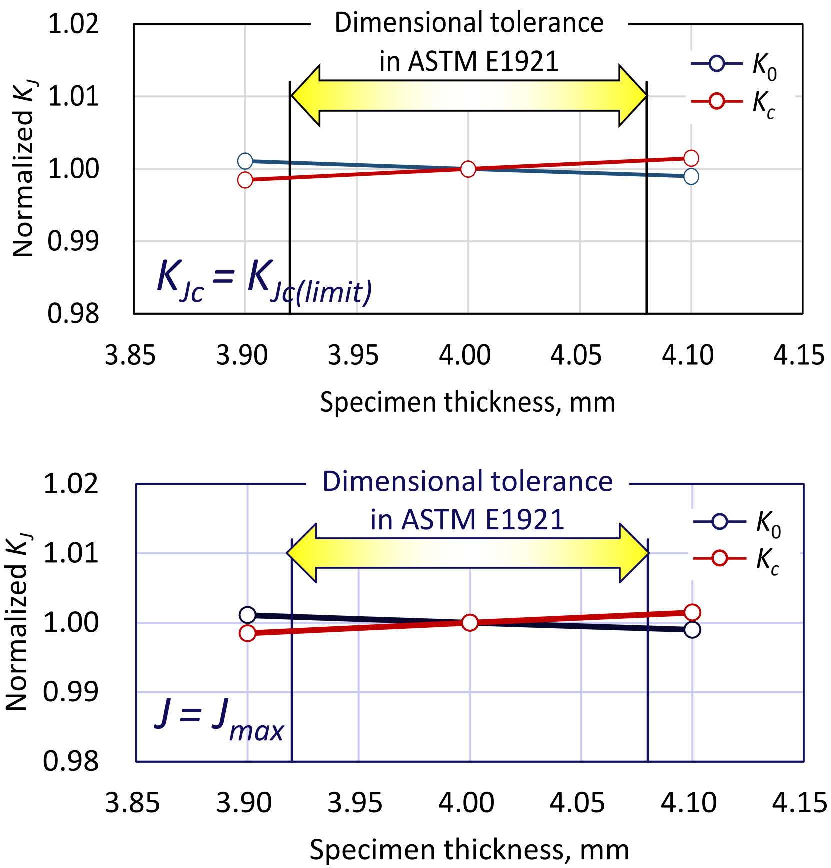

Effect of **thickness** on normalized K_J

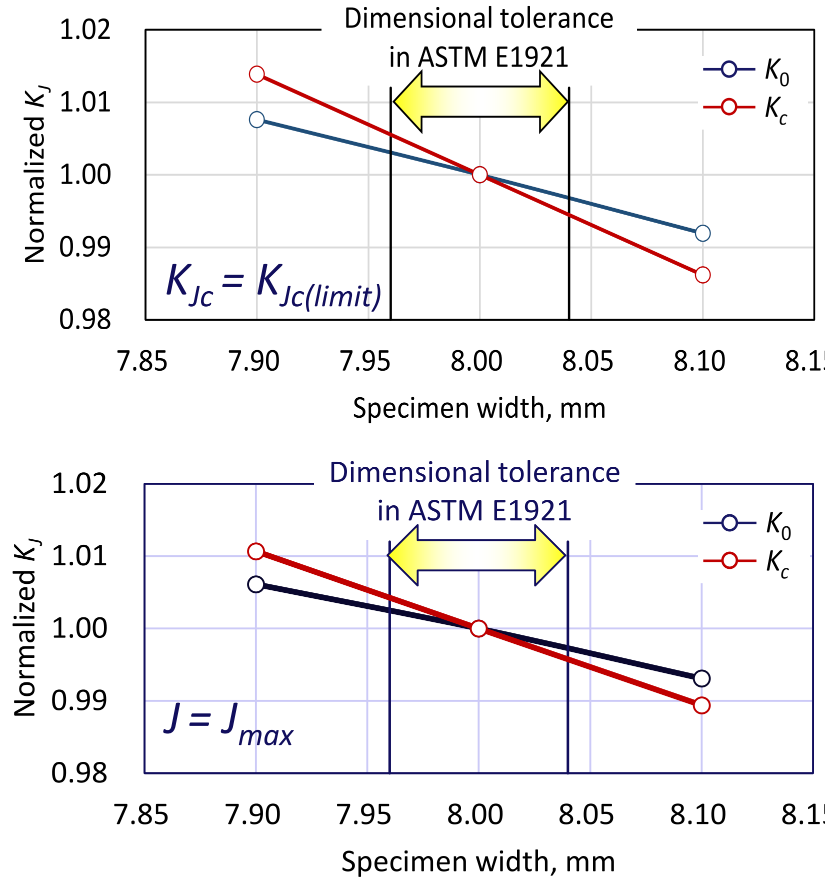

Effect of **width** on normalized K_J

Situation is similar for contributions of B and W

Changes of ±0.1 mm in B or W induce variation of K_J less than ±1%

Effect of Dimensional Tolerances

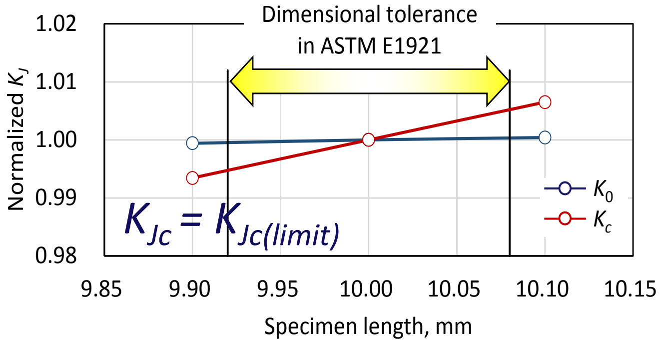

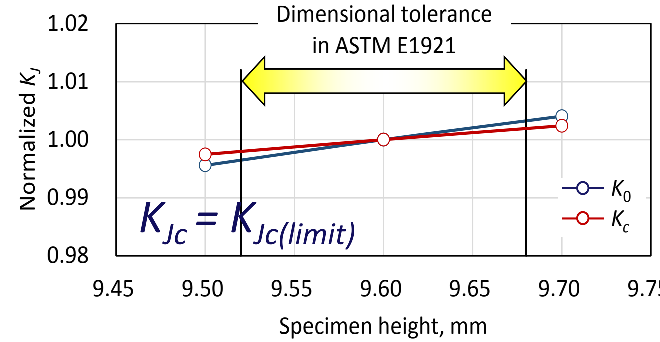

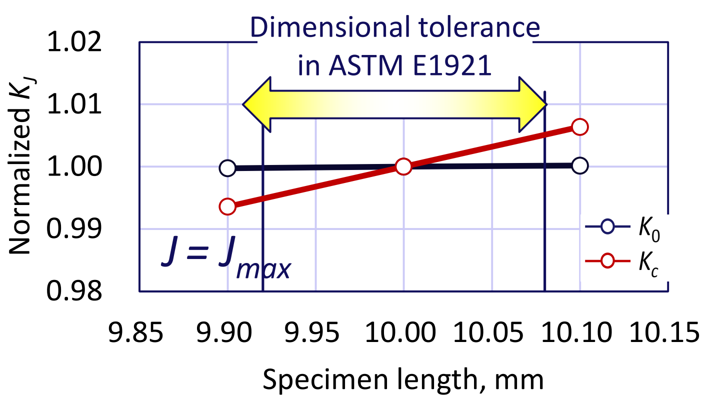

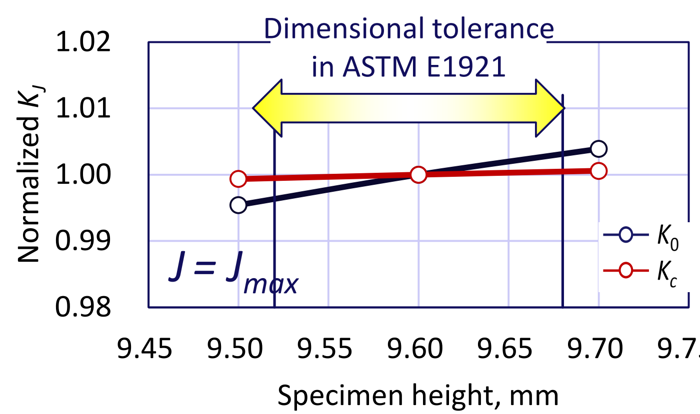

Effect of **length** on normalized K_J

Effect of **height** on normalized K_J

Effects of L, $2H$, GL, and N implicitly considered in K_0, while they cannot be taken into account in K_c

These effects are still limited within assumed range of dimensions

Effect of Dimensional Tolerances

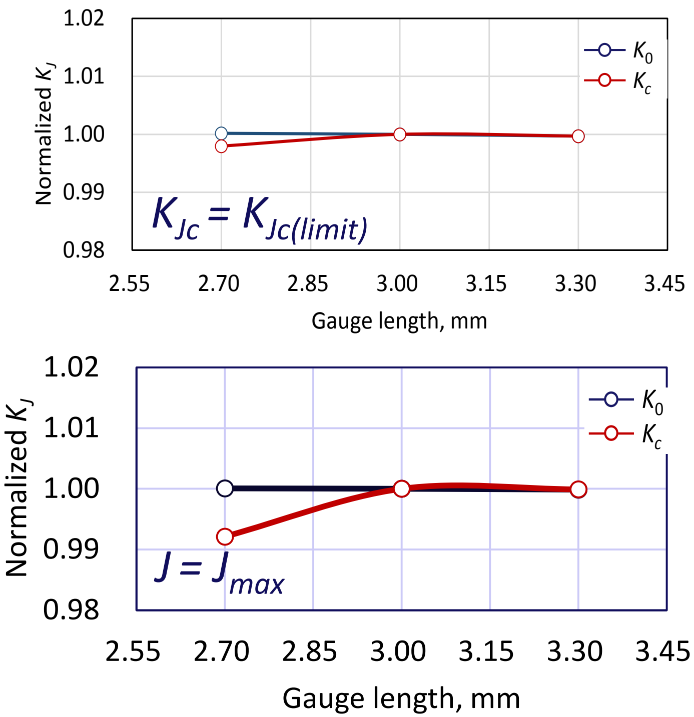

Effect of ***GL*** on normalized K_J

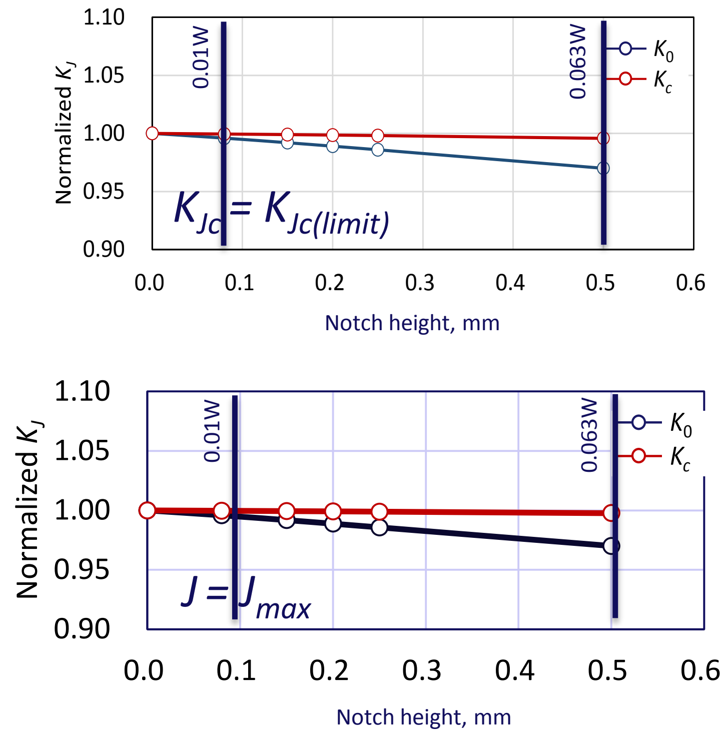

Effect of **notch height** on normalized K_J

Effects of *L*, 2*H*, *GL*, and *N* implicitly considered in K_0, while they cannot be taken into account in K_c

These effects are still limited within assumed range of dimensions

Proposal on tolerances

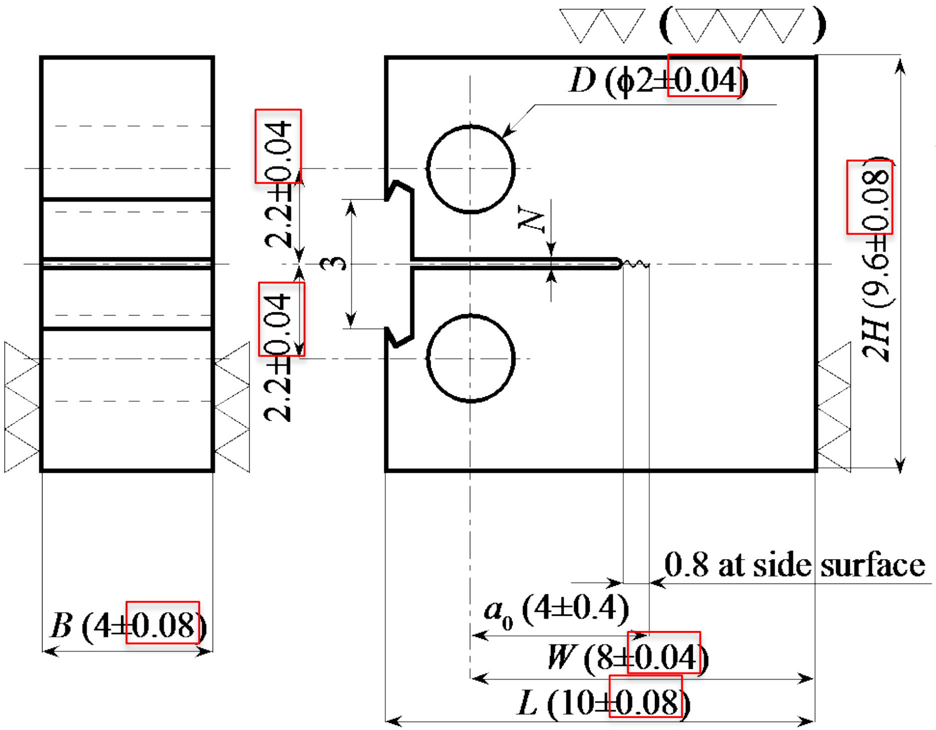

- Mitigation of the red-marked tolerances to 0.0125W (or 0.013W) (0.1mm in Mini-C(T))

	E1921-14e1	Proposal
W, am, D	0.005W	0.0125W
L, B, 2H	0.010W	0.0125W

CHANGE IN MECHANICAL NOTCH SHAPE AND DIMENSION REQUIREMENT

Requirement of mechanical notch shape and dimension

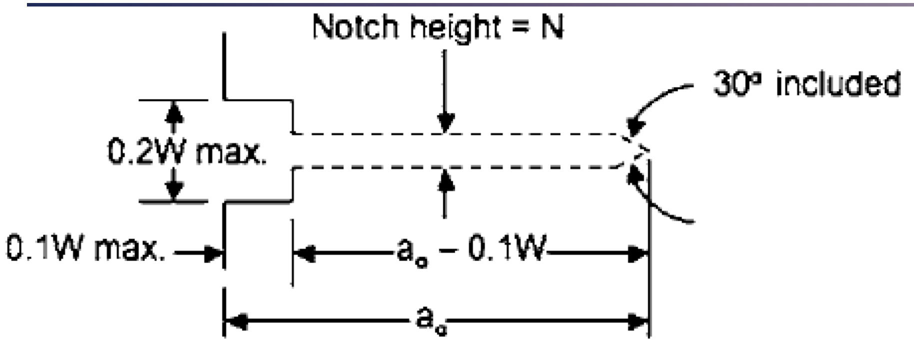

ASTM E1921 specify the acceptable envelope for mechanical notch and pre-crack.

Notch and Precrack Configurations

	Wide Notch	Narrow Notch
Maximum Notch Height	Lesser of 0.063W or 6.25 mm	0.01W
Maximum Notch Angle	60°	As machined
Minimum Precrack Length	Greater of 0.5N or 1.3 mm	Greater of 0.5N or 0.6mm

- Maximum height of narrow groove, N, is **0.01W**, which gives too narrow (0.08mm) for Mini- C(T) specimens.
- Minimum crack requirement Minimum crack length for straight notch is **1.3mm**, which is too large for the Mini-C(T) specimen

Sensitivity of notch envelope angle on K

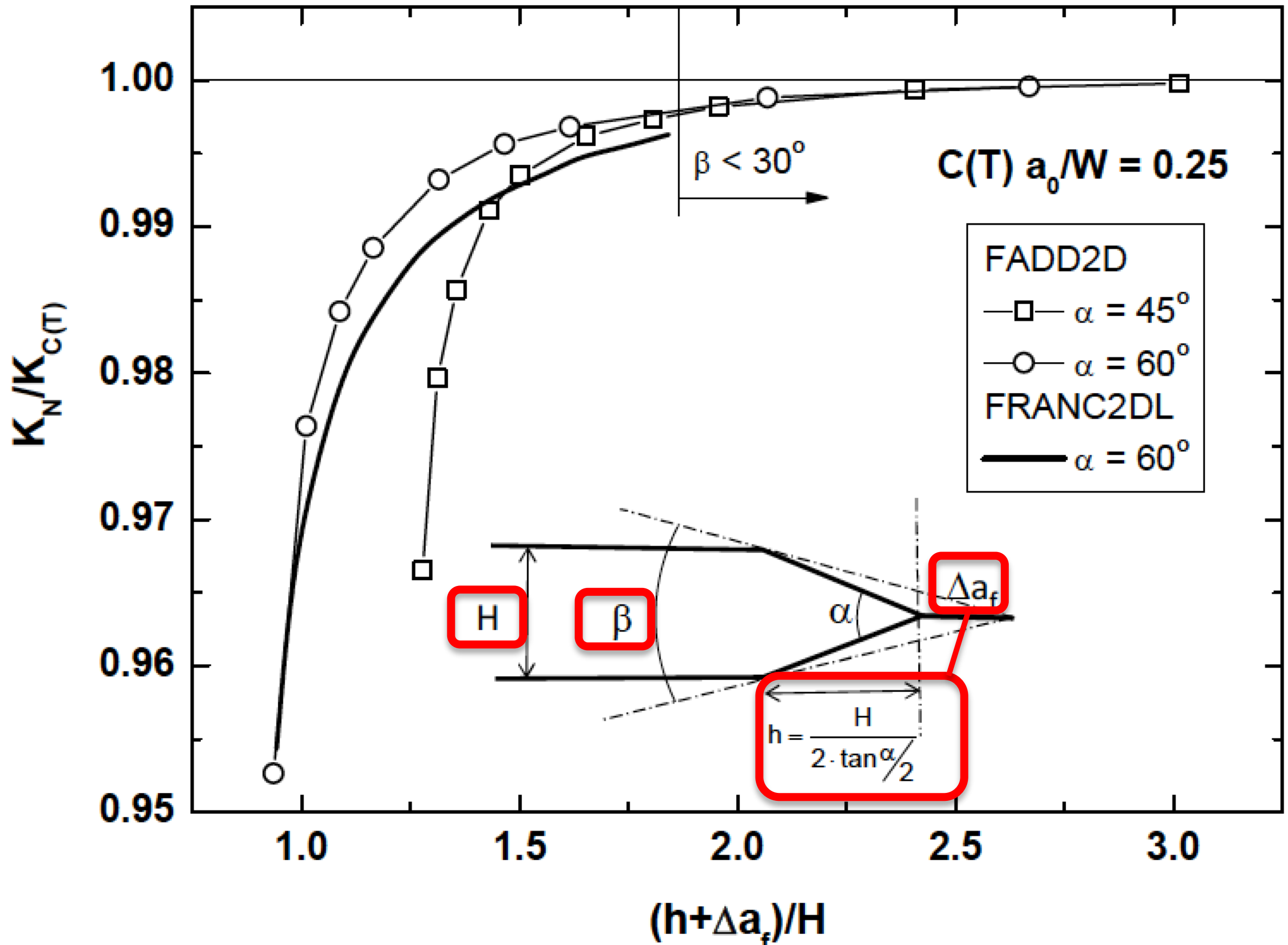

K_N : K for ideal crack (H=0)

$K_{C(T)}$: K for machining notch and precrack

H, h+Δa_f, and angle of β are important to be included as the notch requirement

Notch Shape effect in PVP2015-45505

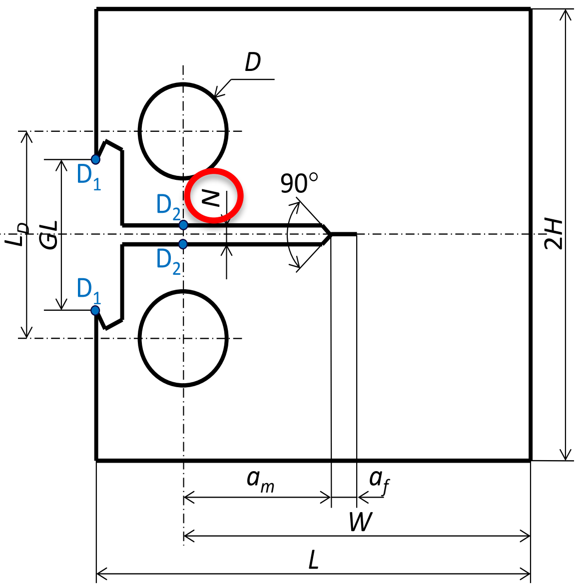

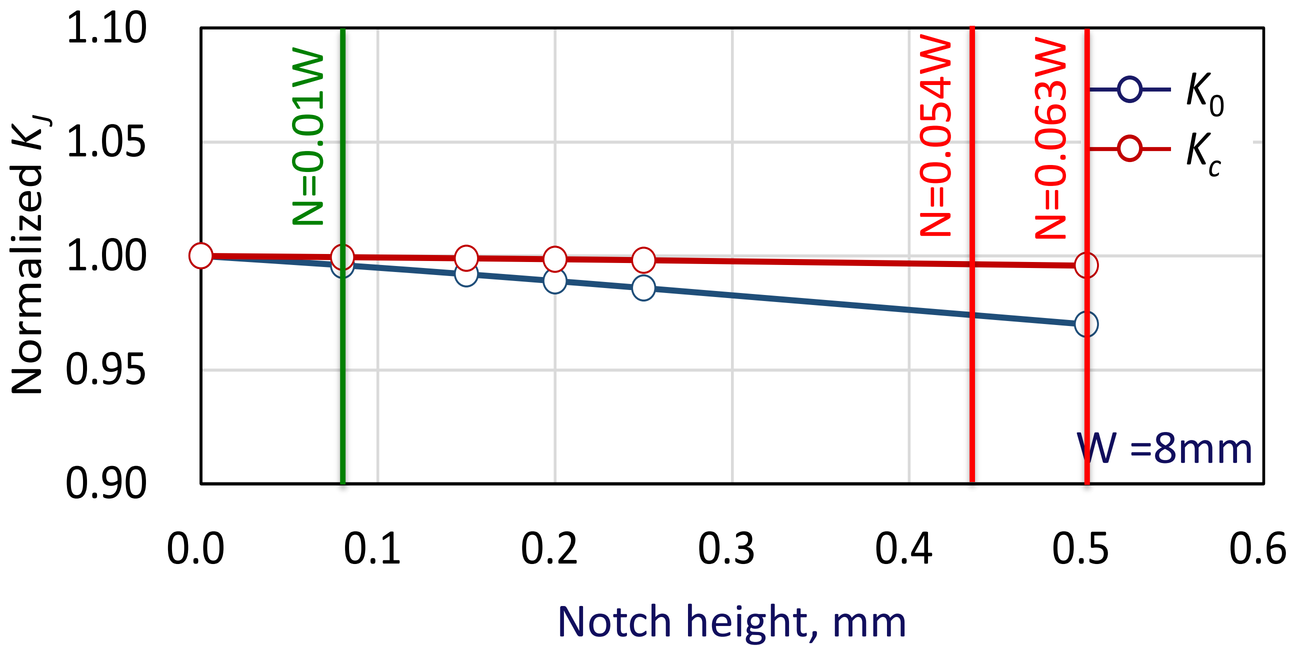

N : 0 – 0.5mm

Δa_{PC} : 0.6 mm

N=0.08mm (0.01W): Maximum notch height for narrow groove

N=0.43mm (0.054W): Maximum notch height to keep envelope requirement with Δa_{PC} = 0.6 mm

N=0.5mm (0.063W): Maximum notch height for straight groove

(Envelope requirement cannot be sufficed with 90˚ groove)

Mitigation of maximum notch height does not significantly affect the evaluation of K_J

Minimum Δa_{pc} to keep the current requirement for notch and crack envelope

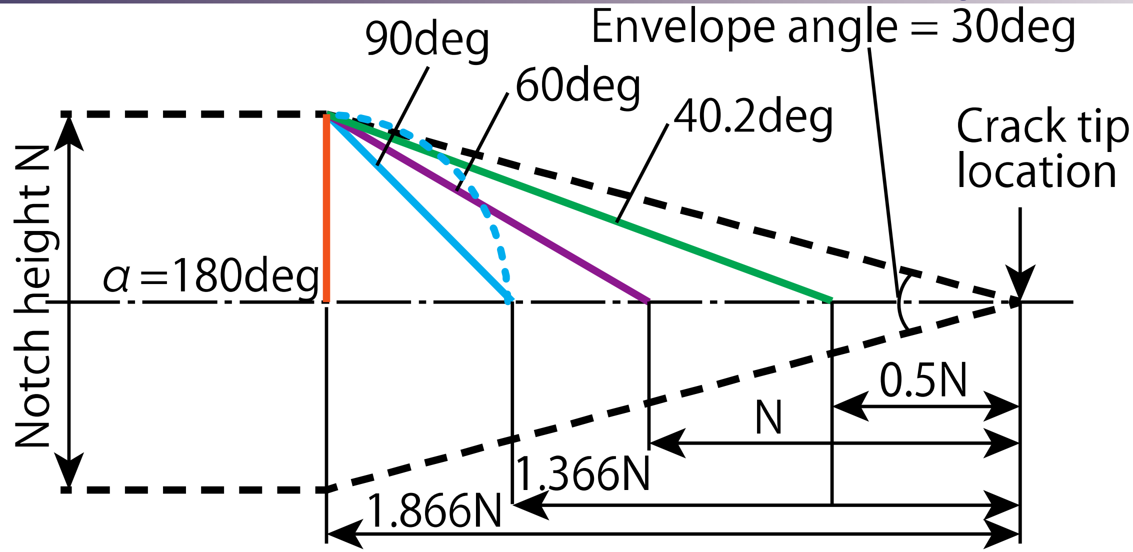

Notch angle, α (deg)	minimum Δa_{pc}	Remark
180	1.866N	Rectangular notch with no sharpened zone
90	1.366N	Similar to narrow notch with circular profile
60	N	Maximum angle for wide notch
< 20.1	0.5N	Angle where 0.5N is sufficient to keep the envelope

Notch and Precrack Configurations

	Wide Notch	Narrow Notch
Maximum Notch Height	Lesser of 0.063W or 6.25 mm	0.01W
Maximum Notch Angle	60°	As machined
Minimum Precrack Length	Greater of 0.5N or 1.3 mm	Greater of 0.5N or 0.6mm

Relationship between required minimum Δa_{pc} and W

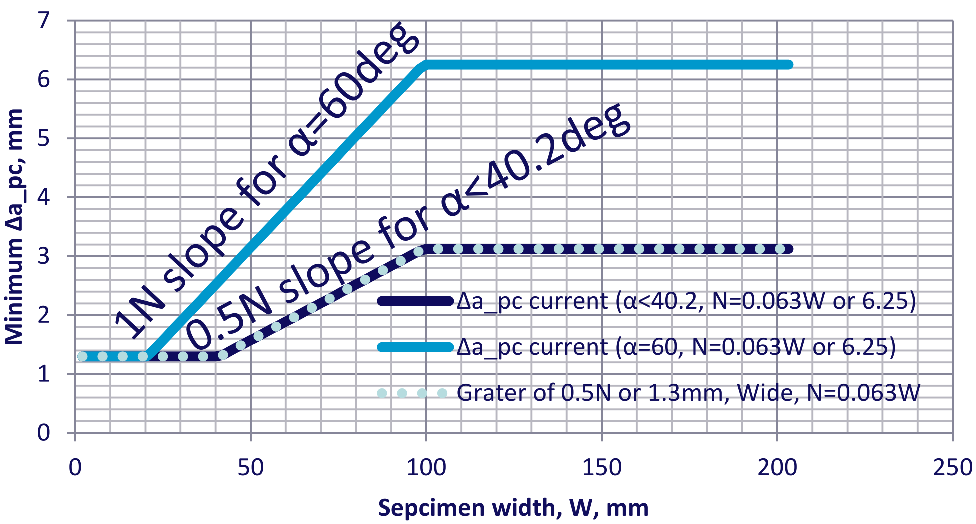

Wide notch with maximum notch height

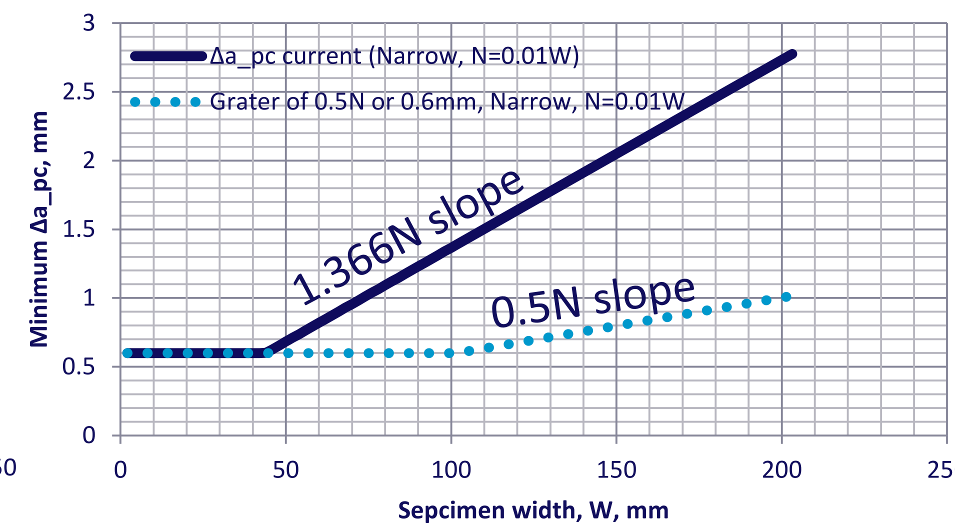

Narrow notch with maximum notch height

- Documented specification in Fig. 5 for both of Narrow and Wide notches not always suffice the envelope requirement

Proposal for notch height requirement (1)

- ✓ Eliminating the specific requirement for "Narrow" and "Wide" notch
- ✓ Any of notch shapes are acceptable if the requirement for
  - ➢ maximum N (relative to W)
  - ➢ Sum of precrack length and sharpened notch length (relative to N)

  are satisfied.

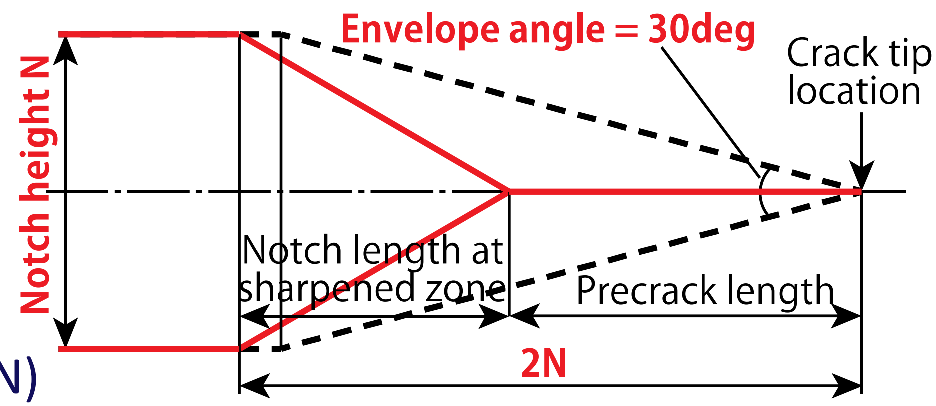

Notch and Precrack Configurations

	Wide Notch	Narrow Notch
Maximum Notch Height	Lesser of 0.063W or 6.25 mm	0.01W
Maximum Notch Angle	60°	As machined
Minimum Precrack Length	Greater of 0.5N or 1.3 mm	Greater of 0.5N or 0.6mm

	Proposal for requirement
Maximum Notch Height	0.063W
Sum of precrack length and sharpened notch length	2.0N
Minimum Precrack Length	0.5N

Comparison of Δa_{pc} between current and proposed requirements